8-2018

Regulation of the Endogenous Antioxidant Defense System in Diabetic Peripheral Neuropathy

Mateusz A. Stochelski
Purdue University

REGULATION OF THE ENDOGENOUS ANTIOXIDANT DEFENSE SYSTEM IN DIABETIC PERIPHERAL NEUROPATHY

by

Mateusz A. Stochelski

A Dissertation

Submitted to the Faculty of Purdue University

In Partial Fulfillment of the Requirements for the degree of

Doctor of Philosophy

Department of Nutrition Science

West Lafayette, Indiana

August 2018

THE PURDUE UNIVERSITY GRADUATE SCHOOL
STATEMENT OF COMMITTEE APPROVAL

Dr. John Burgess, Chair
Department of Nutrition Science
Dr. Edward L. Bartlett
Department of Biomedical Engineering
Dr. Ignacio Camarillo
Department of Biological Sciences
Dr. Kee-Hong Kim
Department of Food Science

Approved by:
Dr. Michelle R. Forman
Head of the Graduate Program

For my wife Jan and our beloved pup Mia

ACKNOWLEDGMENTS

Completion of this dissertation would not have been possible without the love and support of my wife. She stood by my side each and every day of my graduate career and helped me with statistics and SAS programming, editing manuscripts, preparing for presentations, and was my "go-to" person for any and every technical problem I ran into. Words can only begin to describe the amount of gratitude I have for all her love, time, and effort that made this work possible. I would also like to thank my parents for their unwavering love and support throughout all of these years. Visiting them in Chicago provided much needed relief from all the various stresses of graduate life, and I am forever grateful for the loving and welcoming environment they provided and continue to provide for Jan and me. Our pup, Mia, also deserves a heartfelt thank you. She sat by my side, usually begging for walks or pets, through all hours of the day and night as I worked to complete this dissertation. Her companionship is priceless, but I will do my best to return the favor with many tasty snacks and walks in the coming days.

Further gratitude goes out to my mentor, Dr. Jay Burgess. I have worked with Dr. Burgess since my time as an undergraduate at Purdue, and I have wondered many times how/why I was so fortunate. Finding a better mentor is not possible. Dr. Burgess taught me most everything I know about scientific research, from experimental design to lab techniques and data analysis. His scientific integrity and attention to detail have left a lifelong impact on me and set the standard for quality research. Furthermore, Dr. Burgess has taught me that mentorship goes beyond the work environment and requires understanding of your colleagues on a "human" level. This is something sorely missing in academia, and in my opinion is largely responsible for the mental health issues seen in graduate students. The beginning of my graduate career was marred by multiple health complications due to a flu virus that resulted in heart failure. This was a very

difficult time in my life and succeeding in academia without someone like Dr. Burgess would not have been possible. The support that Jan and I had from Dr. Burgess, his wife, and Laura Stevens made us feel like we had a family and support system here in Lafayette. Simply put, I would not be where I am today without their support. I only wish I could do more to acknowledge the effort and mentorship Dr. Burgess puts in for his students. Academia needs more people like him, and these people need to be rewarded for their lifelong commitment to higher education.

Last, but certainly not least, I owe a debt of gratitude to the Burgess lab members. To start, my compatriot Tomasz Wilmanski. Your suggestions, input, ideas, knowledge base, and assistance with manuscripts helped shape the direction of this dissertation. Our friendship, without question, helped me get through graduate school. I would also like to thank Mitchell Walters, who was by far my most helpful undergraduate research assistant. All the meticulous work he did analyzing GSH concentrations is well represented in this dissertation and does not go unappreciated. Further thanks go out to Carrie Terwilliger, the newest Burgess lab member. I appreciate all of your help and support these past few months as I have been writing this dissertation. We have a similar approach to teaching and working as a team, and I look forward to passing on the glutathione reductase paradox to you.

TABLE OF CONTENTS

LIST OF FIGURES

LIST OF ABBREVIATIONS

8-hydroxy-2'-deoxyguanosine	8-OH-dG
2-acetylamino-3-[4-(2-acetylamino-2-carboxyethylsulfanylthiocarbonylamino)phenylthiocarbamoylsulfanyl] propionic acid	AAPA
antibody for advanced glycation end products	Ab-RAGE
advanced glycation end products	AGE
protein kinase B	Akt
AMP activated protein kinase	AMPK
analysis of variance	ANOVA
aldose reductase	AR
antioxidant response element	ARE
Bovine retinal endothelial cells	BRECs
bovine serum albumin	BSA
L-buthionine-sulfoximine	BSO
chlorophenylhydrazone	CCCP
Centers for Disease Control and Prevention	CDC
3H-1-2-dithiole-3-thione	D3T
diacylglycerol	DAG
2′,7′-dichlorofluorescin diacetate	DCFH-DA
dehydroepiandrosterone	DHEA

Dulbecco's Modified Eagle Medium	DMEM
dorsal root ganglion	DRG
dithiol dithiothreitol	DTT
endothelial nitric oxide synthase	eNOS
endothelin-1	ET-1
fetal bovine serum	FBS
glucose-6-phosphate dehydrogenase	G6PD
glyceraldehyde-3-phosphate dehydrogenase	GAPDH
γ-glutamylcysteine ligase	GCL
glutathione peroxidase	Gpx
glutathione reductase	GR
glutaredoxin-1	GRX-1
glutathione	GSH
oxidized glutathione	GSSG
oxidized glutathione methyl ester	GSSGme
glutathione S-transferase	GST
4-hydroxynonenal	HNE
heme oxygenase	HO-1
Kelch-like ECH associated protein 1	Keap 1
keap 1-hepatocyte knockout mice	Keap 1-HKO
low-density lipoprotein	LDL

alpha-lipoic acid	LPA
Ruboxistaurin	LY333531
malondialdehyde	MDA
mitochondrial respiratory chain	MRC
3-(4,5-dimethylthiazol-2-yl)-2,5-diphenyltetrazolium bromide	MTT
N-acetylcysteine	NAC
N-acetyl-p-benzoquinone imine	NAPQI
nerve blood flow	NBF
nerve conduction velocity	NCV
nitric oxide	NO
NAD(P)H:quinone oxidoreductase	NQO1
nuclear factor erythroid 2-related factor 2	Nrf2
oxidative stress	OS
poly(ADP-ribose) polymerase	PARP
phosphatidylinositol-3 kinase	PI3K
protein kinase C	PKC
peripheral neuropathy	PN
peripheral nervous system	PNS
ubiquinol	Q
ubiquinone	QH_2

receptor for advanced glycation end products	RAGE
randomized control trial	RCT
reactive oxygen species	ROS
sorbitol dehydrogenase	SDH
deacetyl silent information regulator 2/sirtulin 1	SIRT1
superoxide dismutase	SOD
soluble advanced glycation end products	SRAGE
tricarboxylic acid	TCA
uncoupling protein-1	UCP-1
vascular endothelial growth factor	VEGF

ABSTRACT

Author: Stochelski, Mateusz, A. PhD
Institution: Purdue University
Degree Received: August 2018
Title: Regulation of the Endogenous Antioxidant Defense System in Diabetic Peripheral Neuropathy.
Major Professor: John R. Burgess

Oxidative stress is implicated as a major contributor to the development of diabetes induced peripheral neuropathy. This debilitating condition significantly impacts the quality of life of patients, yet available treatment options are not optimal. They include tricyclic antidepressants, anticonvulsants, serotonin-norepinephrine reuptake inhibitors, selective serotonin reuptake inhibitors, and opiates. Unfortunately, these treatment options only reduce pain by 30-50%, and many patients discontinue use due to side effects. Furthermore, the current treatment options are focused on pain reduction, but not the protection of the peripheral nerves. Since oxidative stress driven by high glucose concentrations has been implicated as the key factor causing peripheral neuropathy, these studies focused on reducing or increasing protection against oxidative stress using dietary compounds with antioxidant properties to ameliorate diabetic peripheral neuropathy. Two dietary compounds with very different mechanisms of antioxidant protection were explored in detail, N-acetylcysteine (NAC) and 3H-1,2-dithiole-3-thione (D3T). To model diabetic peripheral neuropathy, differentiated SH-SY5Y cells were used and stressed with advanced glycation end products (AGE), which form as a result of high glucose concentrations *in vivo* and cause oxidative stress. In our initial studies, we showed that NAC conferred complete protection against AGE-induced neurite degeneration via a glutathione-mediated mechanism. These studies showed that maintenance of glutathione is critical for neurite structure, as inhibition of glutathione synthesis under non-stressed conditions resulted in significant neurite degeneration. Our next focus

was on D3T, a potent nuclear factor (erythroid-derived 2)-like 2 (Nrf2) inducer. D3T generates its antioxidant effect though upregulation of endogenous cellular antioxidant defenses. Previous studies from our lab have shown that D3T treatment paradoxically exacerbates AGE-induced damage, and these prior results were confirmed in the present studies. The mechanism by which D3T potentiates damage was extensively studied. The results of the experiments indicated that D3T potentiates AGE-induced oxidative stress via two critical pathways in the cell-based system used. First, D3T upregulated the Nrf2 responsive gene glucose-6-phosphate dehydrogenase (G6PD), leading to increased G6PD protein expression. Increased expression of G6PD resulted in generation of reducing equivalents that are used by NADPH oxidases to generate superoxide. The oxidative stress damage caused by superoxide generation was then amplified by D3T-mediated reduction of glutathione reductase activity, which resulted in low cellular reduced glutathione concentrations and high oxidized glutathione concentrations. In this manner, D3T inhibited the effectiveness of the endogenous antioxidant defense system and led to disruption of the thiol redox state. In the final set of studies, we found that AGE-induced oxidative stress resulted in a significant increase of protein glutathionylation. Because D3T further disrupts the thiol redox state, it conferred no protection against AGE-induced protein glutathionylation. However, NAC, which was completely protective against AGE-induced neurite degeneration, was also able to fully protect against protein glutathionylation under challenged conditions. Based on the combined results, we conclude that maintenance of the thiol redox state is critical for maintaining neurite morphology, and antioxidants such as NAC that protect the thiol redox state will confer neurite protection in pro-oxidative conditions.

CHAPTER 1. LITERATURE REVIEW

1.1 Introduction

The incidence of diabetes mellitus has been on the rise, increasing by approximately 1 million new cases every year [1]. Diabetes mellitus is a disease of poor glycemic control and as a result many patients develop serious and sometimes debilitating complications such as cardiovascular complications, retinopathy, nephropathy, and the major focus of this dissertation, peripheral neuropathy (PN) [2–4]. PN is one of the most common and debilitating complications of diabetes affecting at least 50% of patients [5,6]. Unfortunately, the medications available for these patients come with severe side effects causing many people to discontinue their use [7]. The most effective treatment for PN is a return to normoglycemia, however this is not attainable for the majority of patients [8,9]. Oxidative stress as a result of hyperglycemia has been linked to the pathogenesis of peripheral neuropathy [8]. In the hyperglycemic state there is an increased generation of reactive oxygen species (ROS) [2,10,11]. Prolonged exposure can exhaust the endogenous antioxidant defense mechanisms and lead to cellular dysfunction and/or death. The molecular targets of oxidative stress, lipids, DNA, and proteins are briefly reviewed in this literature review. The major pathways of ROS generation, polyol pathway, protein kinase C pathway, mitochondrial pathway, and advanced glycation end product pathway, are also reviewed in great detail in regard to their contributions to the development of diabetic PN. Because there are so few treatment options and because oxidative stress has been implicated in development and progression of PN, antioxidants have been investigated as potential therapeutic treatments for this disease. Here we review four antioxidants that show particular promise, with a focus on cruciferous vegetable constituent 3H-1,2-dithiole-3-thione, and the commonly used supplement N-acetylcysteine.

1.2 Overview of the Prevalence of Diabetes and Complications

Diabetes mellitus, a disease hallmarked by hyperglycemia, is one of the most common chronic diseases worldwide and new diagnoses are on an upward trajectory [1]. Data from the Centers for Disease Control and Prevention (CDC) is startling. In the span of just two years the incidence of diabetes in the US population increased by one percent, amounting to 2.2 million new cases. World prevalence in 2010 was estimated to be 6.4% and is projected to increase to 7.7% in 2030 [1]. Type 2 diabetes accounts for nearly 95% of all diagnosed cases, and lifestyle choices such as inactivity have been linked to the risk of development of this disease [12]. With more people beginning to lead a sedentary lifestyle and with approximately 37% of U.S. adults having prediabetes, the upward trajectory of new cases is likely to continue increasing. This poses a major problem for the healthcare field, as the direct medical costs for treating diabetics in 2012 was a staggering $ 176 billion [13]. With diabetes on the rise, it is important to investigate the possible consequences of poor glycemic control.

1.3 Complications Due to Poor Glycemic Control

1.3.1 Cardiovascular Complications

Cardiovascular complications are the leading cause of diabetes related deaths, and hyperglycemia induced oxidative stress plays a key role in promoting a proatherogenic environment. In diabetic patients, atherosclerosis occurs earlier and is more aggressive compared to nondiabetics [2]. The major sources of ROS generation in the hyperglycemic state include: polyol pathway upregulation, protein kinase c (PKC) activation, the mitochondria, and the formation of advanced glycation end products (AGEs) [14,15]. Studies have shown that the hyperglycemic state can lead to increased endothelial NADPH oxidase activity and a resultant increase in superoxide production [2,10,11]. Increased superoxide concentrations can lead to

depletion of nitric oxide (NO) via oxidation to peroxynitrite, which can induce cardiac remodeling by activation of matrix metalloproteinases and promote necrotic and apoptotic cell death [2,16]. A decrease in NO also leads to inhibition of vasodilation and blood flow abnormalities. This effect is magnified by the upregulation of endothelin-1, a potent vasoconstrictor, which is induced by upregulation of PKC in the diabetic state [15,16]. Peroxynitrite and other ROS may also oxidize insulin receptors on peripheral tissue, further contributing to the insulin resistance observed in diabetes [16]. Furthermore, buildup of peroxynitrite can lead to oxidation of tetrahydrobiopterin, which promotes endothelial nitric oxide synthase (eNOS) uncoupling [2]. Uncoupled eNOS can then transfer electrons to and oxidize molecular oxygen, further increasing superoxide concentrations [2]. High levels of ROS in the vasculature have been suggested to be responsible for increased oxidation of low-density lipoprotein (LDL) [2]. The hyperglycemic condition has been shown to promote lipoprotein lipase synthesis in macrophages, which further promotes lipoprotein accumulation in the vasculature [17]. Macrophages then take up and store oxidized LDL and become foam cells, which leads to an inflammatory state and progression of plaque buildup that is characteristic of atherosclerosis [2,17,18]. Increased oxidative stress can also result in microvascular complications which can contribute to the development of retinopathy, nephropathy, and neuropathy.

1.3.2 Diabetic Retinopathy

Diabetic retinopathy is the leading cause of blindness in adults and is caused by damaged microvasculature in the retina [3]. Prevalence of retinopathy in diabetics increases with the duration of the disease and reaches 90% after 25 years [19]. A prolonged hyperglycemic assault on the retinal microvasculature causes endothelial cell damage and leaky tight junctions that lead

to retinal swelling [19]. Damaged endothelial cells cause further damage to the retina by blocking blood flow in capillaries leading to ischemia [3]. To overcome decreased blood flow, new capillaries begin to form [3]. However, without support, this ultimately leads to the detachment of the retina [3]. The retina is especially susceptible to oxidative injury because it has the highest glucose oxidation and oxygen consumption relative to other tissue [20]. Cell culture models have shown an increase in mitochondrial superoxide accumulation in retinal cells [21] and DNA and lipid peroxidation are observed in the retina under hyperglycemic conditions [3]. Sources of ROS generation in the retina are the same major sources linked to the general hyperglycemic state. Endogenous antioxidant defenses can be compromised in the diabetic state. For example, defects in gamma-glutamyl transpeptidase [22] result in a decrease of the antioxidant glutathione (GSH) [23] in the retina under hyperglycemic conditions leaving it more susceptible to oxidative injury.

1.3.3 Diabetic Nephropathy

Another leading microvascular complication commonly seen in diabetics, nephropathy, has a 25% incidence in patients with type 2 diabetes for 10 years [4]. Diabetic nephropathy is also the leading cause of end stage renal disease and is associated with increased cardiovascular mortality [4,24]. In the hyperglycemic state, glomerular mesangial cells have been shown to poorly regulate their intracellular glucose concentrations [25]. These cells are vital for glomerular capillary structure and for glomerular filtration via smooth muscle activity. In diabetic nephropathy these cells are damaged, and oxidative stress is a major factor [24]. The major pathways of ROS generation are upregulated in the glomerular microvasculature [24]. Markers for oxidative stress are increased in diabetic patients with glomerular hyperfiltration, the first phase of diabetic nephropathy [26]. Glomerular basement membrane thickening, a later

phase of diabetic nephropathy, has been linked to accumulation of AGEs and the corresponding decrease in NO availability [24,27]. Oxidative stress has been clearly implicated in the pathogenesis of diabetic nephropathy [24], and treatment with antioxidants in animal models has shown protection against ROS generation in the glomeruli [28].

1.3.4 Diabetic Neuropathy

PN affects at least 50% of diabetic patients, making it one of the most common complications of diabetes [5,6]. Furthermore, patients with prediabetes or metabolic syndrome are at elevated risk for development of PN [5]. Common symptoms of PN include decreased sensitivity in the extremities and burning and shooting pain [29]. Approximately one third of patients with PN experience pain, which begins in the lower limbs and can later spread to upper limbs[29]. It is important to note that symptoms are not a good indicator of the severity of PN and nerve conduction tests should be performed [29,30]. Approximately 15% of diabetics experience foot ulcers and foot ulcers precede lower leg amputations 84% of the time [31]. Patients that do not develop painful PN and experience numbness in the extremities can be particularly susceptible to developing ulcers. Oxidative stress as a direct result of hyperglycemia has been linked to the pathogenesis of PN and the mechanisms will be described in detail in subsequent sections. A thorough understanding of this debilitating condition is essential for developing treatments for patients and improving their quality of life. The most effective treatment for PN is a return to normoglycemia, however this is not an easy nor relatively feasible task for many patients [8,9]. Current treatments for PN include tricyclic antidepressants, anticonvulsants, serotonin-norepinephrine reuptake inhibitors, selective serotonin reuptake inhibitors, and opiates [7]. Unfortunately, these treatments only reduce pain by at most 30-50%, have a bevy of adverse side effects, and in some cases up to 20% of patients simply discontinue

therapy due to negative side effects [7,32]. Therefore, reducing or increasing protection against oxidative stress should be a key focus for ameliorating diabetic complications, and both animal and human studies have shown protective effects with antioxidant therapy.

1.4 Overview of Oxidative Stress and its Molecular Targets

1.4.1 Oxidative Stress

Oxidative stress has been defined as the generation of toxic ROS that disrupts the balance between antioxidants and oxidants in favor of oxidants [33]. Multiple pathways are responsible for the increased generation of ROS in the hyperglycemic state that eventually leads to oxidative stress. ROS such as superoxide, hydroxyl radical, and singlet oxygen are highly reactive due to unpaired electrons in their outer electron shell [34]. These ROS can then react with molecular targets such as proteins, lipids, and DNA [34]. Prolonged exposure can exhaust the endogenous antioxidant defenses, leaving cellular macromolecules susceptible to oxidation and lead to dysfunction and/or cell death.

1.4.2 Lipid Peroxidation

Damage to lipids caused by an imbalance of ROS can lead to cell dysfunction by impairing the selective permeability of the phospholipid bilayer. Lipid peroxidation leads to the formation of peroxyl fatty acid radicals which themselves are unstable and react with other fatty acids in the phospholipid bilayer which promotes a chain of autocatalytic lipid peroxidation [35]. Vitamin E, the major lipophilic antioxidant, is known as a chain breaking antioxidant that can stop this autocatalytic reaction and protect the integrity of the lipid bilayer. Glutathione also plays a major role in protecting the lipid bilayer, as it is a substrate for the enzyme phospholipid hydroperoxide glutathione peroxidase that reduces oxidized lipids [35]. Therefore, depletion of

endogenous antioxidants under oxidative stress conditions can leave the cell susceptible to lipid peroxidation.

1.4.3 DNA Oxidation

Another target for oxidation in a high ROS environment is DNA. The hydroxyl radical and singlet oxygen can react with DNA nucleobases and lead to the formation of 8-hydroxy-2'-deoxyguanosine (8-OH-dG) [36]. Other nucleobases can react with ROS, but 8-OH-dG is the most common and has also been shown to be promutagenic [36]. For these reasons 8-OH-dG is commonly used as a marker for DNA oxidation. Though there is conflicting data in the literature, it has been shown that when base excision repair mechanisms are defective, ROS can directly induce lethality in cell culture models [35]. In studies from our lab, the antioxidants alpha-tocopherol and N-acetylcysteine conferred protection against DNA oxidation in a cell culture model of peripheral neuropathy using SH-SY5Y cells [37].

1.4.4 Protein Oxidation

Proteins are also susceptible to ROS mediated oxidation. The amino acids most subject to oxidation contain either a sulfhydryl group or an aromatic side chain [34]. Methionine, a thiol ether, can be readily oxidized to methionine sulfoxide under oxidative stress [38]. Most organisms express methionine sulfoxide reductase, as methionine oxidation can impact protein function [35,38]. Oxidative stress can also lead to disulfide bond formation, and both thioredoxin and glutaredoxin systems in eukaryotic cells work to reduce protein disulfides [39]. Other amino acids can form carbonyls when oxidized, but unlike thiol oxidation, this is not reversible. Carbonylated proteins can form into toxic aggregates and accumulate overtime [35]. To counter this, carbonylated proteins are ubiquitinated and then degraded by the proteasome [35]. However, the proteasome itself can be inactivated via oxidation, allowing for the buildup of toxic

aggregates in a pro-oxidative environment [35]. The oxidation and inactivation of other antioxidant enzymes such as superoxide dismutase can further disrupt the cellular endogenous antioxidant defense mechanisms and promote a pro-oxidative condition [35].

1.5 Peripheral Neurons and Hyperglycemia

Peripheral nerves are highly susceptible to damage in the hyperglycemic state due to their high expression of the glucose transporter GLUT1[40]. Both neuronal cells and Schwann cells are unable to decrease glucose transport in response to increased blood glucose concentrations [25]. GLUT1 has a very high affinity for glucose and operates at V_{max} under normal blood glucose concentrations (4.4 – 6.1 mM) and hyperglycemic conditions [41]. In mesangial cells, saturation of this transporter has been reported at glucose concentrations of 30-35 mM [41]. Peripheral nerves have also been shown to have low GSH, glutathione peroxidase, and glutathione reductase levels, making them especially susceptible to oxidative stress [42]. Therefore, peripheral nerves, due to their high expression of GLUT1 and low GSH status, would be especially susceptible to hyperglycemia induced damage.

To better understand glucose uptake in the peripheral nervous system (PNS), a solid understanding of glucose uptake physiology is required. According to an extensive review of glucose transport in peripheral nerves by Magnani and colleagues, peripheral nerves have a very high demand for glucose, as it is their major source of energy. In the neuron, the highest energy demands are in nodes of Ranvier, where large amounts of ATP are required for the Na^+/K^+ ATPase. For glucose to enter the neuron, it must first pass both the perineurial diffusion barrier and the blood-nerve barrier in the endoneurium. GLUT1 is highly expressed in these areas. After passing through the endoneurium, glucose still needs to traverse through the Schwann cell and the axolemma itself. Due to the anatomical structures of the Schwann cell and axolemma at the

paranodal region, which makes up the paranodal diffusion barrier, it is believed to be the major site of axonal glucose transport. Glucose is transported across the Schwann cell via GLUT1, however it is not conclusive as to which glucose transporter is responsible for glucose transport across the axolemma. In other lesser energy requiring sections of the axon such as the internode, glucose enters the axon at the Schmidt-Lanterman incisure via GLUT1 mediated transport [40]. In summary, GLUT1 is the major glucose transporter in the peripheral nerve and is highly expressed in the perineurium, endoneurium, and Schwann cells. It is also responsible for axonal glucose uptake at the Schmidt-Lanterman incisures, but a novel glucose uptake pathway may exist at the paranodal region of the axon.

Many studies and reviews that discuss oxidative stress in peripheral neuropathy generalize the condition to the entire peripheral nerve. It is important to note that the peripheral nerve consists of the epineurium, perineurium, endoneurium, Schwann cells, and the neuron (Fig. 1.1). Hyperglycemia induced injury in the PNS can occur in any of these locations *in vivo,* and where the cascade that initiates the development of diabetic PN originates is still a subject of much debate [14]. In a review of the pathogenesis of diabetic PN, Cameron and colleagues stated that even though hyperglycemia has been shown to directly affect the neuron, these effects could be caused by compromised blood delivery [43]. The endoneurium has been shown to be hypo-perfused and hypoxic in the diabetic state, a condition that is secondary to a reduction in nerve blood flow (NBF) and increased endoneurial vascular resistance [44]. Vasodilators such as NO are decreased in the diabetic state, and a strong positive correlation has been shown between correction of endoneurial perfusion deficits and nerve conduction improvements [43]. The pathogenesis of diabetic PN is multi-factorial, and the following sections will cover the major

pathways of hyperglycemia induced oxidative stress and their role in the development of this debilitating diabetic complication.

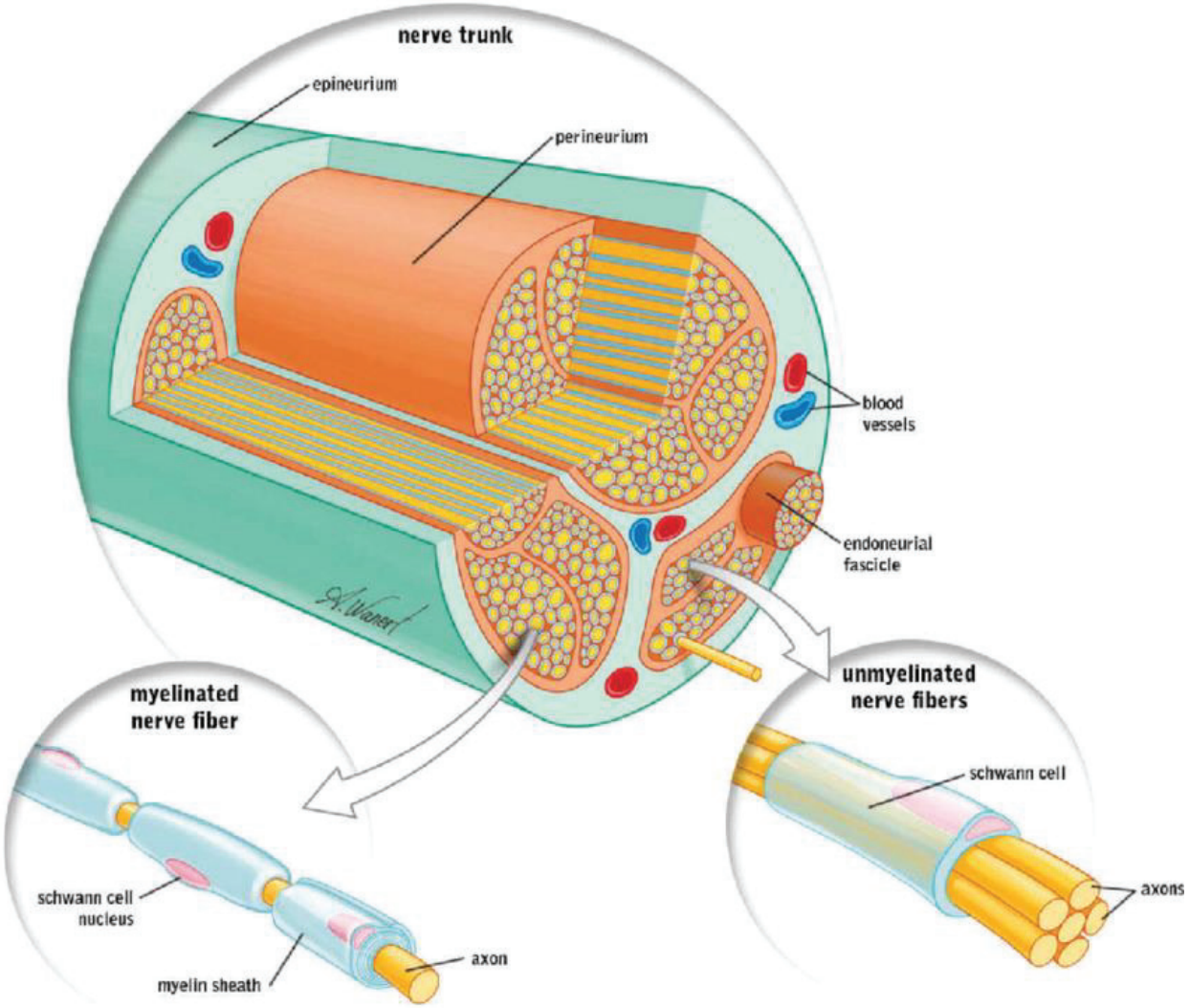

Figure 1.1 Structure of the peripheral nerve.
Reprinted with permission from Taylor & Francis [45].

1.6 Four Major Sources of ROS Generation in Diabetic Peripheral Neuropathy

1.6.1 Polyol Pathway

The role of the polyol pathway in diabetic PN has been extensively studied and reviewed. This pathway consists of two enzymes, aldose reductase (AR) and sorbitol dehydrogenase (SDH)

(Fig. 1.2). AR has a low affinity for glucose, but in the hyperglycemic state glucose flux through this pathway increases [15]. Via an NADPH dependent process, AR then reduces glucose to sorbitol [15]. A large number of studies have been conducted that have identified why increased polyol pathway flux leads to development and progression of diabetic PN, and the Obrosova review provides an excellent summary [46].

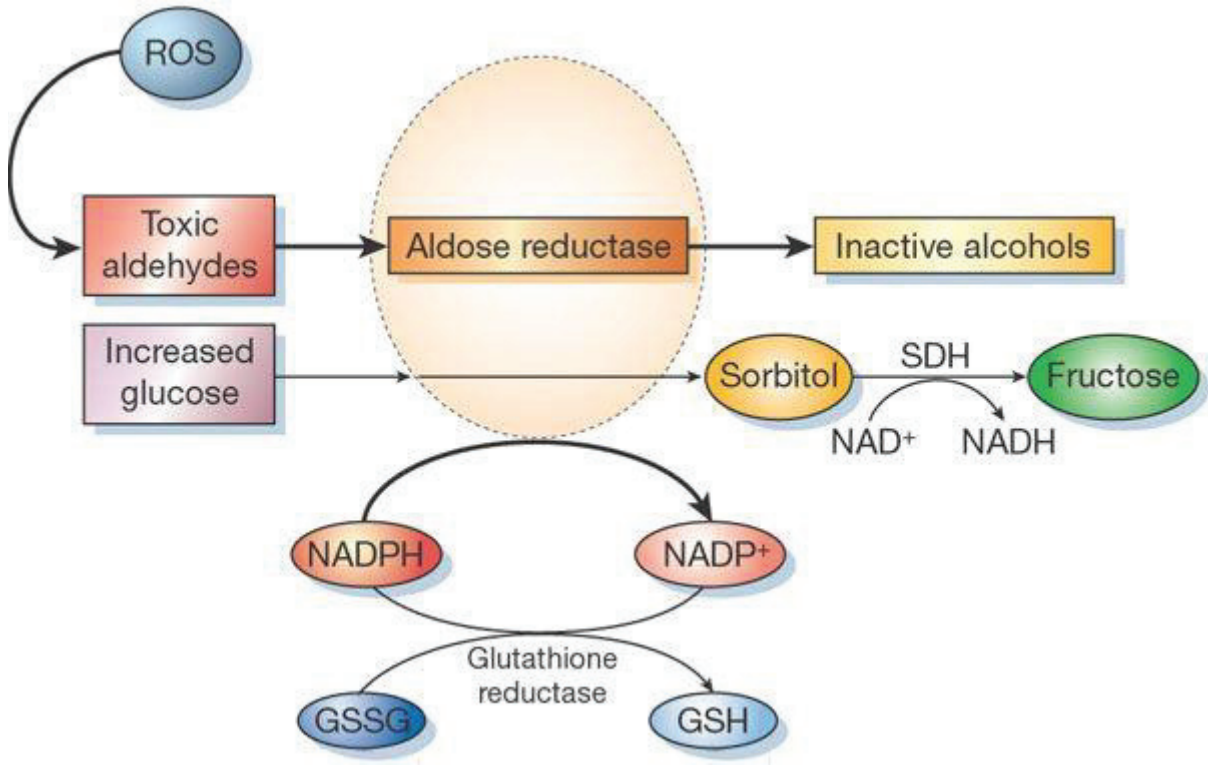

Figure 1.2 Polyol pathway.
Reprinted with permission from Springer Nature and Copyright Clearance Center, Inc. [15].

Increased glucose flux through the polyol pathway leads to increased generation of fructose. Fructose is a ten times more powerful glycating agent compared to glucose which can have the effect of increased formation of AGEs (discussed in detail in subsequent section), activation of the receptor for advanced glycation end products (RAGE), and the downstream

increased production of ROS [46]. Oxidation of sorbitol to fructose by SDH is mediated by reduction of NAD^+ to NADH. An increase in the NADH:NAD^+ ratio can lead to decreased activity of glyceraldehyde-3-phospahte dehydrogenase (GAPDH) [15]. GAPDH catalyzes the formation of 1,3- Diphosphoglycerate from triose phosphate via an NAD^+ dependent mechanism in glycolysis. Inhibition of this enzyme leads to build up of triose phosphate which itself can increase formation of methylglyoxal, a precursor of AGE formation, and diacylglycerol (DAG), a PKC activator [15,47]. SDH inhibitors or mutations however, have not been shown to be protective against development of PN suggesting that AR is the responsible enzyme [43,48,49].

AR reduces glucose to sorbitol via an NADPH dependent mechanism, and as such increased flux through the polyol pathway can deplete cellular NADPH stores [15]. Depletion of NADPH stores would limit the activity of glutathione reductase and increase the ratio of oxidized glutathione (GSSG) to GSH. Depletion of glutathione, the bodies' major biological antioxidant, has been linked to increased intracellular oxidative stress and diabetic complications [43,50]. Animal studies have shown promising effects in both the use of AR inhibitors and AR knockout.

Studies done on diabetic rats have shown that diabetes leads to a decrease in total nerve GSH, an increase in buildup of nerve malondialdehyde (MDA), a decrease in nerve conduction velocity (NCV), and a decrease in NBF [49]. Treatment with AR inhibitor restores GSH loss, counters superoxide production in the vasa nervorum, corrects NBF deficits, and prevents elevation of nerve MDA [46,49]. The AR inhibitor Fidarestat was also able to correct motor and sensory never conduction velocity in a dose dependent fashion in a diabetic rat model [46,51]. Furthermore, Chung and colleagues developed an AR gene knockout mouse model. Under diabetic conditions, wild-type mice had significantly depleted nerve GSH levels and decreased

NCV. Under these same conditions, AR null mice were able to maintain normal GSH levels, and there was no change in NCV [48]. These results clearly implicate AR as a major contributor of oxidative stress and nerve function impairment that is seen in diabetic peripheral neuropathy. Human studies however, have had mixed results.

It is reported that patients with diabetes on average experience an approximate 0.5m/s drop in NCV [52]. In a 60-week study of the AR inhibitor Ranirestat, a 20mg/day dose decreased sorbitol levels by 83.5% and had a significant effect on increasing NCV in peroneal motor, right sural, and proximal median sensory nerves. Peroneal motor and right sural NCV improved by ~1m/s whereas the proximal median sensory nerve saw an improvement of 3.4 m/s [53]. However, this study was not placebo controlled, and a follow up placebo-controlled study was performed by the same group. In the follow up study, 20 mg/day Ranirestat showed similar improvement to peroneal motor NCV. Sensory nerve function was not improved compared to placebo, but this was largely due to an overall increase in NCV in the placebo group [54]. The authors attributed this to lifestyle modifications of the patients in the study. Another study using a different AR inhibitor, Zenarestat, at dosages decreasing sorbitol levels by more than 80% increased small-diameter sural nerve myelinated fiber density [53,55]. AR inhibitors have shown promise for patients with diabetic PN, but further follow up studies should be conducted to better ascertain the clinical efficacy of AR inhibitors.

1.6.2 PKC Pathway

PKC overactivation has also been linked with the development of diabetic PN, so a brief overview of activation and the downstream targets is warranted [56]. There are at least 11 isoforms of PKC, with 9 activated by DAG [15]. Hyperglycemic conditions promote *de novo* synthesis of DAG in vascular tissue due to increases in glycolytic pathway intermediates. *De*

novo synthesis of DAG requires glycolytic intermediate triose phosphate and stepwise acylation catalyzed by glycerol-3-phosphate acyltransferase and monoacylglycerol-3-phosphate acyltransferase [57]. The hyperglycemic state has been shown to increase activity of the polyol pathway, with as much as 30% of glucose shunted through this pathway [48]. Increased activity of SDH can lead to a depletion of cellular NAD^+ and suppressed activity of GAPDH[15]. Suppressed activity of GAPDH in the glycolytic pathway will lead to build up of triose phosphate, and as such can contribute to the increase in DAG seen in the hyperglycemic state. The interaction between the polyol and PKC pathways is shown in Figure 1.3.

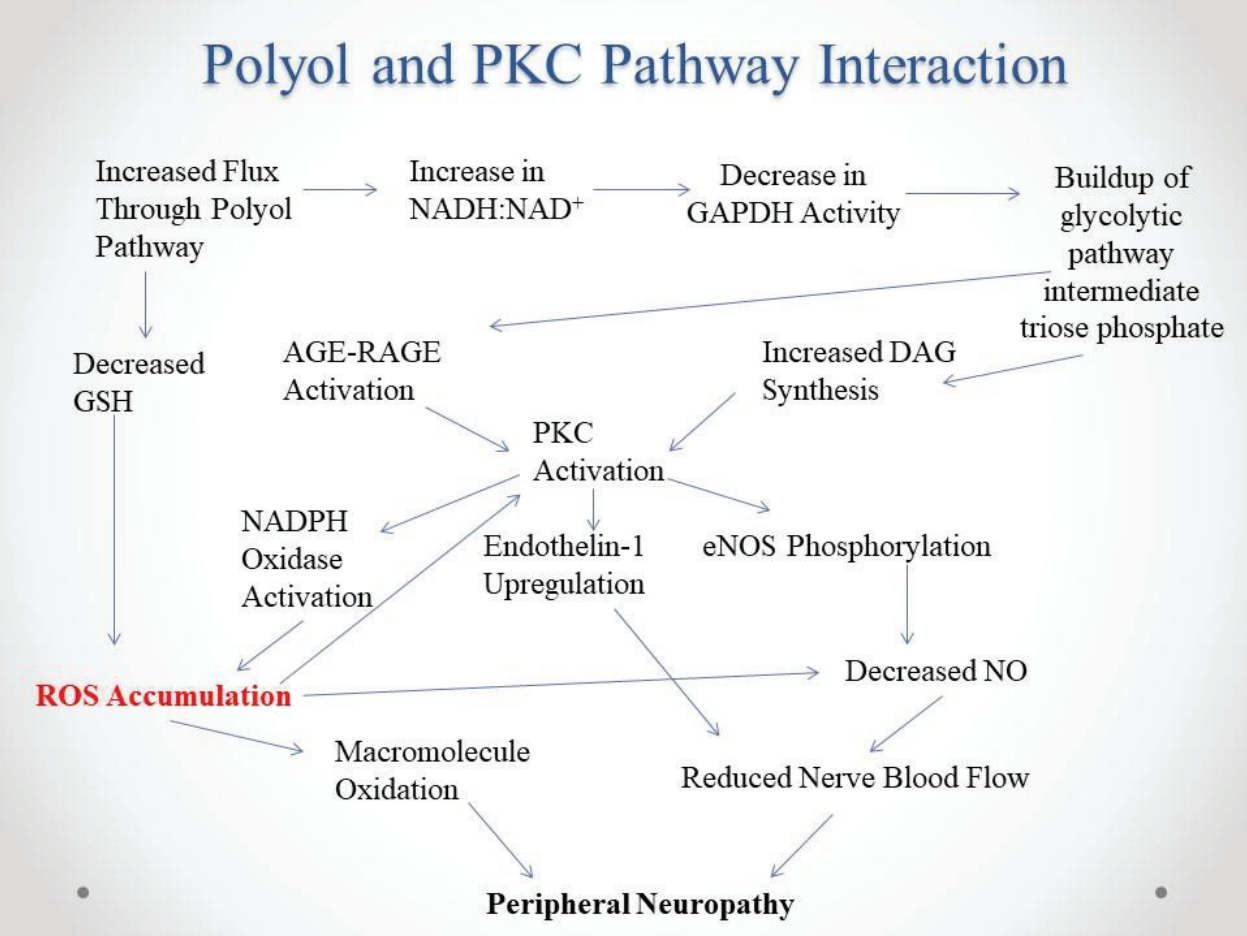

Figure 1.3 Polyol and PKC pathway interaction.

Of all the isoforms of PKC, PKC-β has gathered the most attention with regards to the development of diabetic PN. Overactivation of PKC-β has been associated with diabetic PN mainly through dysregulation of the microvasculature [56]. Upregulation of PKC-β has been linked with inhibition of eNOS and upregulation of endothelin 1 (ET-1), vascular endothelial growth factor (VEGF), and NADPH oxidase [58]. Phosphorylation of eNOS leads to a decrease in NO production, leading to blood flow abnormalities due to inhibited vasodilation [15,59]. This effect is multiplied by increased expression of ET-1, a powerful vasoconstrictor [58]. Increased VEGF expression can promote vascular permeability [15], and PKC activation in diabetes has been linked with increased permeability of endothelial cells to macromolecules [58]. Upregulation of NADPH oxidase leads to an increase in generation of superoxide which can promote formation of peroxynitrite, leading to uncoupling of eNOS and decreased NO availability. PKC activation of NADPH oxidase is linked to the AGE-RAGE pathway that will be discussed in a later section. Taken together, these effects lead to a decrease in nerve perfusion and oxygenation which can lead to nerve damage and neuropathy.

The role for PKC-β in the development of diabetic PN, however, has been disputed. Early studies showed that PKC activity was decreased in the diabetic peripheral nerve and corresponding DAG was also shown to be decreased [60,61]. In a more recent study specifically looking at the neovasculature of diabetic rats, the authors found that the PKC-β inhibitor LY333531 (Ruboxistaurin) was able to correct nerve dysfunction. In diabetic animals, endoneurial blood flow was reduced by approximately 50%, and motor and sensory NCV was reduced by 19.7% and 13.9%, respectively. A high dose of LY333531 (10 mg kg^{-1} day^{-1}) was able to completely reverse both the endoneurial blood flow and decrease in NCV [59]. This data supports other studies that have been done on PKC inhibitors that show improvement in NBF

and NCV in diabetic rats [49]. Further evidence supporting that PKC-β promotes diabetic PN via a neurovascular method comes from a study using a nitric oxide synthase inhibitor. This inhibitor attenuated the protective effects of PKC inhibition on diabetic rat peripheral nerves [62]. PKC-β has been shown to be tyrosine phosphorylated by H_2O_2 treatment in a cell culture model of monkey kidney cells [63]. Other studies have implicated oxidative stress and oxidized LDL in PKC stimulation [49,64]. These other methods of activation are of importance because some studies have shown that DAG concentrations are decreased in diabetic peripheral nerves [65].

Though PKC-β inhibition has shown improvements in neurovascular blood flow and sensory and motor nerve conduction, human studies have at best shown a trend towards significance. A recent systematic review was conducted on randomized control trials (RCTs) for Ruboxistaurin. Of the six reviewed RCTs, four studies reported significant improvements in the neurological total symptoms score. Vibration detection threshold was only measured in one study and showed minor improvements in a subgroup of patients with clinically significant symptoms. Importantly, out of four studies that measured C-fiber mediated skin microvascular blood flow, three studies showed a significant increase from baseline after Ruboxistaurin treatment. The authors concluded that even though treatment did show some benefits, there was not enough data available to make any conclusions [66]. In future studies, it may be of interest to co-treat patients with both Ruboxistaurin and antioxidants such as vitamin E and alpha-lipoic acid (LPA). Co-treatment with a low dose of Ruboxistaurin and vitamin E or LPA in diabetic rats completely corrected both endoneurial blood flow and NCV. Without co-treatment with antioxidants, only ~20% improvement was observed [59]. The possible mechanism of action for antioxidants could be that they protect against the buildup of superoxide and eNOS uncoupling,

thus preventing peroxynitrite formation and NO depletion. Furthermore, vitamin E should be of vital interest due to its ability to lower DAG levels by stimulating DAG kinase [49,59].

1.6.3 Mitochondrial Pathway

Hyperglycemia also induces mitochondrial ROS generation. To better understand mitochondrial ROS generation, a brief overview of the electron transport chain is warranted. In glycolysis, glucose oxidation yields the formation of pyruvate and generation of NADH. Pyruvate can then be transported to the mitochondria and enter the tricarboxylic acid cycle (TCA). Pyruvate oxidation then yields NADH (4) and $FADH_2$ (1) electron donors. At complex one, NADH transfers two electrons to ubiquinol (Q) and reduces it to ubiquinone (QH_2). QH_2 then leaves complex one and enters the interior of the membrane. This cycle leads to pumping of four protons out of the mitochondria and into the cytosol. Complex two also generates QH_2, but the electrons are initially donated from $FADH_2$. Electrons from QH_2 are then transferred to complex three. At complex three (ubiquinol:cytochrome c oxidoreductase) electrons are transferred to cytochrome c by the ubisemiquinone radical generating Q cycle [67]. Four protons are transferred to the cytosol, two from QH_2, and two directly from the matrix. At complex four (cytochrome c oxidase), cytochrome c is oxidized and electron transfer proceeds to molecular oxygen resulting in the release of water. This electron transport process creates a proton concentration that is much lower in the matrix, generating an electric field with the matrix side being negative. The proton gradient is crucial for ATP generation at complex five (ATP synthase). Figure 1.4 illustrates the electron transport chain.

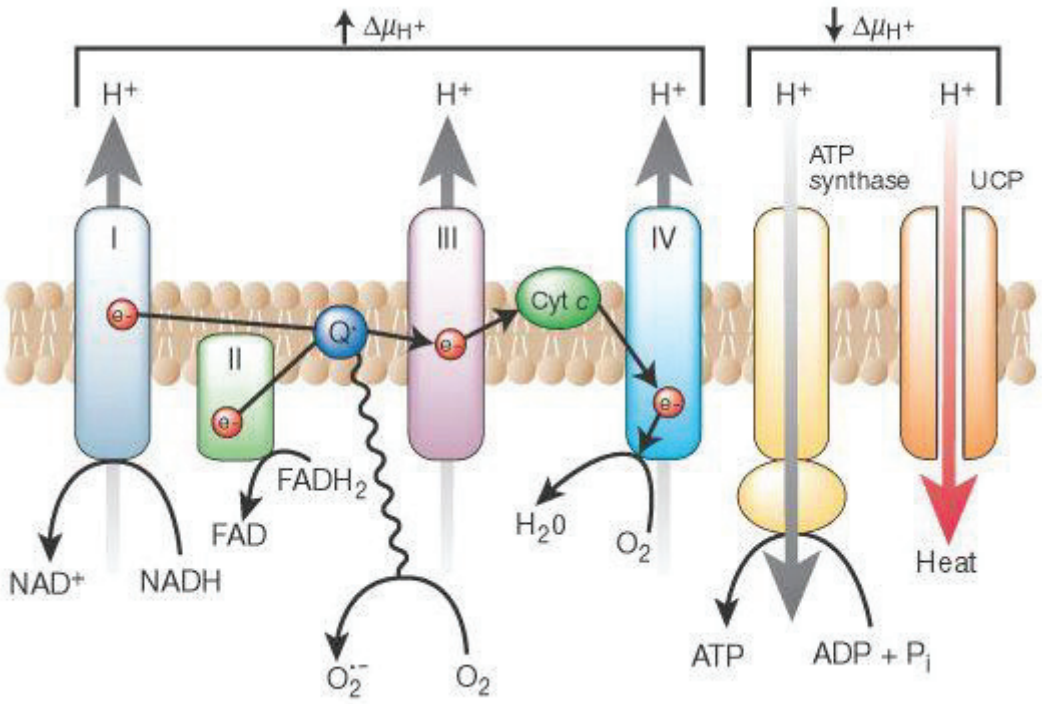

Figure 1.4 The electron transport chain.
Reprinted with permission from Springer Nature and Copyright Clearance Center, Inc. [15].

Hyperglycemia induces perturbations in glycolysis that lead to increased transport of pyruvate into the mitochondria and an increase of TCA derived electron transporters (NADH and $FADH_2$). An increase of these electron transporters increases the efflux of protons into the cytosol (10 protons per electron pair from NADH, 6 for $FADH_2$) and generates a high electrochemical gradient. When the electrochemical gradient is high it increases the life of superoxide generating electron transport intermediates such as ubisemiquinone [67]. Overexpression of Mn superoxide dismutase (SOD), uncoupling protein-1 (UCP-1), and treatment with chlorophenylhydrazone (CCCP) (an uncoupler of oxidative phosphorylation that abolishes the proton gradient) all prevent hyperglycemia induced intracellular ROS production in bovine aortic endothelial cells [67].

It has been proposed that mitochondrial superoxide production in the hyperglycemic state is the initiating event for activating mechanisms such as polyol pathway, PKC activation, and AGE formation that lead to progression of diabetic complications [15]. Brownlee and colleagues were able to show that disrupting oxidative phosphorylation with CCCP, decreasing the electrochemical gradient by upregulating UCP-1, and decreasing mitochondrial ROS by upregulating MnSOD prevented activation of all three mechanisms [15,67]. They proposed that the mechanism linking all these pathways of hyperglycemia induced damage is hyperglycemia induced GAPDH inhibition. The authors claim that GAPDH activity under these conditions is suppressed because increased mitochondrial ROS production induces DNA damage and activates poly(ADP-ribose) polymerase (PARP). PARP can then make polymers of ADP-ribose which accumulate on GAPDH and prevent its activity [68]. Inhibition of GAPDH could lead to increased glucose shunted through the polyol pathway, and the increase in triose phosphate can lead to increased DAG production and PKC activation, and AGE formation from methylglyoxal [15]. In cultured aortic endothelial cells, GAPDH inhibition elevated the three pathways of hyperglycemic damage to the same extent as hyperglycemia [68,69]. Mitochondrial generation of ROS may be a unifying mechanism for ROS generation under hyperglycemic conditions in endothelial cells, but recent studies on DRG neurons isolated from diabetic rats suggest there may be other mechanisms.

A thorough review of mitochondrial dysfunction in sensory neuropathy was recently written by Fernyhough *et al* [70]. In brief, mitochondrial respiratory chain (MRC) activity was analyzed in DRG neurons of diabetic rats. Interestingly, at 22 weeks of diabetes there was a significant decrease in MRC activity. Gene expression studies confirmed this phenomenon by showing that components of both complex I and complex IV were downregulated. In vitro

studies using sensory neurons from diabetic rats showed that the mitochondria of diabetic axons are more depolarized compared to control cells. A decrease in generation of the electrochemical gradient will decrease energy production through complex V. Further studies confirmed that the decrease in mitochondrial function correlated with decreased ROS production in diabetic mitochondria axons compared to control. The authors concluded that though there is an increase in ROS production in diabetic axons, the likely source is not the mitochondria. However, the observed decrease in ATP production is an important factor to consider in PN, as it decreases excitation, axonal transport, and growth cone motility [70].

1.6.4 AGE Pathway

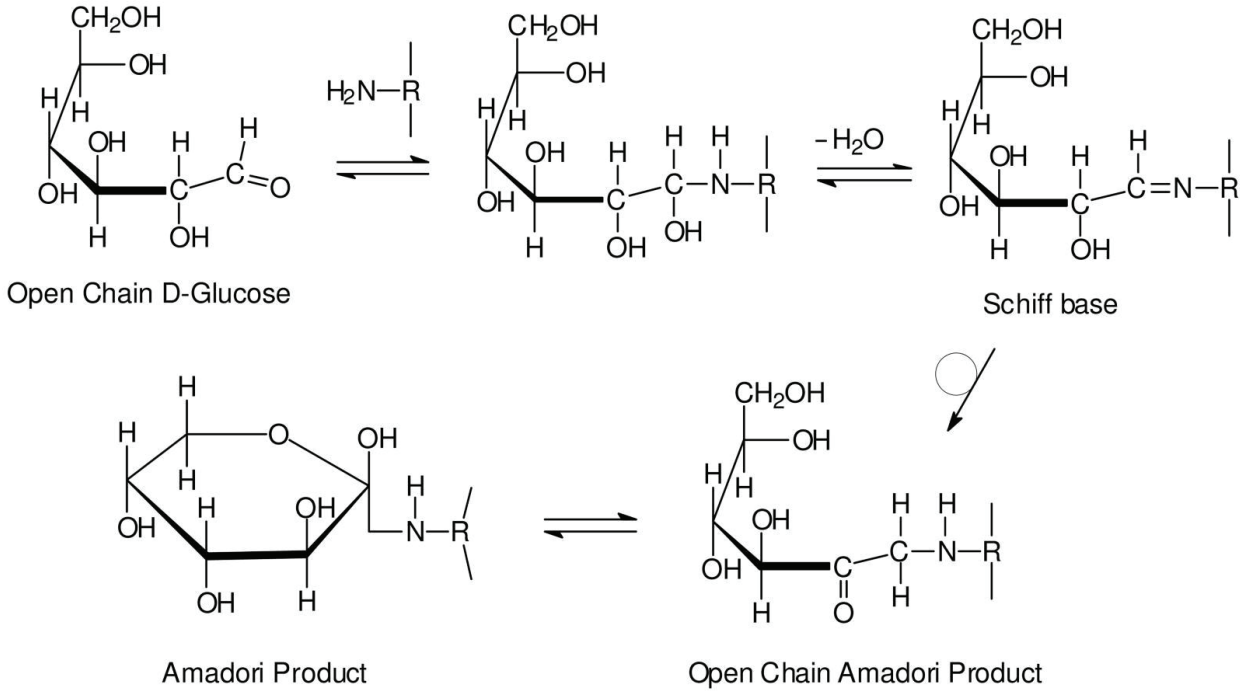

Figure 1.5 Formation of Amadori products.
Reprinted with permission from the American Chemical Society [71].

Another pathway commonly linked with the progression of diabetic PN is the formation of AGEs and their interaction with receptors such as RAGE. For an extensive review of AGE synthesis, the Nessar Ahmed review is a great source [72]. In the classical AGE pathway, glucose or other reducing sugars such as fructose react with a free amino group on a protein forming an unstable Schiff base. The Schiff base then degrades into a more stable Amadori product (Fig. 1.5) which with further rearrangement, oxidation, and elimination leads to the formation of AGEs [73]. Reactive dicarbonyls also contribute to AGE synthesis, especially in the diabetic condition [73]. As was discussed previously, a decrease in GAPDH activity is observed under hyperglycemic conditions. As a direct result of hyperglycemia, more glucose is shunted through the polyol pathway, leading to an increase in fructose. Fructose is more reactive than glucose, and elevated levels lead to AGE synthesis [72,73]. There is also a build-up of triose phosphate which leads to increased conversion to methylglyoxal, a reactive dicarbonyl. Reactive dicarbonyls are gaining traction as one of the main mechanisms driving AGE synthesis as they are 20,000 times more reactive than glucose [73]. In the diabetic state there is a significant increase in both dicarbonyl and AGE synthesis, as well as AGE accumulation in the peripheral nerves (axoplasm, Schwann cells, endoneurial and epineurial microvessels, perineurial basal lamina, and perineurium) [73,74].

In the peripheral nerve, RAGE is localized in the microvasculature and on the axons themselves. Experiments done on mice have shown the importance of RAGE in the development of diabetic complications. RAGE knockout mice were partially protected from diabetes induced pain perception loss. Wild type animals treated with soluble RAGE (sRAGE) showed similar results. RAGE knockout mice were also protected from increased activation of PKC-β and NF-Kβ pathways [46]. In rats the use of an inhibitor of AGE formation, pyridoxamine, reversed

diabetes induced decrease in NBF and motor and sensory NCV [46]. The AGE-RAGE axis has clearly been implicated with the progression of diabetic PN in animal models; therefore, a further look into the mechanism of action of this axis is warranted.

To elucidate the mechanism of action of the AGE-RAGE axis, Vincent *et al* first isolated dorsal root ganglia (DRG) from Sprague Dawley rats. RAGE was shown to be localized throughout the entire neuron. DRG neurons were then treated with the RAGE ligand S100, which lead to a significant increase in ROS production. Cells that were incubated with sRAGE or an antibody to rage (Ab-RAGE), which prevents RAGE from binding to ligands, showed a 70% and 80% decrease in ROS formation, respectively. NADPH oxidase was upregulated with the activation of RAGE, accounting for the observed increase in ROS. NADPH oxidase upregulation was inhibited with both sRAGE and Ab-RAGE treatment. The authors concluded that RAGE activates NADPH oxidase via a phosphatidylinositol-3 kinase (PI3K)/ protein kinase B (Akt) pathway. However, activation of Akt alone was not sufficient to increase NADPH oxidase activity, suggesting further downstream mechanisms of activation [75].

Studies done on endothelial and mesangial cells have shed more light on establishing a pathway of NADPH oxidase activation. In both an animal model of diabetic nephropathy and cell culture model using primary rat mesangial cells, Thallas-Bonke *et al* observed that inhibition of PKC-α had similar results to apocynin inhibited NADPH oxidase in preventing cytosolic ROS generation. PKC-α likely phosphorylates $p47^{phox}$ which allows for the assembly and activation of NADPH oxidase [76]. In endothelial cells it has been shown that PKC-ζ is responsible for phosphorylating $p47^{phox}$, and that the upstream activation of PI3K is critical in the activation of NADPH oxidase [77]. This pathway may be the missing step that was observed in the Vincent *et al* study in DRG neurons. Further studies done on bovine retinal endothelial cells (BRECs)

confirmed that AGE treatment enhanced ROS generation. It was also observed that $p47^{phox}$ was activated and translocated to the membrane from the cytosol after AGE treatment (Fig. 1.6). Inhibition of NADPH oxidase with apocynin prevented the increase in ROS generation. Use of PKC-β inhibitor LY379196 also completely prevented ROS production and $p47^{phox}$ translocation [78]. These studies confirm that the AGE-RAGE axis plays a key role in ROS generation, and that ROS is generated by NADPH oxidase activated by PKC. Future studies will need to be done on peripheral nerves to confirm that these pathways are also specific to the nerve vasculature and to neurons and axons themselves.

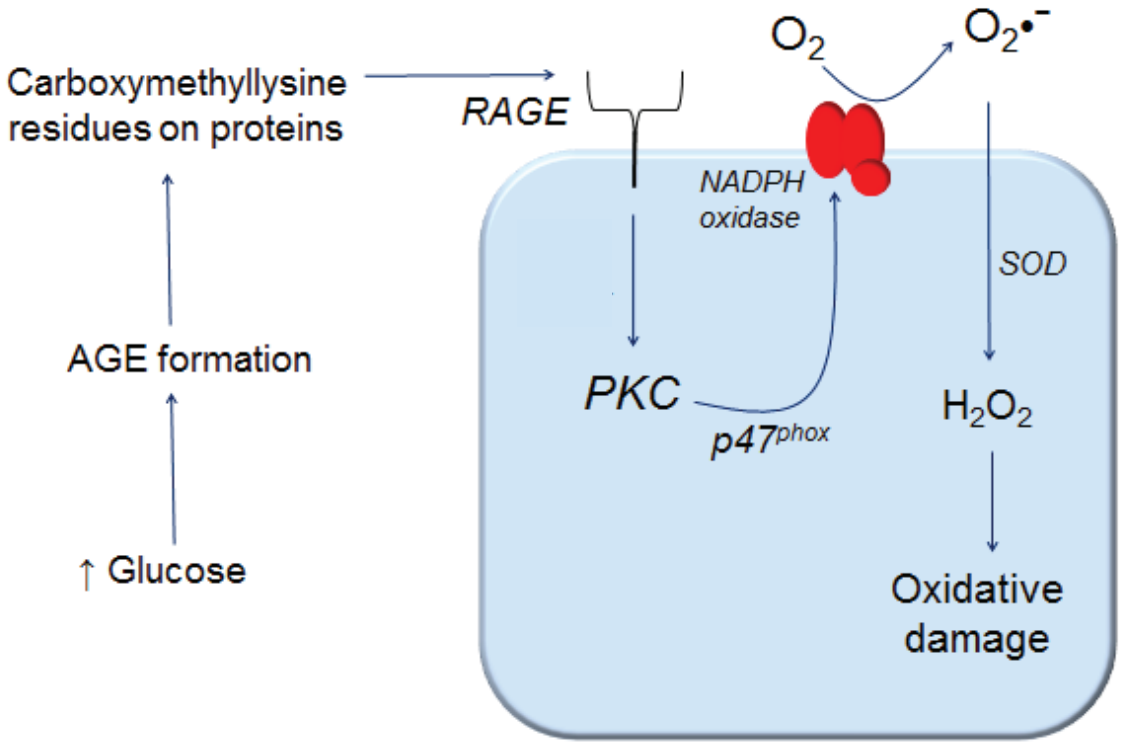

Figure 1.6 AGE-RAGE-mediated activation of NADPH oxidase.

The AGE-RAGE axis may be especially critical in the generation of ROS and subsequent development of diabetic PN because of the link to NF-Kβ. Activation of RAGE leads to

intracellular signaling and activation of NF-Kβ [79]. Translocation of NF-Kβ to the nucleus induces expression of many genes including ET-1, one of the most potent vasoconstrictors, and RAGE itself [80]. NF-Kβ is also redox sensitive [67,74,80] and activation can lead to increased RAGE expression which can lead to increased activation of the AGE-RAGE axis and ROS generation. This creates a positive feedback loop and prolonged NF-Kβ activation that overwhelms the endogenous autoregulatory feedback inhibition loop [79]. Prolonged NF-Kβ activation leading to increased ET-1 expression can also contribute to endothelial cell dysfunction and be partly responsible for the observed decrease in endoneurial blood flow that is seen in diabetic PN [80]. Since NF-Kβ is also a regulator of many apoptotic genes such as Fas-Ligand, it is possible that prolonged activation may also directly lead to apoptosis [81]. Therefore, intracellular signaling initiated by activation of the AGE-RAGE axis plays a critical role in the development of diabetic PN.

1.6.5 Summary of ROS Generating Pathways

All of the ROS generating pathways described in this literature review are interconnected and can activate each other in a variety of different ways. As an example, the hyperglycemic state leads to more glucose being shunted through the polyol pathway as well as more pyruvate entering the mitochondria. In the mitochondria this can lead to a disruption of the electrochemical gradient, and as a consequence increased ROS generation. Increased activity of AR can deplete NADPH stores and limit the activity of glutathione reductase. Further oxidation of sorbitol to fructose would increase the NADH:NAD^+ ratio which could decrease the activity of GAPDH. The resulting buildup of triose phosphate would lead to increased synthesis of AGEs. Activation of the AGE-RAGE axis would lead to downstream activation of PKC, which would then activate NADPH oxidase and promote further ROS generation. Increased ROS and

reduced activity of glutathione reductase would increase the GSSG:GSH ratio, impairing the endogenous antioxidant defense of neurons and making them more susceptible to macromolecule oxidation. Returning to normoglycemia would reduce ROS generation through these interconnected pathways, but because this is not readily achievable for many patients it is important to look at alternative treatments.

1.7 Potential Therapeutic Antioxidants

1.7.1 Lipoic Acid

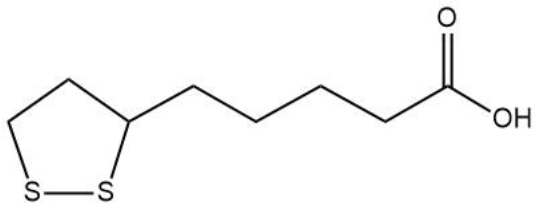

Figure 1.7 Structure of lipoic acid.

Lipoic acid (LPA) is a potent thiol antioxidant that plays a key role in the antioxidant network. When vitamin E becomes oxidized, it can be reduced back by vitamin C. Oxidized vitamin C can then be reduced back to its reduced form by GSH. In the mitochondria, LPA can be further reduced to dihydrolipoate by lipoamide dehydrogenase. Dihydrolipoate is a powerful reductant that is capable of direct scavenging of radicals, regenerating vitamins E and C, increasing potency of the entire redox antioxidant network, and upregulating levels of GSH [82]. Endothelial cells treated with AGE showed a 64% reduction in GSH levels and dramatic reduction in reduced ascorbic acid. The increased oxidative stress was shown to activate NF-Kβ. Treatment with LPA restored intracellular GSH and reduced ascorbic acid levels as well as prevented nuclear translocation of NF- Kβ [80]. In diabetic rats with PN, LPA treatment

significantly improved sensory NCV, endoneurial nutritive NBF, GSH levels, and normalized the GSH:GSSG ratio [83]. Most importantly, the protective results of LPA treatment have also been observed in humans. LPA has been shown to improve neuropathic symptoms in patients with diabetic PN in multiple studies [84–86].

1.7.2 Resveratrol

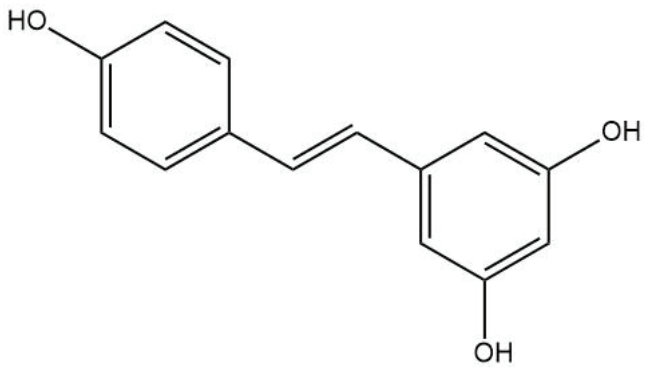

Figure 1.8 Structure of resveratrol.

Resveratrol is gaining traction as a neuroprotectant because it has been shown to be an effective hydroxyl and superoxide radical scavenger [87]. Resveratrol has also shown protection against ROS-induced lipid peroxidation and DNA damage [87]. Resveratrol, through deacetylase silent information regulator 2/sirtuin 1 (SIRT1), also upregulates MnSOD and increases cellular GSH levels in endothelial cells [88]. SIRT1 also protects against GAPDH translocation from the cytosol to the nucleus [89]. GAPDH normally resides in the cytosol, but is translocated to the nucleus after apoptotic stimulation [90]. Here it regulates acetylation and subsequent activation of proteins such as p53 that are part of the apoptotic cascade [89]. In the axons of diabetic neurons, mitochondrial activity is decreased, and the AMP/ATP ratio begins to rise. AMP-activated protein Kinase (AMPK) is a sensor for high AMP levels that becomes phosphorylated

under these conditions. It can then enhance mitochondrial function to increase ATP production. DRG sensory neurons of diabetic rats have depressed AMPK signaling. Treatment with resveratrol was able to cause direct activation of AMPK and normalize thermal sensitivity [70]. In another study, resveratrol treatment of rats with diabetic PN significantly improved motor NCV, NBF, and decreased thermal hyperalgesia [91]. Clinical trials in diabetic patients with PN have not been done on resveratrol, but this would be the logical next step given the positive results seen in animal models.

1.7.3 3H-1,2-dithiole-3-thione (D3T)-Upregulation of the endogenous antioxidant defense system

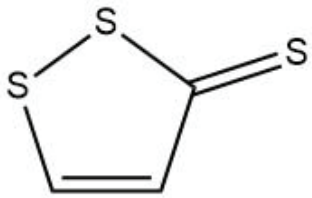

Figure 1.9 Structure of 3H-1,2-dithiole-3-thione.

3H-1,2-dithiole-3-thione (D3T) is a dithiolethione found in cruciferous vegetables such as Brussels sprouts. This compound has garnered interest as a potential neuroprotectant due to its nuclear factor-erythroid 2-related factor 2 (Nrf2) inducing properties and corresponding upregulation of antioxidant genes [92–95]. Nrf2 is a transcription factor regulated by Kelch-like ECH-associated protein 1 (Keap1). Nrf2 when bound by Keap1 is targeted for proteasomal degradation via the Cullin-3-based E3 ligase complex. However, in response to oxidants or electrophiles, Nrf2 is released from Keap1 by phosphorylation of Nrf2 or modification of critical cysteine thiols on either Keap1 or Nrf2 and then translocates to the nucleus. Nrf2 then binds to the antioxidant response element (ARE) and forms a heterodimer to transcriptionally activate a

host of antioxidant genes (Fig. 1.10). Upregulation of phase II metabolism enzymes such as NAD(P)H:quinone oxidoreductase 1 (NQO1), glutathione S-transferase (GST), γ-glutamylcysteine ligase (GCL), and heme oxygenase 1 (HO-1) has made Nrf2 a target for research on chemoprotection and oxidative stress [96].

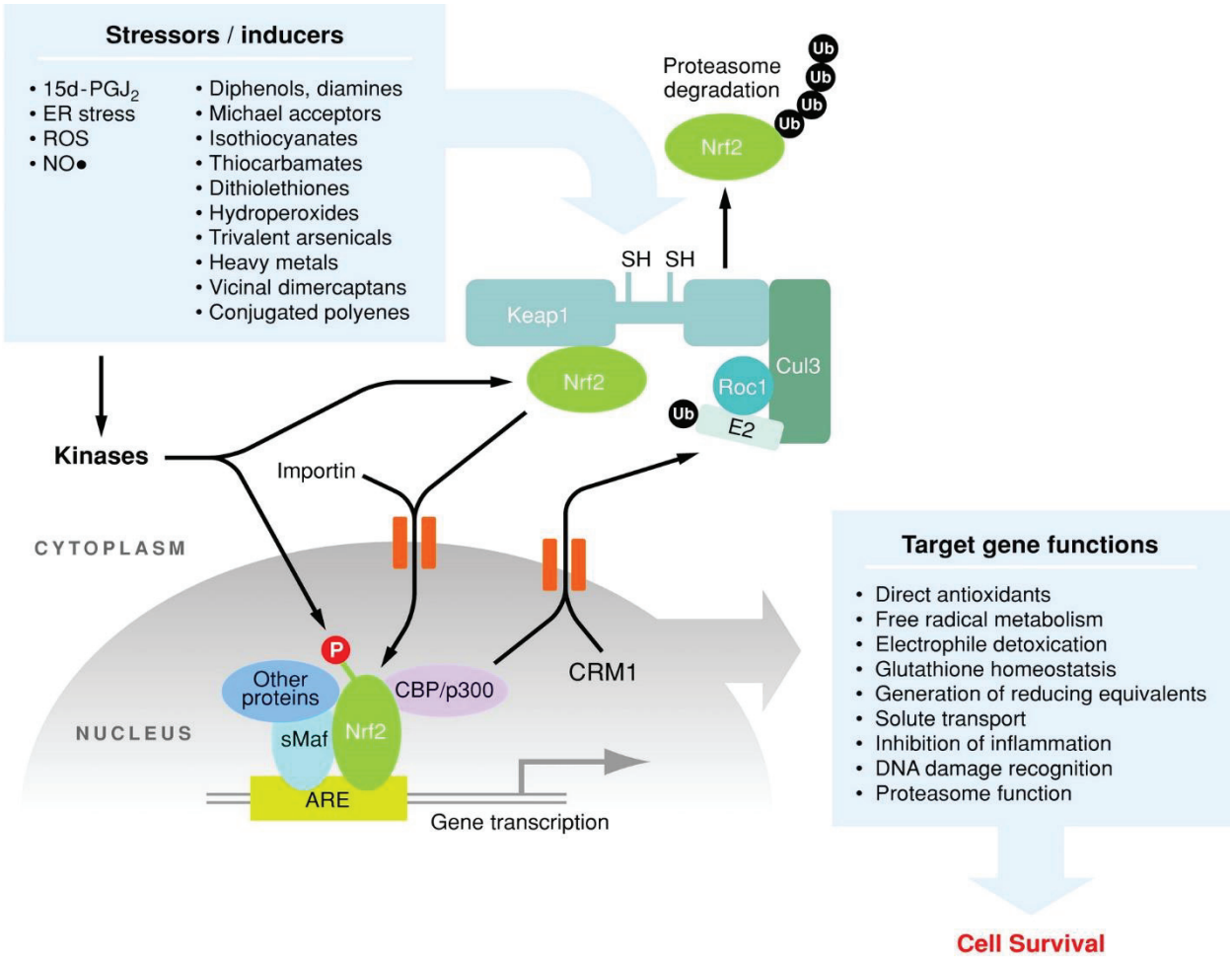

Figure 1.10 Regulation of Nrf2 activation and Nrf2-mediated gene transcription. Permission to reprint obtained from Copyright Clearance Center, Inc. [97]

The mechanism for how D3T upregulates Nrf2 expression is not entirely elucidated and more than one mechanism may be responsible. In zebra fish embryos, D3T was shown to

conjugate to regulatory cysteine 151 on Keap1 and lower Nrf2 degradation [95]. Keap1 has 25 reactive cysteines that can be modified by oxidation, reduction, or alkylation. Nrf2 has only seven reactive cysteine residues; therefore, Keap1 has been referred to as being a "redox sensor." However, cysteine 199 on Nrf2 may be of particular importance as it has been shown to regulate nuclear localization [98]. Interestingly, D3T may show protection by increasing superoxide generation when reacting with thiols. Jia *et al.* measured superoxide generation during the reaction of D3T with the dithiol dithiothreitol (DTT) and the thiol GSH. Reaction with either molecule resulted in increased oxygen consumption and superoxide generation in a concentration dependent manner. Superoxide production was more readily induced with DTT which may more readily mimic the adjacent sulfhydryl groups located on Keap1 [94]. Therefore, D3T may upregulate nuclear translocation of Nrf2 by directly interacting with reactive cysteine residues on Keap1 as well as by generating ROS when reacting with sulfhydryl groups such as those found on Keap1.

D3T treatment has been shown to be protective against neurotoxicity in SH-SY5Y cells, primary human neurons, and human primary astrocytes [99,100]. In SH-SY5Y and primary human neuronal cells, treatment with up to 100 μM D3T increased both total and mitochondrial GSH and increased NQO1 activity. Dopaminergic neurons may be particularly susceptible to oxidative stress as dopamine is readily oxidized to 6-hydroxydopamine. D3T pretreatment was protective against 6-hydroxydopamine stress in SH-SY5Y and primary human neuronal cells [99]. *In vivo* experiments with D3T have been carried out in mouse and rat models, but protection against PN has not been directly studied [101–104]. In both mouse and rat models, D3T treatment lead to upregulation of many Nrf2 responsive genes. However, the pattern of response varied among different genes and tissues [101–103]. Therefore, further studies will

need to be carried out in *in vivo* models of diabetic PN to determine whether D3T's Nrf2 inducing properties confer protection in the peripheral nerve.

1.7.4 N-acetylcysteine (NAC)

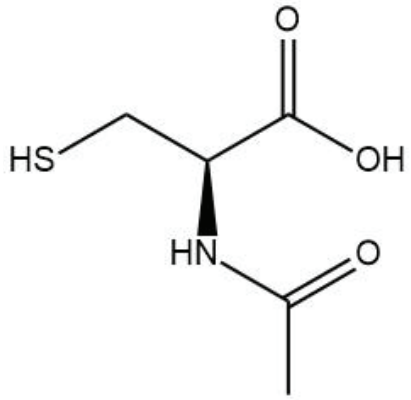

Figure 1.11 Structure of N-acetylcysteine.

N-acetylcysteine (NAC) is an antioxidant that has been commonly used since the mid-1970s as a first line of defense against acetaminophen poisoning [105,106]. Metabolism of acetaminophen leads to the formation of reactive intermediate N-acetyl-p-benzoquinoneimine (NAPQI), which is cleared after conjugation with GSH [107]. Once GSH is depleted, NAPQI reacts with proteins and enzymes, which can lead to toxicity and cell death [105]. NAC protects against acetaminophen toxicity by both increasing GSH production, and as a free radical scavenger reducing NAPQI to acetaminophen [105,107]. Therefore, further review of these potential mechanisms of action is warranted.

Cysteine is the rate limiting amino acid of GSH synthesis, and under physiological conditions GCL is not operating at its maximal rate [106]. Therefore, increasing the cysteine pool results in increased GSH synthesis and replenishment [106,108,109]. Active transport is required for cysteine transport into the cell via the alanine-serine-cysteine system [106].

However, NAC is membrane permeable and does not require active transport to be taken up [106,109]. After entering the cell NAC is hydrolyzed to yield cysteine, increasing substrate for GCL and allowing for increased GSH synthesis (Fig. 1.12) [109]. Due to these reasons, NAC is commonly used as a supplement to increase GSH levels [106,109,110]. In human clinical trials, NAC has been shown to confer protection by replenishing GSH in HIV-infected individuals [111] and in acetaminophen toxicity [107]. NAC supplementation has also been shown to reduce postprandial markers of oxidative stress in patients with type 2 diabetes or impaired glucose tolerance, however the mechanism of NAC protection was not established [112]. In a cell culture model of diabetic neuropathy using SH-SY5Y cells, NAC treatment protected against AGE-induced GSH depletion and conferred full protection against neurite degeneration [37]. In cultured cerebellar granule neurons, the addition of lipid peroxidation byproduct 4-hyroxynonenal (HNE) induced neuronal death. HNE treatment resulted in depletion of GSH and a significant decrease in mitochondrial membrane potential. NAC supplementation prior to HNE treatment resulted in complete protection against neuronal death and decrease in mitochondrial membrane potential, and partial but significant protection of GSH. The mechanism of NAC protection was attributed to maintenance of intracellular GSH, as GSH-HNE conjugation is required for HNE detoxification [113]. NAC supplementation in cell culture has also shown protection against ROS through a potential glutathione dependent mechanism in spinal motor neurons [114], oligodendrocytes [115], cortical neurons [116], and PC-12 cells [117]. In diabetic rats, NAC supplementation protected both reduced protein thiols and GSH levels and conferred protection against the diabetes induced lipid peroxidation byproduct, MDA. Furthermore, the diabetic rats experienced significant impairment of motor coordination, and NAC supplementation was able to significantly improve motor coordination to 77.84% of control. The

authors attribute the protective effects of NAC observed in this study to both its free radical scavenging and GSH maintaining properties [118].

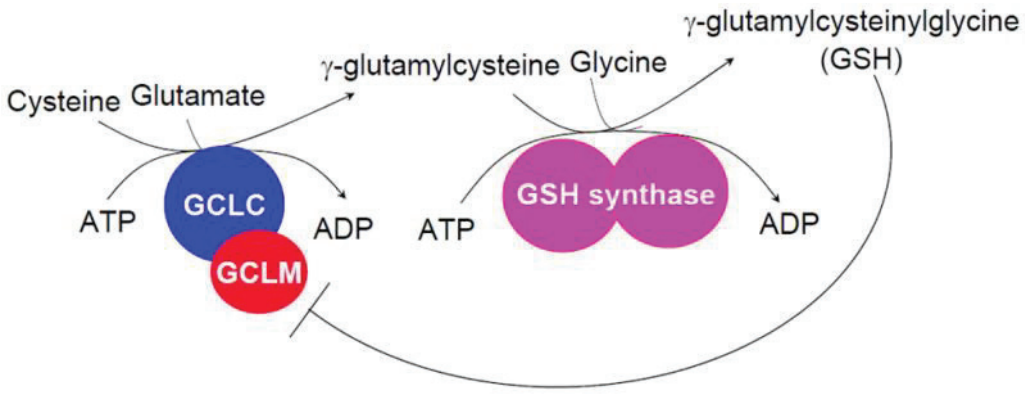

Figure 1.12 Glutathione synthesis pathway.
Reprinted with permission from Elsevier and Copyright Clearance Center, Inc. [119].

1.8 Research Questions

As was summarized in this literature review, ROS and oxidative stress play a significant role in the development of diabetic PN. Both *in vitro* and *in vivo* studies have shown the potential beneficial effects of antioxidants on protection against diabetic PN. Further research on establishing the mechanisms of protection of antioxidants in PN is critical, as this may provide diabetic patients more information and tools to improve their quality of life. This dissertation will focus on two particular antioxidants, NAC and D3T, in a validated cell culture model of diabetic PN.

The second chapter of this dissertation focuses on the mechanism of protection of NAC. Previously in our lab, we were able to show that when differentiated SH-SY5Y cells were stressed with AGE they experienced neurite and viability loss along with depletion of intracellular GSH. NAC pre-treatment was able to completely protect against AGE-induced

damage, and also maintained intracellular GSH concentrations. However, what was not established was whether NAC was also conferring protection via its intrinsic antioxidant scavenging properties. The mechanism of NAC protection is critical to understand for both the role of GSH in neurite protection as well as later translation into *in vivo* studies. It was hypothesized that NAC confers protection against AGE-induced neurite degeneration entirely through maintaining intracellular reduced GSH concentrations, and not through the chemical's intrinsic antioxidant properties.

The third chapter of this dissertation focuses on the D3T paradox that was previously discovered. Initially, it was hypothesized that D3T would confer protection against AGE-induced damage in much the same way as NAC. D3T is potent Nrf2 inducer that has been shown to upregulate enzymes required for GSH synthesis. However, D3T was only able to protect against hydrogen peroxide-induced stress, but paradoxically exacerbated AGE-induced damage. Unexpectedly, D3T pre-treatment increased oxidized GSH concentrations, but decreased reduced GSH concentrations in AGE-stressed cells. This led to testing the extent to which D3T affected Nrf2 target genes: glucose-6-phosphate dehydrogenase (G6PD) and glutathione reductase (GR). Therefore, in chapter 3 we provide an explanation for the D3T paradox.

In the fourth chapter of this dissertation, we present the results of studies directed at determining the specific mechanisms for neurite retraction in SH-SY5Y cells. Study results from previous chapters have shown that maintenance of intracellular reduced GSH was critical for neurite protection under stressed conditions. Accumulation of oxidized GSH was associated with greater amounts of neurite degeneration. Thus, the role of glutathionylation in driving neurite retraction was explored. A better understanding of the mechanisms of neurite retraction can help in the development of a targeted approach to prevention and protection against diabetic PN.

1.9 References

[1] J.E. Shaw, R.A. Sicree, P.Z. Zimmet, Global estimates of the prevalence of diabetes for 2010 and 2030., Diabetes Res. Clin. Pract. 87 (2010) 4–14. doi:10.1016/j.diabres.2009.10.007.

[2] D. Jay, H. Hitomi, K.K. Griendling, Oxidative stress and diabetic cardiovascular complications., Free Radic. Biol. Med. 40 (2006) 183–92. doi:10.1016/j.freeradbiomed.2005.06.018.

[3] R.A. Kowluru, P.-S. Chan, Oxidative stress and diabetic retinopathy., Exp. Diabetes Res. 2007 (2007) 43603. doi:10.1155/2007/43603.

[4] J.L. Gross, M.J. de Azevedo, S.P. Silveiro, L.H. Canani, M.L. Caramori, T. Zelmanovitz, Diabetic nephropathy: diagnosis, prevention, and treatment., Diabetes Care. 28 (2005) 164–76. http://www.ncbi.nlm.nih.gov/pubmed/15616252 (accessed October 17, 2014).

[5] A.M. Stino, A.G. Smith, Peripheral neuropathy in prediabetes and the metabolic syndrome., J. Diabetes Investig. 8 (2017) 646–655. doi:10.1111/jdi.12650.

[6] Effect of intensive therapy on the microvascular complications of type 1 diabetes mellitus., JAMA. 287 (2002) 2563–9. http://www.pubmedcentral.nih.gov/articlerender.fcgi?artid=2622728&tool=pmcentrez&rendertype=abstract (accessed October 28, 2014).

[7] T.J. Lindsay, B.C. Rodgers, V. Savath, K. Hettinger, Treating diabetic peripheral neuropathic pain., Am. Fam. Physician. 82 (2010) 151–8. http://www.ncbi.nlm.nih.gov/pubmed/20642268 (accessed September 16, 2014).

[8] E.L. Feldman, Oxidative stress and diabetic neuropathy: a new understanding of an old problem., J. Clin. Invest. 111 (2003) 431–3. doi:10.1172/JCI17862.

[9] J.W. Baynes, S.R. Thorpe, Role of oxidative stress in diabetic complications: a new perspective on an old paradigm., Diabetes. 48 (1999) 1–9. http://www.ncbi.nlm.nih.gov/pubmed/9892215 (accessed September 2, 2014).

[10] T. Inoguchi, P. Li, F. Umeda, H.Y. Yu, M. Kakimoto, M. Imamura, T. Aoki, T. Etoh, T. Hashimoto, M. Naruse, H. Sano, H. Utsumi, H. Nawata, High glucose level and free fatty acid stimulate reactive oxygen species production through protein kinase C--dependent sactivation of NAD(P)H oxidase in cultured vascular cells., Diabetes. 49 (2000) 1939–45. http://www.ncbi.nlm.nih.gov/pubmed/11078463 (accessed October 26, 2014).

[11] T. Inoguchi, T. Sonta, H. Tsubouchi, T. Etoh, M. Kakimoto, N. Sonoda, N. Sato, N. Sekiguchi, K. Kobayashi, H. Sumimoto, H. Utsumi, H. Nawata, Protein kinase C-dependent increase in reactive oxygen species (ROS) production in vascular tissues of diabetes: role of vascular NAD(P)H oxidase., J. Am. Soc. Nephrol. 14 (2003) S227-32. http://www.ncbi.nlm.nih.gov/pubmed/12874436 (accessed October 26, 2014).

[12] L. Fontana, Modulating human aging and age-associated diseases., Biochim. Biophys. Acta. 1790 (2009) 1133–8. doi:10.1016/j.bbagen.2009.02.002.

[13] Centers for Disease Control Prevention, Diabetes 2014 Report Card, 2014. www.cdc.gov/diabetes/library/reports/congress.html (accessed April 29, 2018).

[14] D.A. Greene, M.J. Stevens, I. Obrosova, E.L. Feldman, Glucose-induced oxidative stress and programmed cell death in diabetic neuropathy., Eur. J. Pharmacol. 375 (1999) 217–23. http://www.ncbi.nlm.nih.gov/pubmed/10443578 (accessed September 16, 2014).

[15] M. Brownlee, Biochemistry and molecular cell biology of diabetic complications., Nature. 414 (2001) 813–20. doi:10.1038/414813a.

[16] Z. V Varga, Z. Giricz, L. Liaudet, G. Haskó, P. Ferdinandy, P. Pacher, Interplay of oxidative, nitrosative/nitrative stress, inflammation, cell death and autophagy in diabetic cardiomyopathy., Biochim. Biophys. Acta. 1852 (2015) 232–42. doi:10.1016/j.bbadis.2014.06.030.

[17] M.-C. Beauchamp, S.-E. Michaud, L. Li, M.R. Sartippour, G. Renier, Advanced glycation end products potentiate the stimulatory effect of glucose on macrophage lipoprotein lipase expression., J. Lipid Res. 45 (2004) 1749–57. doi:10.1194/jlr.M400169-JLR200.

[18] R. Ross, Atherosclerosis — An Inflammatory Disease, N. Engl. J. Med. 340 (1999) 115–126. doi:10.1056/NEJM199901143400207.

[19] N.S. Harhaj, D.A. Antonetti, Regulation of tight junctions and loss of barrier function in pathophysiology., Int. J. Biochem. Cell Biol. 36 (2004) 1206–37. doi:10.1016/j.biocel.2003.08.007.

[20] R.E. Anderson, L.M. Rapp, R.D. Wiegand, Lipid peroxidation and retinal degeneration., Curr. Eye Res. 3 (1984) 223–7. http://www.ncbi.nlm.nih.gov/pubmed/6606531 (accessed October 26, 2014).

[21] R.A. Kowluru, S.N. Abbas, Diabetes-induced mitochondrial dysfunction in the retina., Invest. Ophthalmol. Vis. Sci. 44 (2003) 5327–34. http://www.ncbi.nlm.nih.gov/pubmed/14638734 (accessed October 26, 2014).

[22] R. Kowluru, T.S. Kern, R.L. Engerman, Abnormalities of retinal metabolism in diabetes or galactosemia. II. Comparison of gamma-glutamyl transpeptidase in retina and cerebral cortex, and effects of antioxidant therapy., Curr. Eye Res. 13 (1994) 891–6. http://www.ncbi.nlm.nih.gov/pubmed/7720397 (accessed October 26, 2014).

[23] T.S. Kern, R.A. Kowluru, R.L. Engerman, Abnormalities of retinal metabolism in diabetes or galactosemia: ATPases and glutathione., Invest. Ophthalmol. Vis. Sci. 35 (1994) 2962–7. http://www.ncbi.nlm.nih.gov/pubmed/8206713 (accessed October 26, 2014).

[24] S. Dronavalli, I. Duka, G.L. Bakris, The pathogenesis of diabetic nephropathy., Nat. Clin. Pract. Endocrinol. Metab. 4 (2008) 444–52. doi:10.1038/ncpendmet0894.

[25] J.M. Forbes, M.T. Coughlan, M.E. Cooper, Oxidative stress as a major culprit in kidney disease in diabetes., Diabetes. 57 (2008) 1446–54. doi:10.2337/db08-0057.

[26] R. Hernández-Marco, P. Codoñer-Franch, S. Pons Morales, C. Del Castillo Villaescusa, L. Boix García, V. Valls Bellés, Oxidant/antioxidant status and hyperfiltration in young patients with type 1 diabetes mellitus., Pediatr. Nephrol. 24 (2009) 121–7. doi:10.1007/s00467-008-0961-4.

[27] M. Hogan, A. Cerami, R. Bucala, Advanced glycosylation endproducts block the antiproliferative effect of nitric oxide. Role in the vascular and renal complications of diabetes mellitus., J. Clin. Invest. 90 (1992) 1110–5. doi:10.1172/JCI115928.

[28] D. Koya, K. Hayashi, M. Kitada, A. Kashiwagi, R. Kikkawa, M. Haneda, Effects of antioxidants in diabetes-induced oxidative stress in the glomeruli of diabetic rats., J. Am. Soc. Nephrol. 14 (2003) S250-3. http://www.ncbi.nlm.nih.gov/pubmed/12874441 (accessed October 30, 2014).

[29] S. Tesfaye, D. Selvarajah, Advances in the epidemiology, pathogenesis and management of diabetic peripheral neuropathy., Diabetes. Metab. Res. Rev. 28 Suppl 1 (2012) 8–14. doi:10.1002/dmrr.2239.

[30] S. Tesfaye, A.J.M. Boulton, P.J. Dyck, R. Freeman, M. Horowitz, P. Kempler, G. Lauria, R.A. Malik, V. Spallone, A. Vinik, L. Bernardi, P. Valensi, Diabetic neuropathies: update on definitions, diagnostic criteria, estimation of severity, and treatments., Diabetes Care. 33 (2010) 2285–93. doi:10.2337/dc10-1303.

[31] H. Brem, M. Tomic-Canic, Cellular and molecular basis of wound healing in diabetes., J. Clin. Invest. 117 (2007) 1219–22. doi:10.1172/JCI32169.

[32] T. Saarto, P.J. Wiffen, Antidepressants for neuropathic pain: a Cochrane review., J. Neurol. Neurosurg. Psychiatry. 81 (2010) 1372–3. doi:10.1136/jnnp.2008.144964.

[33] H. Sies, Oxidative stress: oxidants and antioxidants., Exp. Physiol. 82 (1997) 291–5. http://www.ncbi.nlm.nih.gov/pubmed/9129943 (accessed September 26, 2014).

[34] V. Cecarini, J. Gee, E. Fioretti, M. Amici, M. Angeletti, A.M. Eleuteri, J.N. Keller, Protein oxidation and cellular homeostasis: Emphasis on metabolism., Biochim. Biophys. Acta. 1773 (2007) 93–104. doi:10.1016/j.bbamcr.2006.08.039.

[35] S. V Avery, Molecular targets of oxidative stress., Biochem. J. 434 (2011) 201–10. doi:10.1042/BJ20101695.

[36] A. Valavanidis, T. Vlachogianni, C. Fiotakis, 8-hydroxy-2’ -deoxyguanosine (8-OHdG): A critical biomarker of oxidative stress and carcinogenesis., J. Environ. Sci. Health. C. Environ. Carcinog. Ecotoxicol. Rev. 27 (2009) 120–39. doi:10.1080/10590500902885684.

[37] R. Pazdro, J.R. Burgess, Differential effects of α-tocopherol and N-acetyl-cysteine on advanced glycation end product-induced oxidative damage and neurite degeneration in SH-SY5Y cells., Biochim. Biophys. Acta. 1822 (2012) 550–6. doi:10.1016/j.bbadis.2012.01.003.

[38] J. Lu, A. Holmgren, The thioredoxin antioxidant system, Free Radic. Biol. Med. 66 (2014) 75–87. doi:10.1016/J.FREERADBIOMED.2013.07.036.

[39] A.P. Fernandes, A. Holmgren, Glutaredoxins: Glutathione-Dependent Redox Enzymes with Functions Far Beyond a Simple Thioredoxin Backup System, Antioxid. Redox Signal. 6 (2004) 63–74. doi:10.1089/152308604771978354.

[40] P. Magnani, P.V. Cherian, G.W. Gould, D.A. Greene, A.A.F. Sima, F.C.B. Iii, Glucose Transporters in Rat Peripheral Nerve : P a r a n o d a l Expression of GLUT1 and GLUT3, Metabolism. 45 (1996) 1466–1473.

[41] C.W. Heilig, L.A. Concepcion, B.L. Riser, S.O. Freytag, M. Zhu, P. Cortes, Overexpression of glucose transporters in rat mesangial cells cultured in a normal glucose milieu mimics the diabetic phenotype., J. Clin. Invest. 96 (1995) 1802–14. doi:10.1172/JCI118226.

[42] F.J. Romero, E. Monsalve, C. Hermenegildo, F.J. Puertas, V. Higueras, E. Nies, J. Segura-Aguilar, J. Romá, Oxygen toxicity in the nervous tissue: comparison of the antioxidant defense of rat brain and sciatic nerve., Neurochem. Res. 16 (1991) 157–61. http://www.ncbi.nlm.nih.gov/pubmed/1908956 (accessed November 2, 2014).

[43] P. Sytze Van Dam, M.A. Cotter, B. Bravenboer, N.E. Cameron, Pathogenesis of diabetic neuropathy: focus on neurovascular mechanisms., Eur. J. Pharmacol. 719 (2013) 180–6. doi:10.1016/j.ejphar.2013.07.017.

[44] P.A. Low, K.K. Nickander, H.J. Tritschler, The roles of oxidative stress and antioxidant treatment in experimental diabetic neuropathy., Diabetes. 46 Suppl 2 (1997) S38-42. http://www.ncbi.nlm.nih.gov/pubmed/9285497 (accessed September 16, 2014).

[45] B.M. Ilfeld, J. Preciado, A.M. Trescot, Novel cryoneurolysis device for the treatment of sensory and motor peripheral nerves., Expert Rev. Med. Devices. 13 (2016) 713–25. doi:10.1080/17434440.2016.1204229.

[46] I.G. Obrosova, Diabetes and the peripheral nerve., Biochim. Biophys. Acta. 1792 (2009) 931–40. doi:10.1016/j.bbadis.2008.11.005.

[47] J.R. Williamson, K. Chang, M. Frangos, K.S. Hasan, Y. Ido, T. Kawamura, J.R. Nyengaard, M. van den Enden, C. Kilo, R.G. Tilton, Hyperglycemic pseudohypoxia and diabetic complications., Diabetes. 42 (1993) 801–13. http://www.ncbi.nlm.nih.gov/pubmed/8495803 (accessed November 4, 2014).

[48] S.S.M. Chung, E.C.M. Ho, K.S.L. Lam, S.K. Chung, Contribution of polyol pathway to diabetes-induced oxidative stress., J. Am. Soc. Nephrol. 14 (2003) S233-6. http://www.ncbi.nlm.nih.gov/pubmed/12874437 (accessed September 24, 2014).

[49] M.A. Cotter, N.E. Cameron, Antioxidants in the Treatment of Diabetic Polyneuropathy: Synergy with Essential Fatty Acids, in: L. Packer, P. Rosen, H.J. Tritschler, G.L. King, A. Azzi (Eds.), Antioxidants Diabetes Manag., 1st ed., Marcel Dekker, INC, New York, 2000: pp. 129–153.

[50] I.G. Obrosova, D.A. Greene, Antioxidative Defense in Diabetic Peripheral Nerve: Effects of DL-alpha-Lipoic Acid, Aldose Reductase Inhibitor, and Sorbitol Dehydrogenase Inhibitor, in: L. Packer, P. Rosen, H.J. Tritschler, G.L. King, A. Azzi (Eds.), Antioxidants Diabetes Manag., 1st ed., Marcel Dekker, INC, New York, 2000: pp. 93–110.

[51] N. Kato, K. Mizuno, M. Makino, T. Suzuki, S. Yagihashi, Effects of 15-month aldose reductase inhibition with fidarestat on the experimental diabetic neuropathy in rats., Diabetes Res. Clin. Pract. 50 (2000) 77–85. http://www.ncbi.nlm.nih.gov/pubmed/10960717 (accessed November 18, 2014).

[52] J.C. Arezzo, The use of electrophysiology for the assessment of diabetic neuropathy, Neurosci. Res. Commun. 21 (1997) 13–23. doi:10.1002/(SICI)1520-6769(199707)21:1<13::AID-NRC203>3.0.CO;2-P.

[53] V. Bril, R.A. Buchanan, Long-term effects of ranirestat (AS-3201) on peripheral nerve function in patients with diabetic sensorimotor polyneuropathy., Diabetes Care. 29 (2006) 68–72. http://www.ncbi.nlm.nih.gov/pubmed/16373898 (accessed November 10, 2014).

[54] V. Bril, T. Hirose, S. Tomioka, R. Buchanan, Ranirestat for the management of diabetic sensorimotor polyneuropathy., Diabetes Care. 32 (2009) 1256–60. doi:10.2337/dc08-2110.

[55] D.A. Greene, J.C. Arezzo, M.B. Brown, Effect of aldose reductase inhibition on nerve conduction and morphometry in diabetic neuropathy. Zenarestat Study Group., Neurology. 53 (1999) 580–91. http://www.ncbi.nlm.nih.gov/pubmed/10449124 (accessed November 10, 2014).

[56] C.M. Casellini, P.M. Barlow, A.L. Rice, M. Casey, K. Simmons, G. Pittenger, E.J. Bastyr, A.M. Wolka, A.I. Vinik, A 6-month, randomized, double-masked, placebo-controlled study evaluating the effects of the protein kinase C-beta inhibitor ruboxistaurin on skin microvascular blood flow and other measures of diabetic peripheral neuropathy., Diabetes Care. 30 (2007) 896–902. doi:10.2337/dc06-1699.

[57] N. Das Evcimen, G.L. King, The role of protein kinase C activation and the vascular complications of diabetes., Pharmacol. Res. 55 (2007) 498–510. doi:10.1016/j.phrs.2007.04.016.

[58] P. Geraldes, G.L. King, Activation of protein kinase C isoforms and its impact on diabetic complications., Circ. Res. 106 (2010) 1319–31. doi:10.1161/CIRCRESAHA.110.217117.

[59] N.E. Cameron, M.A. Cotter, Effects of protein kinase Cbeta inhibition on neurovascular dysfunction in diabetic rats: interaction with oxidative stress and essential fatty acid dysmetabolism., Diabetes. Metab. Res. Rev. 18 315–23. doi:10.1002/dmrr.307.

[60] X. Zhu, J. Eichberg, 1,2-diacylglycerol content and its arachidonyl-containing molecular species are reduced in sciatic nerve from streptozotocin-induced diabetic rats., J. Neurochem. 55 (1990) 1087–90. http://www.ncbi.nlm.nih.gov/pubmed/2117050 (accessed November 22, 2014).

[61] D.A. Greene, A.A. Sima, M.J. Stevens, E.L. Feldman, S.A. Lattimer, Complications: neuropathy, pathogenetic considerations., Diabetes Care. 15 (1992) 1902–25. http://www.ncbi.nlm.nih.gov/pubmed/1464245 (accessed November 22, 2014).

[62] N.E. Cameron, M.A. Cotter, A.M. Jack, M.D. Basso, T.C. Hohman, Protein kinase C effects on nerve function, perfusion, Na(+), K(+)-ATPase activity and glutathione content in diabetic rats., Diabetologia. 42 (1999) 1120–30. doi:10.1007/s001250051280.

[63] H. Konishi, M. Tanaka, Y. Takemura, H. Matsuzaki, Y. Ono, U. Kikkawa, Y. Nishizuka, Activation of protein kinase C by tyrosine phosphorylation in response to H2O2., Proc. Natl. Acad. Sci. U. S. A. 94 (1997) 11233–7. http://www.pubmedcentral.nih.gov/articlerender.fcgi?artid=23425&tool=pmcentrez&rendertype=abstract (accessed November 21, 2014).

[64] J.F. Keaney, Y. Guo, D. Cunningham, G.T. Shwaery, A. Xu, J.A. Vita, Vascular incorporation of alpha-tocopherol prevents endothelial dysfunction due to oxidized LDL by inhibiting protein kinase C stimulation., J. Clin. Invest. 98 (1996) 386–94. doi:10.1172/JCI118804.

[65] K. Uehara, S.-I. Yamagishi, S. Otsuki, S. Chin, S. Yagihashi, Effects of polyol pathway hyperactivity on protein kinase C activity, nociceptive peptide expression, and neuronal structure in dorsal root ganglia in diabetic mice., Diabetes. 53 (2004) 3239–47. http://www.ncbi.nlm.nih.gov/pubmed/15561956 (accessed November 22, 2014).

[66] D. Bansal, Y. Badhan, K. Gudala, F. Schifano, Ruboxistaurin for the treatment of diabetic peripheral neuropathy: a systematic review of randomized clinical trials., Diabetes Metab. J. 37 (2013) 375–84. doi:10.4093/dmj.2013.37.5.375.

[67] T. Nishikawa, D. Edelstein, X.L. Du, S. Yamagishi, T. Matsumura, Y. Kaneda, M.A. Yorek, D. Beebe, P.J. Oates, H.P. Hammes, I. Giardino, M. Brownlee, Normalizing mitochondrial superoxide production blocks three pathways of hyperglycaemic damage., Nature. 404 (2000) 787–90. doi:10.1038/35008121.

[68] F. Giacco, M. Brownlee, Oxidative stress and diabetic complications., Circ. Res. 107 (2010) 1058–70. doi:10.1161/CIRCRESAHA.110.223545.

[69] X. Du, T. Matsumura, D. Edelstein, L. Rossetti, Z. Zsengellér, C. Szabó, M. Brownlee, Inhibition of GAPDH activity by poly(ADP-ribose) polymerase activates three major pathways of hyperglycemic damage in endothelial cells., J. Clin. Invest. 112 (2003) 1049–57. doi:10.1172/JCI18127.

[70] P. Fernyhough, M. Jonathan, Mechanisms of disease: Mitochondrial dysfunction in sensory neuropathy and other complications in diabetes., Handb. Clin. Neurol. 126 (2014) 353–77. doi:10.1016/B978-0-444-53480-4.00027-8.

[71] Q. Zhang, J.M. Ames, R.D. Smith, J.W. Baynes, T.O. Metz, A Perspective on the Maillard Reaction and the Analysis of Protein Glycation by Mass Spectrometry: Probing the Pathogenesis of Chronic Disease, J. Proteome Res. 8 (2009) 754–769. doi:10.1021/pr800858h.

[72] N. Ahmed, Advanced glycation endproducts--role in pathology of diabetic complications., Diabetes Res. Clin. Pract. 67 (2005) 3–21. doi:10.1016/j.diabres.2004.09.004.

[73] M. Jack, D. Wright, Role of advanced glycation endproducts and glyoxalase I in diabetic peripheral sensory neuropathy., Transl. Res. 159 (2012) 355–65. doi:10.1016/j.trsl.2011.12.004.

[74] I.K. Lukic, P.M. Humpert, P.P. Nawroth, A. Bierhaus, The RAGE pathway: activation and perpetuation in the pathogenesis of diabetic neuropathy., Ann. N. Y. Acad. Sci. 1126 (2008) 76–80. doi:10.1196/annals.1433.059.

[75] A.M. Vincent, L. Perrone, K. a Sullivan, C. Backus, A.M. Sastry, C. Lastoskie, E.L. Feldman, Receptor for advanced glycation end products activation injures primary sensory neurons via oxidative stress., Endocrinology. 148 (2007) 548–58. doi:10.1210/en.2006-0073.

[76] V. Thallas-Bonke, S.R. Thorpe, M.T. Coughlan, K. Fukami, F.Y.T. Yap, K.C. Sourris, S.A. Penfold, L.A. Bach, M.E. Cooper, J.M. Forbes, Inhibition of NADPH oxidase prevents advanced glycation end product-mediated damage in diabetic nephropathy through a protein kinase C-alpha-dependent pathway., Diabetes. 57 (2008) 460–9. doi:10.2337/db07-1119.

[77] R.S. Frey, X. Gao, K. Javaid, S.S. Siddiqui, A. Rahman, A.B. Malik, Phosphatidylinositol 3-kinase gamma signaling through protein kinase Czeta induces NADPH oxidase-mediated oxidant generation and NF-kappaB activation in endothelial cells., J. Biol. Chem. 281 (2006) 16128–38. doi:10.1074/jbc.M508810200.

[78] L. Li, G. Renier, Activation of nicotinamide adenine dinucleotide phosphate (reduced form) oxidase by advanced glycation end products links oxidative stress to altered retinal vascular endothelial growth factor expression., Metabolism. 55 (2006) 1516–23. doi:10.1016/j.metabol.2006.06.022.

[79] A. Bierhaus, P.M. Humpert, M. Morcos, T. Wendt, T. Chavakis, B. Arnold, D.M. Stern, P.P. Nawroth, Understanding RAGE, the receptor for advanced glycation end products., J. Mol. Med. (Berl). 83 (2005) 876–86. doi:10.1007/s00109-005-0688-7.

[80] A. Bierhaus, S. Chevion, M. Chevion, M. Hofmann, P. Quehenberger, T. Illmer, T. Luther, E. Berentshtein, H. Tritschler, M. Müller, P. Wahl, R. Ziegler, P.P. Nawroth, Advanced glycation end product-induced activation of NF-kappaB is suppressed by alpha-lipoic acid in cultured endothelial cells., Diabetes. 46 (1997) 1481–90. http://www.ncbi.nlm.nih.gov/pubmed/9287050 (accessed November 30, 2014).

[81] S. Wang, S. Kotamraju, E. Konorev, S. Kalivendi, J. Joseph, B. Kalyanaraman, Activation of nuclear factor-kappaB during doxorubicin-induced apoptosis in endothelial cells and myocytes is pro-apoptotic: the role of hydrogen peroxide., Biochem. J. 367 (2002) 729–40. doi:10.1042/BJ20020752.

[82] L. Packer, Oxidative Stress and Antioxidants: The Antioxidant Network, alpha-Lipoic Acid, and Diabetes, in: L. Packer, P. Rosen, H.J. Tritschler, G.L. King, A. Azzi (Eds.), Antioxidants Diabetes Manag., 1st ed., Marcel Dekker, INC, New York, 2000: pp. 1–15.

[83] M.J. Stevens, I. Obrosova, X. Cao, C. Van Huysen, D.A. Greene, Effects of DL-alpha-lipoic acid on peripheral nerve conduction, blood flow, energy metabolism, and oxidative stress in experimental diabetic neuropathy., Diabetes. 49 (2000) 1006–15. http://www.ncbi.nlm.nih.gov/pubmed/10866054 (accessed September 23, 2014).

[84] M. Reljanovic, G. Reichel, K. Rett, M. Lobisch, K. Schuette, W. Möller, H.J. Tritschler, H. Mehnert, Treatment of diabetic polyneuropathy with the antioxidant thioctic acid (alpha-lipoic acid): a two year multicenter randomized double-blind placebo-controlled trial (ALADIN II). Alpha Lipoic Acid in Diabetic Neuropathy., Free Radic. Res. 31 (1999) 171–9. http://www.ncbi.nlm.nih.gov/pubmed/10499773 (accessed September 23, 2014).

[85] A.S. Ametov, A. Barinov, P.J. Dyck, R. Hermann, N. Kozlova, W.J. Litchy, P.A. Low, D. Nehrdich, M. Novosadova, P.C. O'Brien, M. Reljanovic, R. Samigullin, K. Schuette, I. Strokov, H.J. Tritschler, K. Wessel, N. Yakhno, D. Ziegler, The sensory symptoms of diabetic polyneuropathy are improved with alpha-lipoic acid: the SYDNEY trial., Diabetes Care. 26 (2003) 770–6. http://www.ncbi.nlm.nih.gov/pubmed/12610036 (accessed September 23, 2014).

[86] D. Ziegler, A. Ametov, A. Barinov, P.J. Dyck, I. Gurieva, P.A. Low, U. Munzel, N. Yakhno, I. Raz, M. Novosadova, J. Maus, R. Samigullin, Oral treatment with alpha-lipoic acid improves symptomatic diabetic polyneuropathy: the SYDNEY 2 trial., Diabetes Care. 29 (2006) 2365–70. doi:10.2337/dc06-1216.

[87] S.S. Leonard, C. Xia, B.-H. Jiang, B. Stinefelt, H. Klandorf, G.K. Harris, X. Shi, Resveratrol scavenges reactive oxygen species and effects radical-induced cellular responses., Biochem. Biophys. Res. Commun. 309 (2003) 1017–26. http://www.ncbi.nlm.nih.gov/pubmed/13679076 (accessed December 4, 2014).

[88] Z. Ungvari, N. Labinskyy, P. Mukhopadhyay, J.T. Pinto, Z. Bagi, P. Ballabh, C. Zhang, P. Pacher, A. Csiszar, Resveratrol attenuates mitochondrial oxidative stress in coronary arterial endothelial cells., Am. J. Physiol. Heart Circ. Physiol. 297 (2009) H1876-81. doi:10.1152/ajpheart.00375.2009.

[89] H.-Y. Joo, S.R. Woo, Y.-N. Shen, M.Y. Yun, H.-J. Shin, E.-R. Park, S.-H. Kim, J.-E. Park, Y.-J. Ju, S.H. Hong, S.-G. Hwang, M.-H. Cho, J. Kim, K.-H. Lee, SIRT1 interacts with and protects glyceraldehyde-3-phosphate dehydrogenase (GAPDH) from nuclear translocation: implications for cell survival after irradiation., Biochem. Biophys. Res. Commun. 424 (2012) 681–6. doi:10.1016/j.bbrc.2012.07.006.

[90] M. Ventura, F. Mateo, J. Serratosa, I. Salaet, S. Carujo, O. Bachs, M.J. Pujol, Nuclear translocation of glyceraldehyde-3-phosphate dehydrogenase is regulated by acetylation., Int. J. Biochem. Cell Biol. 42 (2010) 1672–80. doi:10.1016/j.biocel.2010.06.014.

[91] A. Kumar, R.K. Kaundal, S. Iyer, S.S. Sharma, Effects of resveratrol on nerve functions, oxidative stress and DNA fragmentation in experimental diabetic neuropathy., Life Sci. 80 (2007) 1236–44. doi:10.1016/j.lfs.2006.12.036.

[92] K.-R. Li, S.-Q. Yang, Y.-Q. Gong, H. Yang, X.-M. Li, Y.-X. Zhao, J. Yao, Q. Jiang, C. Cao, 3H-1,2-dithiole-3-thione protects retinal pigment epithelium cells against Ultra-violet radiation via activation of Akt-mTORC1-dependent Nrf2-HO-1 signaling., Sci. Rep. 6 (2016) 25525. doi:10.1038/srep25525.

[93] J. Dong, D. Yan, S. Chen, Stabilization of Nrf2 Protein by D3T Provides Protection against Ethanol-Induced Apoptosis in PC12 Cells, PLoS One. 6 (2011) e16845. doi:10.1371/journal.pone.0016845.

[94] Z. Jia, H. Zhu, M.A. Trush, H.P. Misra, Y. Li, Generation of superoxide from reaction of 3H-1,2-dithiole-3-thione with thiols: implications for dithiolethione chemoprotection., Mol. Cell. Biochem. 307 (2008) 185–91. doi:10.1007/s11010-007-9598-z.

[95] M. Kobayashi, L. Li, N. Iwamoto, Y. Nakajima-Takagi, H. Kaneko, Y. Nakayama, M. Eguchi, Y. Wada, Y. Kumagai, M. Yamamoto, The antioxidant defense system Keap1-Nrf2 comprises a multiple sensing mechanism for responding to a wide range of chemical compounds., Mol. Cell. Biol. 29 (2009) 493–502. doi:10.1128/MCB.01080-08.

[96] E. Bhakkiyalakshmi, D. Sireesh, P. Rajaguru, R. Paulmurugan, K.M. Ramkumar, The emerging role of redox-sensitive Nrf2-Keap1 pathway in diabetes., Pharmacol. Res. 91 (2015) 104–14. doi:10.1016/j.phrs.2014.10.004.

[97] T.W. Kensler, N. Wakabayashi, S. Biswal, Cell survival responses to environmental stresses via the Keap1-Nrf2-ARE pathway., Annu. Rev. Pharmacol. Toxicol. 47 (2007) 89–116. doi:10.1146/annurev.pharmtox.46.120604.141046.

[98] X. He, Q. Ma, NRF2 cysteine residues are critical for oxidant/electrophile-sensing, Kelch-like ECH-associated protein-1-dependent ubiquitination-proteasomal degradation, and transcription activation., Mol. Pharmacol. 76 (2009) 1265–78. doi:10.1124/mol.109.058453.

[99] Z. Jia, H. Zhu, H.P. Misra, Y. Li, Potent induction of total cellular GSH and NQO1 as well as mitochondrial GSH by 3H-1,2-dithiole-3-thione in SH-SY5Y neuroblastoma cells and primary human neurons: protection against neurocytotoxicity elicited by dopamine, 6-hydroxydopamine, 4-hydroxy-2-no, Brain Res. 1197 (2008) 159–69. doi:10.1016/j.brainres.2007.12.044.

[100] Z. Jia, H. Zhu, Y. Li, H.P. Misra, Cruciferous nutraceutical 3H-1,2-dithiole-3-thione protects human primary astrocytes against neurocytotoxicity elicited by MPTP, MPP(+), 6-OHDA, HNE and acrolein., Neurochem. Res. 34 (2009) 1924–34. doi:10.1007/s11064-009-9978-8.

[101] M.K. Kwak, K. Itoh, M. Yamamoto, T.R. Sutter, T.W. Kensler, Role of transcription factor Nrf2 in the induction of hepatic phase 2 and antioxidative enzymes in vivo by the cancer chemoprotective agent, 3H-1, 2-dimethiole-3-thione., Mol. Med. 7 (2001) 135–45. http://www.ncbi.nlm.nih.gov/pubmed/11471548 (accessed March 14, 2018).

[102] M.A. Otieno, T.W. Kensler, K.Z. Guyton, Chemoprotective 3H-1,2-dithiole-3-thione induces antioxidant genes in vivo, Free Radic. Biol. Med. 28 (2000) 944–952. doi:10.1016/S0891-5849(00)00175-1.

[103] R. Munday, C.M. Munday, Induction of phase II enzymes by 3H-1,2-dithiole-3-thione: dose-response study in rats, Carcinogenesis. 25 (2004) 1721–1725. doi:10.1093/carcin/bgh162.

[104] H. Kumar, I.-S. Kim, S.V. More, B.-W. Kim, D.-K. Choi, Natural product-derived pharmacological modulators of Nrf2/ARE pathway for chronic diseases, Nat. Prod. Rep. 31 (2014) 109–139. doi:10.1039/C3NP70065H.

[105] A.L. Jones, Mechanism of action and value of N-acetylcysteine in the treatment of early and late acetaminophen poisoning: a critical review., J. Toxicol. Clin. Toxicol. 36 (1998) 277–85. http://www.ncbi.nlm.nih.gov/pubmed/9711192 (accessed April 18, 2018).

[106] M. Arakawa, Y. Ito, N-acetylcysteine and neurodegenerative diseases: Basic and clinical pharmacology, The Cerebellum. 6 (2007) 308–314. doi:10.1080/14734220601142878.

[107] J.T. Slattery, J.M. Wilson, T.F. Kalhorn, S.D. Nelson, Dose-dependent pharmacokinetics of acetaminophen: Evidence of glutathione depletion in humans, Clin. Pharmacol. Ther. 41 (1987) 413–418. doi:10.1038/clpt.1987.50.

[108] K.R. Atkuri, J.J. Mantovani, L.A. Herzenberg, L.A. Herzenberg, N-Acetylcysteine--a safe antidote for cysteine/glutathione deficiency., Curr. Opin. Pharmacol. 7 (2007) 355–9. doi:10.1016/j.coph.2007.04.005.

[109] D. Marmolino, M. Manto, Past, present and future therapeutics for cerebellar ataxias., Curr. Neuropharmacol. 8 (2010) 41–61. doi:10.2174/157015910790909476.

[110] B. Schmitt, M. Vicenzi, C. Garrel, F.M. Denis, Effects of N-acetylcysteine, oral glutathione (GSH) and a novel sublingual form of GSH on oxidative stress markers: A comparative crossover study., Redox Biol. 6 (2015) 198–205. doi:10.1016/J.REDOX.2015.07.012.

[111] S.C. De Rosa, M.D. Zaretsky, J.G. Dubs, M. Roederer, M. Anderson, A. Green, D. Mitra, N. Watanabe, H. Nakamura P, I. Tjioe, S.C. Deresinski, W.A. Moore, S.W. Ela, D. Parks, L.A. Herzenberg, L.A. Herzenberg, N-acetylcysteine replenishes glutathione in HIV infection, Eur. J. Clin. Invest. 30 (2000) 915–929. doi:10.1046/j.1365-2362.2000.00736.x.

[112] S. Neri, S.S. Signorelli, B. Torrisi, D. Pulvirenti, B. Mauceri, G. Abate, L. Ignaccolo, F. Bordonaro, D. Cilio, S. Calvagno, C. Leotta, Effects of antioxidant supplementation on postprandial oxidative stress and endothelial dysfunction: a single-blind, 15-day clinical trial in patients with untreated type 2 diabetes, subjects with impaired glucose tolerance, and healthy controls., Clin. Ther. 27 (2005) 1764–73. doi:10.1016/j.clinthera.2005.11.006.

[113] M. Arakawa, N. Ushimaru, N. Osada, T. Oda, K. Ishige, Y. Ito, N-acetylcysteine selectively protects cerebellar granule cells from 4-hydroxynonenal-induced cell death, Neurosci. Res. 55 (2006) 255–263. doi:10.1016/J.NEURES.2006.03.008.

[114] J.D. Rothstein, L.A. Bristol, B. Hosler, R.H. Brown, R.W. Kuncl, Chronic inhibition of superoxide dismutase produces apoptotic death of spinal neurons, Proc. Natl. Acad. Sci. 91 (1994) 4155–4159. doi:10.1073/PNAS.91.10.4155.

[115] M. Mayer, M. Noble, N-acetyl-L-cysteine is a pluripotent protector against cell death and enhancer of trophic factor-mediated cell survival in vitro., Proc. Natl. Acad. Sci. U. S. A. 91 (1994) 7496–500. doi:10.1073/PNAS.91.16.7496.

[116] R.R. Ratan, T.H. Murphy, J.M. Baraban, Macromolecular synthesis inhibitors prevent oxidative stress-induced apoptosis in embryonic cortical neurons by shunting cysteine from protein synthesis to glutathione., J. Neurosci. 14 (1994) 4385–92. doi:10.1523/JNEUROSCI.14-07-04385.1994.

[117] G. Ferrari, C.Y. Yan, L.A. Greene, N-acetylcysteine (D- and L-stereoisomers) prevents apoptotic death of neuronal cells., J. Neurosci. 15 (1995) 2857–66. doi:10.1523/JNEUROSCI.15-04-02857.1995.

[118] S.S. Kamboj, R.K. Vasishta, R. Sandhir, N-acetylcysteine inhibits hyperglycemia-induced oxidative stress and apoptosis markers in diabetic neuropathy., J. Neurochem. 112 (2010) 77–91. doi:10.1111/j.1471-4159.2009.06435.x.

[119] S.C. Lu, Glutathione synthesis., Biochim. Biophys. Acta. 1830 (2013) 3143–53. doi:10.1016/j.bbagen.2012.09.008.

[120] C.A. Haber, T.K.T. Lam, Z. Yu, N. Gupta, T. Goh, E. Bogdanovic, A. Giacca, I.G. Fantus, N-acetylcysteine and taurine prevent hyperglycemia-induced insulin resistance in vivo: possible role of oxidative stress., Am. J. Physiol. Endocrinol. Metab. 285 (2003) E744-53. doi:10.1152/ajpendo.00355.2002.

[121] A. Dhar, I. Dhar, K.M. Desai, L. Wu, Methylglyoxal scavengers attenuate endothelial dysfunction induced by methylglyoxal and high concentrations of glucose., Br. J. Pharmacol. 161 (2010) 1843–56. doi:10.1111/j.1476-5381.2010.01017.x.

[122] V. Martina, A. Masha, V.R. Gigliardi, L. Brocato, E. Manzato, A. Berchio, P. Massarenti, F. Settanni, L. Della Casa, S. Bergamini, A. Iannone, Long-term N-acetylcysteine and L-arginine administration reduces endothelial activation and systolic blood pressure in hypertensive patients with type 2 diabetes., Diabetes Care. 31 (2008) 940–4. doi:10.2337/dc07-2251.

[123] C.Y. Yan, G. Ferrari, L.A. Greene, N-acetylcysteine-promoted survival of PC12 cells is glutathione-independent but transcription-dependent., J. Biol. Chem. 270 (1995) 26827–32. doi:10.1074/JBC.270.45.26827.

[124] I.A. Cotgreave, N-acetylcysteine: pharmacological considerations and experimental and clinical applications., Adv. Pharmacol. 38 (1997) 205–27. http://www.ncbi.nlm.nih.gov/pubmed/8895810 (accessed April 27, 2018).

[125] M.R. Holdiness, Clinical Pharmacokinetics of N-Acetylcysteine, Clin. Pharmacokinet. 20 (1991) 123–134. doi:10.2165/00003088-199120020-00004.

CHAPTER 2. N-ACETYLCYSTEINE CONFERS PROTECTION AGAINST ADVANCED GLYCATION END-PRODUCT INDUCED NEURITE RETRACTION OF SH-SY5Y CELLS VIA A GLUTATHIONE-DEPENDENT MANNER

2.1 Abstract

N-acetylcysteine (NAC) is a commonly used thiol-containing substance widely known for its antioxidant properties. NAC can function as an antioxidant by increasing cellular glutathione (GSH) production, as a free radical scavenger, or a combination of these mechanisms. These properties make NAC a compound of interest for research as a therapeutic substance for diabetic peripheral neuropathy (PN). Diabetic PN is one of the most common complications of diabetes and affects at least 50% of patients. Hyperglycemia-induced oxidative stress is a primary driver in the development of PN. Peripheral nerves are particularly susceptible to oxidative stress as they express low levels of antioxidants such as GSH. In our lab we use differentiated SH-SY5Y cells treated with advanced glycation end products (AGE) as a model to mimic diabetic conditions and to study the mechanisms of oxidative stress-mediated cell damage and antioxidant protection. We have previously shown that NAC was able to completely protect against AGE-induced depletion of GSH and neurite damage. In the present study we explore the mechanisms of NAC action on neurite protection by inhibiting GSH synthesis. Depletion of GSH resulted in neurite retraction, even under non-stressed conditions, suggesting GSH plays a critical role in baseline neurite maintenance. Critically, inhibition of GSH synthesis blocked all protective effects of NAC against AGE-induced neurite damage, suggesting that the compound's free radical scavenging properties were not involved in neurite protection. Understanding the mechanisms responsible for both neurite retraction and antioxidant protection can provide an

outline for developing and/or identifying new therapeutic substances for patients with diabetic PN.

2.2 Introduction

N-acetylcysteine (NAC) is a thiol-containing compound widely known for its potent antioxidant properties. One of the most well-known uses for NAC is as an antidote to acetaminophen poisoning [1]. Metabolism of acetaminophen leads to the formation of reactive intermediate N-acetyl-p-benzoquinoneimine (NAPQI), which is cleared after conjugation with glutathione (GSH) [2]. Once GSH is depleted, NAPQI reacts with proteins and enzymes, which can lead to toxicity and cell death [1]. NAC protects against acetaminophen toxicity by both increasing GSH production, and as a free radical scavenger reducing NAPQI to acetaminophen [1,2]. These two mechanisms of NAC protection, maintenance of GSH and free radical scavenging, have been commonly cited as conferring protection in numerous conditions and disease states. NAC has been shown to confer protection against muscle fatigue [3,4], insulin resistance [5], post prandial oxidative stress [6], endothelial dysfunction [6,7], T cell function in HIV-infected individuals [8], and diabetic neuropathy [9].

The use of NAC to maintain GSH is due to its ability to provide the rate limiting substrate of GSH synthesis, cysteine [10]. NAC is membrane permeable and does not require active transport to be taken up, unlike cysteine [10,11]. After entering the cell NAC is hydrolyzed to yield cysteine, increasing substrate for γ-glutamylcysteine ligase (GCL) and allowing for increased GSH synthesis [11]. The free radical scavenging properties of NAC have also been cited as a potential mechanism of protection in many studies and reviews [1,5–7,9,12–16]. NAC has been shown to directly reduce the hydroxyl radical, hydrogen peroxide, and hypochlorous acid [16], and the ability to scavenge methylglyoxal [14] and NAPQI [1].

However, the protective effects of NAC as a free radical scavenger have predominantly been shown *in vitro* [16]. This discrepancy between *in vivo* and *in vitro* studies can be largely attributed to *in vivo* metabolism and low bioavailability of native NAC [13,16].

In our laboratory, we use differentiated SH-SY5Y cells stressed with advanced glycation end products (AGE) as a model system for diabetic peripheral neuropathy (PN) [17–19]. Oxidative stress is implicated as one of the major underlying mechanisms for diabetes-induced PN [20]. AGEs, products of non-enzymatic glycation of proteins, accumulate in circulation and tissue in the diabetic state and are a major contributor to oxidative-stress induced complications of diabetes, including PN [21–26]. AGE accumulation increases oxidative stress via binding to the receptor for advanced glycation end products (RAGE) and downstream activation of NADPH oxidase in a PKCδ-dependent manner [27,28]. The resulting increase in reactive oxygen species (ROS) facilitates damage to peripheral nerves [21]. Peripheral nerves are particularly susceptible to ROS, as they have low GSH levels [29], which are further depleted in diabetic conditions [9]. These characteristics of peripheral nerves led us to evaluate the effects of NAC in our model system of PN.

Previous results from our laboratory showed that when differentiated SH-SY5Y cells were stressed with AGEs, there was significant neurite loss [17,18]. Cells stressed with AGEs also experienced GSH depletion, however NAC treatment was able to protect against both GSH depletion and neurite loss [17]. Antioxidants that did not maintain GSH in the stressed (AGE-treated) condition, such as α-tocopherol and 3H-1,2-dithiole-3-thione (D3T), did not confer protection against neurite loss [17,18]. These results led us to conclude that maintaining intracellular GSH was critical for protection against AGE-induced neurite degeneration. In the present studies, the mechanism of NAC protection was investigated. As was previously

mentioned, NAC can confer protection through both its intrinsic antioxidant properties as well as through maintenance of GSH. However, the free radical scavenging properties of NAC observed in *in vitro* models have not translated to *in vivo* models. Consequently, the applicability of NAC as a potential therapeutic substance for diabetic PN is highly dependent on its mechanism of action. It was hypothesized that in our model NAC confers protection against AGE-induced neurite degeneration via maintenance of GSH levels and not through free-radical scavenging.

2.3 Methods

2.3.1 Materials

Dulbecco's Modified Medium (DMEM), Ham's F12 Medium, penicillin-streptomycin, and fetal bovine serum (FBS) were purchased from Invitrogen (Waltham, MO). All standard cell culture flasks and plates were purchased from ThermoFisher Scientific (Waltham, MO). All reagents such as retinoic acid, L-buthionine-sulfoximine (BSO), NAC, and reagents for GSH analysis were purchased from Sigma-Aldrich (St. Louis, MO) unless otherwise stated.

2.3.2 Cell Culture

SH-SY5Y cells were purchased from ATCC (Manassas, VA) and were cultured initially in growth media (DMEM, 10% FBS, 1% penicillin-streptomycin, 8 mM glucose) for 24 hours to allow for adherence. Following adherence, growth media was replaced with differentiating media (1:1 DMEM: F12, 1% FBS, 8 mM glucose, 10 μM retinoic acid) for five days to allow for neuronal cell phenotype development. Treatments for all experiments took place following the five-day differentiation period. Cells treated with NAC had .5-2 mM NAC (<1% PBS) added to the media 24 hours prior to 5 mg/mL BSA or AGE treatment. This treatment was then replenished in BSA and AGE treatment groups for 24 hours. For BSO-treated cells, 10-1000 μM

BSO (< 1% PBS) was added to the media 72 hours prior to BSA or AGE treatment and replenished during the 24-hour BSA or AGE treatment. For cells that were treated with BSO and NAC, NAC was added concurrently with BSO. Both NAC and BSO were replenished during BSA or AGE treatment.

2.3.3 Preparation of AGE-BSA and BSA Control

AGE-BSA was prepared as previously reported [18]. Briefly, 5 mg/ML BSA in PBS was incubated with 33 mM glycolaldehyde dimer for 20 hours at 37°C. Control BSA was treated in the same manner, but without the addition of glycolaldehyde. Both control and glycated BSA were then concentrated via ammonium sulfate precipitation. Ammonium sulfate was added to glycated BSA and control solutions (80% ammonium sulfate solution), and then centrifuged at 10,000g for 30 minutes. Precipitated proteins were resuspended with the minimal amount of PBS required for resuspension. Solutions were then dialyzed in PBS for three days, with daily replacement of PBS. Following dialysis, solutions were sterile filtered. The final concentrations of both glycated and control BSA were approximately 15 mg/mL.

2.3.4 GSH Assay

Total GSH was quantified using a colorimetric based assay as described by Rahman *et al*. [30]. SH-SY5Y cells were plated in 6-well plates (9 cm^2) at a concentration of 0.4 x 10^6. Each well was then pretreated with either NAC or vehicle (<1% PBS) for 24 hours followed by co-treatment and addition of AGE-BSA or BSA-control for an additional 24 hours. For groups treated with BSO and NAC, NAC was added concurrently with BSO treatment. Absorption was measured using a Bio-Tek Powerwave X200 (Winooski, VT) spectrophotometer (abs. 412nm). All values were normalized to protein content using a BCA assay kit (Pierce, Rockford, IL).

2.3.5 Cell Viability

Cell viability was estimated by protein content using a BCA assay kit (Pierce, Rockford, IL). Briefly, cells were plated in 6-well plates (9 cm^2) at a concentration of .4 x 10^6. At time of analysis, each well was washed three times with warm PBS (37°C) followed by harvesting with 500 µL trypsin-EDTA solution. The solution was neutralized with 500 µL growth media, and the cell suspension was centrifuged at 1000g for 5 min. Supernatant was then discarded, and the pellet resuspended in ice-cold PBS. This suspension was centrifuged and once again resuspended in PBS as a rinse step. At this step, nuclei for several samples was calculated as a validation for using protein content as an estimate for viability. Following the second PBS rinse, cells were centrifuged and the pellet was resuspended in 250 µL extraction buffer as listed by Rahman and colleagues [30]. To ensure complete lysis, suspensions were freeze-thawed at total of three times in a -80°C freezer, briefly sonicated, and the centrifuged at 3000g for 5 min. Following centrifugation, the supernatant was collected and used to measure protein content and GSH concentrations.

2.3.6 Neurite Quantification

At the completion of experiments, photos were taken to document morphological changes of differentiated SH-SY5Y cells. Images were captured at 10x magnification using a Zeiss Axio Vert. A1 microscope (Oberkochen, Germany). A Zeiss AxioCam ICm1 camera was used to take photos using Zeiss Zen2 imaging software. All images were 1388 x 1038 pixels, and exposure time for all photos was 32.03 ms. Images were then analyzed using ImageJ (NIH) software with NeuronJ (ImageScience) plugin. Individual neurites were traced, and neurite length was reported as length in pixels. Neurites present in the field of view were quantified from three to four independent experiments for each treatment group. Exclusion criteria included counting only

neurites with clearly defined start and end locations. Neurites that were shorter than the width of the cell body were not counted. For each treatment group, a minimum of 169 total neurites was quantified. To quantify the impact of treatments on the longest neurites, the number of neurites greater than or equal to the average length of neurites in the BSA control group was calculated for each treatment group.

2.3.7 Statistical Methods

Values are presented as group means ±S.E.M. Treatment effects were tested using a Student's t-test for two variables, or analysis of variance (ANOVA) for multiple variables. A significant ANOVA result was followed by a multiple comparisons of means test (Dunnett or Tukey HSD), with $P<0.05$ considered statistically significant.

2.4 Results

2.4.1 Impact of NAC on GSH Concentrations

To establish the most effective concentration of NAC to increase total GSH levels, a dose response was done with 0.5, 1.0, and 2.0 mM concentrations of NAC. The impact of NAC treatment on GSH concentrations for both BSA and AGE-treated cells is shown in Figure 2.1. Control (BSA treated) differentiated SH-SY5Y cells contained approximately 39 nmol/mg protein of GSH. As expected, AGE-treated cells experienced a significant drop in GSH (~18.3 nmol/mg protein). 1 mM NAC treatment in BSA-treated cells resulted in the highest GSH levels, however 2 mM NAC treatment did not increase GSH levels above BSA control (Fig. 2.1). NAC did not significantly increase [GSH] at any concentration when cells were treated with AGE, however a trend towards an increase was observed at 1 and 2 mM NAC concentrations (Fig. 2.1). Based on these initial results, 1 mM NAC was chosen as the optimal concentration for

further experiments. The effect of 1 mM NAC treatment on GSH levels of AGE-treated cells was revaluated and follow up experiments showed that 1 mM NAC treatment significantly increased GSH (Fig. 2.2).

2.4.2 The Effect of 1 mM NAC on Protection Against AGE-Induced Neurite Loss

Previously in our laboratory, we were able to show that 2 mM NAC treatment was able to completely protect against AGE-induced neurite loss [17]. In our current studies, we have shown that 1 mM NAC treatment resulted in the highest levels of intracellular [GSH] in BSA-treated SH-SY5Y cells. Furthermore, 1 mM NAC treatment significantly increased GSH in AGE-treated cells. To assess the effects of NAC in AGE-mediated neurite degeneration, the following functional outcomes were analyzed: neurite length and average number of long neurites per field of view. Consistent with our previous work, AGE treatment significantly compromised neurite morphology as measured by neurite length (Fig. 2.3) and the average number of long neurites per field of view (Fig 2.4). NAC (1 mM) conferred protection against AGE-mediated decrease in neurite length (Fig. 2.3) and loss of long neurites (Fig. 2.4).

2.4.3 BSO Does Response for Depletion of Intracellular GSH

To confirm whether NAC confers protection via its GSH maintaining properties, inhibition of GSH synthesis was required. BSO at concentrations of 10, 100, and 1000 μM was added to media for 72 hours following differentiation. 100 μM BSO led to near complete depletion of GSH, and 1000 μM BSO treatment fell below the level of detection (Fig. 2.5). A 72-hour treatment of 1000 μM BSO was determined to be optimum for complete GSH depletion in differentiated SH-SY5Y cells.

2.4.4 The Effect of BSO Treatment on Control SH-SY5Y Cells

While establishing the dose response for BSO-induced GSH depletion, it was noted that there were also changes in cell morphology with BSO treatment. Treatment of SH-SY5Y cells with 1000 μM BSO resulted in a decrease in neurite length (Fig. 2.6). Co-treatment of cells with both BSO and 2 mM NAC protected neurite morphology, however 1 mM NAC co-treatment did not confer protection (Fig. 2.6). No significant differences among groups were observed for number of long neurites, but trends were similar (Fig. 2.7). Representative photos of each group are shown in figure 2.8. BSO (1000 μM) also significantly decreased viability, and both 1 and 2 mM NAC co-treatment conferred partial protection (Fig. 2.9). Co-treatment of cells with 1000 μM BSO and NAC had a very minor impact on intracellular GSH (~0.6 and 0.3 nmol/mg for 1 mM and 2 mM NAC, respectively), suggesting NAC protection was not GSH-dependent (Fig. 2.10).

2.4.5 The Effect of BSO Treatment on AGE-treated SH-SY5Y Cells

Depletion of intracellular GSH followed by AGE treatment led to a complete loss of neurites in SH-SY5Y cells (Figs. 2.11, 2.12, 2.13). Only SH-SY5Y cells treated with vehicle (no BSO) for 3 days followed by AGE treatment had quantifiable neurites (Fig. 2.12 & 2.13). BSO (1000 μM) completely depleted GSH (~0-.003 nmol/mg protein) in all groups (Fig. 2.14), and NAC conferred no protection against either AGE or AGE-BSO-induced loss of viability (Fig. 2.15). When GSH synthesis was inhibited with BSO, NAC did not confer protection against AGE-mediated neurite damage, decrease in viability, and loss of GSH.

2.5 Discussion

Hyperglycemia induced oxidative stress is a major source of damage to peripheral neurons in diabetic patients [31]. Therefore, understanding mechanisms leading to the protection and maintenance of endogenous antioxidants, such as GSH, is the first step to discovery of novel therapeutic treatments and/or substances. In this study, we confirmed previous results from our laboratory showing that NAC confers complete protection against AGE-induced neurite retraction in differentiated SH-SY5Y cells. Analysis of changes to neurite morphology was done by quantifying the length of neurites in each treatment group as well as the total number of neurites that exceeded the average length of the control group. This method was developed to quantify the retraction of neurites that was observed when cells were exposed to a stressed condition. The analysis of long neurites was particularly important as diabetic neuropathy commonly presents in a "stocking-glove" distribution, where the longest neurons are damaged first, leading to sensory and motor nerve dysfunction in the extremities [31,32].

In previous studies, we have shown that AGE treatment results in a significant increase in NADPH oxidase-mediated ROS generation [18], and that NAC treatment confers protection against AGE-induced depletion of GSH, DNA oxidation, and protein carbonyl formation [17]. Importantly, only antioxidants that maintained GSH were able to protect against AGE-induced neurite degeneration [17,18]. GSH plays a critical role in protection against ROS and oxidative stress in neurons [33] via multiple mechanisms including its role in maintaining redox status and reduced thiols [34–37], direct interaction with ROS [38], and working synergistically with other antioxidants as part of the endogenous antioxidant defense system (Fig. 2.16) [38]. In our model, NAC treatment clearly results in increased concentrations of GSH in both control and AGE-treated cells. However, it was possible that NAC conferred protection through its intrinsic antioxidant properties as well as through maintenance/protection of GSH.

To determine whether intrinsic antioxidant properties of NAC were responsible for the protection observed, we inhibited GSH synthesis. GSH synthesis was inhibited using BSO, a specific inhibitor of GCL [39]. GCL is the first, and rate limiting, enzyme in GSH synthesis with inhibition resulting in GSH depletion [40]. BSO (1000 μM) treatment for 72 hours resulted in complete GSH depletion in differentiated SH-SY5Y cells. GSH depletion alone led to significantly decreased viability, neurite length, and trended towards loss of long neurites ($p=.053$) demonstrating that GSH plays a critical role in maintenance of neurites in SH-SY5Y cells. To test whether NAC could confer protection against BSO-induced damage, cells were co-treated with BSO and 1-2 mM NAC. Both concentrations of NAC conferred partial protection against BSO-induced viability loss, but only 2 mM NAC protected neurite morphology. These results suggest that NAC, particularly at higher concentrations, can confer protection via a non-GSH mediated mechanism.

Non-GSH mediated protection of NAC was observed under control conditions (no AGE stress) against BSO-induced neurite retraction. However, NAC did not confer any protection against AGE-treated SH-SY5Y cells that were depleted of GSH. The combination of GSH depletion followed by AGE-induced stress resulted in a complete loss of neurites and dramatic loss in viability. Again, NAC conferred no protection under these conditions. We had previously shown that NAC was able to confer complete protection against AGE-induced viability loss [17], and in this study we have shown that NAC also confers complete protection against AGE-induced neurite damage. That NAC loses the entirety of its protective effect upon inhibition of GSH synthesis is strong evidence that NAC confers protection against AGE-induced neurite damage via a GSH-mediated mechanism.

Bioavailability of native NAC in humans is low due to intestinal deacetylation (oral formulation) and first-pass metabolism, and by deacetylation in the liver (oral and intravenous formulation) [16,41]. Therefore, the protective effects of NAC that are due to its intrinsic antioxidant properties observed in *in vitro* studies may not translate in *in vivo* models. In agreement with our results, NAC has been shown to confer protection in *in vivo* models against peripheral nerve injury. Intraperitoneal injection of NAC in rats conferred protection against chronic constriction injury-induced mechanical, thermal, and cold allodynia [33]. In another rat model, sciatic nerve axotomy induced a 21% loss of neurons in the axotomized ganglia. Rats treated with intravenous NAC post-operatively experienced near complete protection of neurons in the axotomized ganglia, with only a 3% loss of neurons [42]. In a long-term study of diabetic neuropathy in rats, seven weeks of oral administration of NAC in diabetic animals conferred significant protection against diabetes-induced thermal hyperalgesia and motor deficits. Analysis of the sciatic nerve showed that diabetic animals experienced depletion of GSH and protein thiols, however NAC-treated diabetic animals did not differ from controls [9].

In our study we have shown that GSH is critical for the maintenance of neurites, as simple inhibition of GSH synthesis leads to neurite retraction. We have also shown that NAC confers protection against AGE-induced neurite damage via an exclusively GSH-mediated mechanism. Future studies will focus on evaluating the effectiveness of other GSH-inducing substances, identifying the mechanisms of neurite retraction, and identifying why GSH is critical for neurite protection.

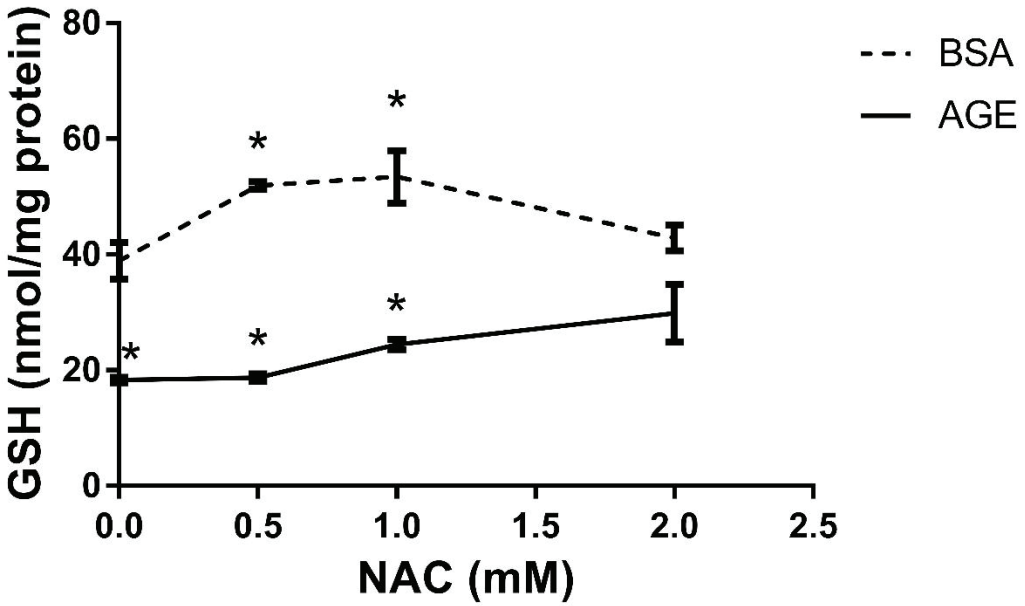

Figure 2.1 Effect of NAC pre-treatment on GSH concentrations of BSA- and AGE-treated SH-SY5Y cells.

Differentiated cells were treated with vehicle, 0.5, 1, and 2 mM NAC for 24 hours prior to BSA or AGE treatment. Cells were treated with 5 mg/mL BSA or AGE for 24 hours with replenishment of NAC treatment. GSH concentrations were normalized to total protein. Data were analyzed by one-way ANOVA with Dunnett's post-hoc analysis from 3 independent experiments. Data points with an * are significantly different ($p < 0.05$) from the vehicle treated BSA group.

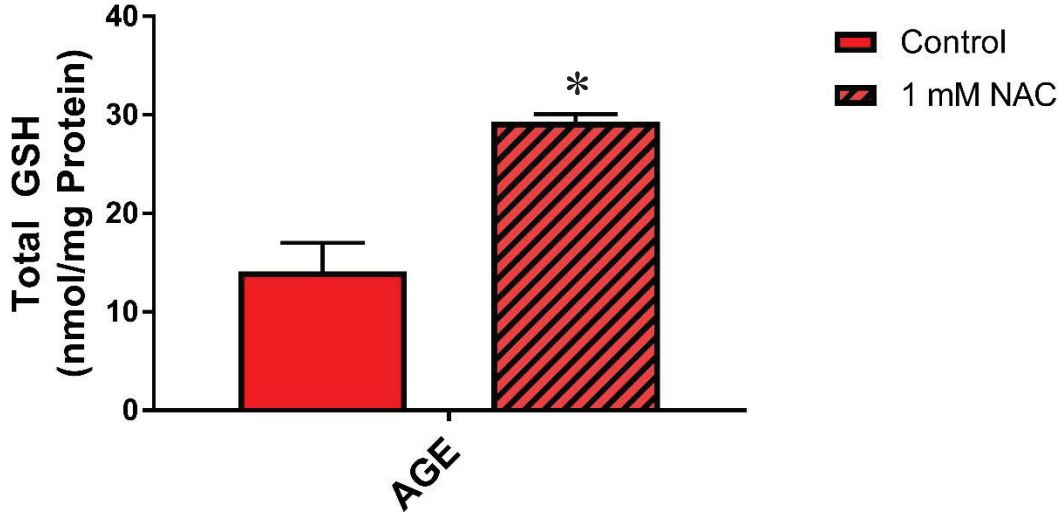

Figure 2.2 NAC (1 mM) pre-treatment protects against AGE-induced GSH depletion.

Differentiated cells were treated with 1 mM NAC 24 hours prior to a 24-hour 5 mg/mL AGE treatment. NAC (1 mM) was replenished during the 24-hour AGE treatment. GSH concentrations were normalized to total protein. Data were analyzed via 2-tailed unpaired Student's t-test from 3 independent experiments. Bars with an * are significantly different ($p < 0.05$) from the control group.

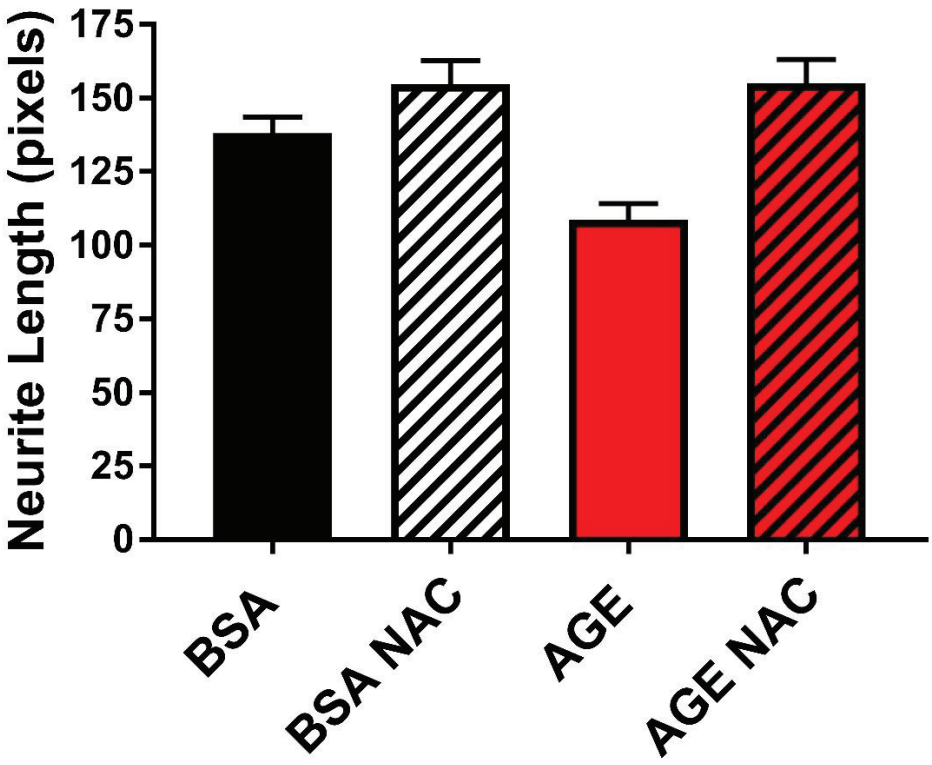

Figure 2.3 NAC pre-treatment confers complete protection against AGE-induced neurite retraction.

Differentiated cells were treated with 1 mM NAC 24 hours prior to 5 mg/mL BSA or AGE treatment. NAC (1 mM) was replenished during the 24-hour BSA and AGE treatments. Data were analyzed by one-way ANOVA with Tukey's post-hoc analysis from 6 independent experiments. At least 190 neurites were analyzed per treatment group. Bars with superscript letters different from each other are significantly different ($p < 0.05$).

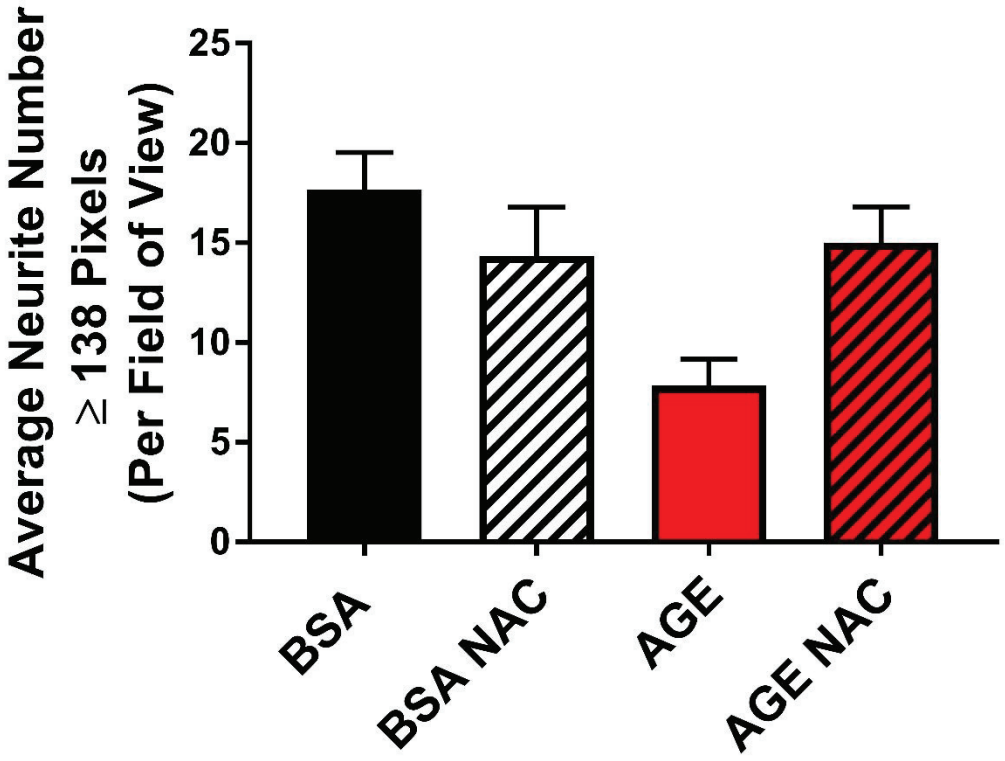

Figure 2.4 NAC pre-treatment confers complete protection against AGE-induced long neurite loss.

Differentiated cells were treated with 1 mM NAC 24 hours prior to 5 mg/mL BSA or AGE treatment. NAC (1 mM) was replenished during the 24-hour BSA and AGE treatments. Data were analyzed by one-way ANOVA with Tukey's post-hoc analysis from 6 independent experiments. At least 190 neurites were analyzed per treatment group. Bars with superscript letters different from each other are significantly different ($p < 0.05$).

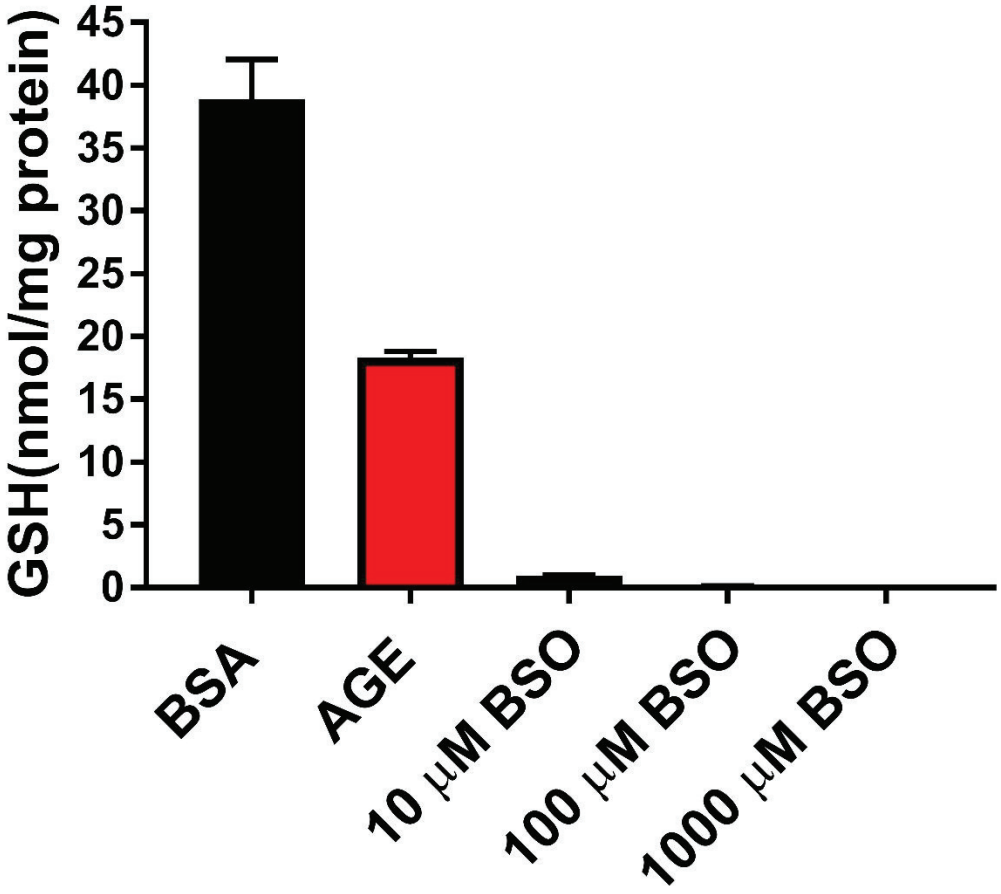

Figure 2.5 BSO (1000 μM) treatment results in depletion of cellular GSH.

Following differentiation, 10, 100, and 1000 μM BSO was added to the media for 72 hours. BSA and AGE groups were treated with 5 mg/mL BSA or AGE, respectively, for 24 hours following differentiation. GSH concentrations were normalized to total protein. Data were analyzed by one-way ANOVA with Tukey's post-hoc analysis from 3-6 independent experiments. Bars with superscript letters different from each other are significantly different ($p < 0.05$).

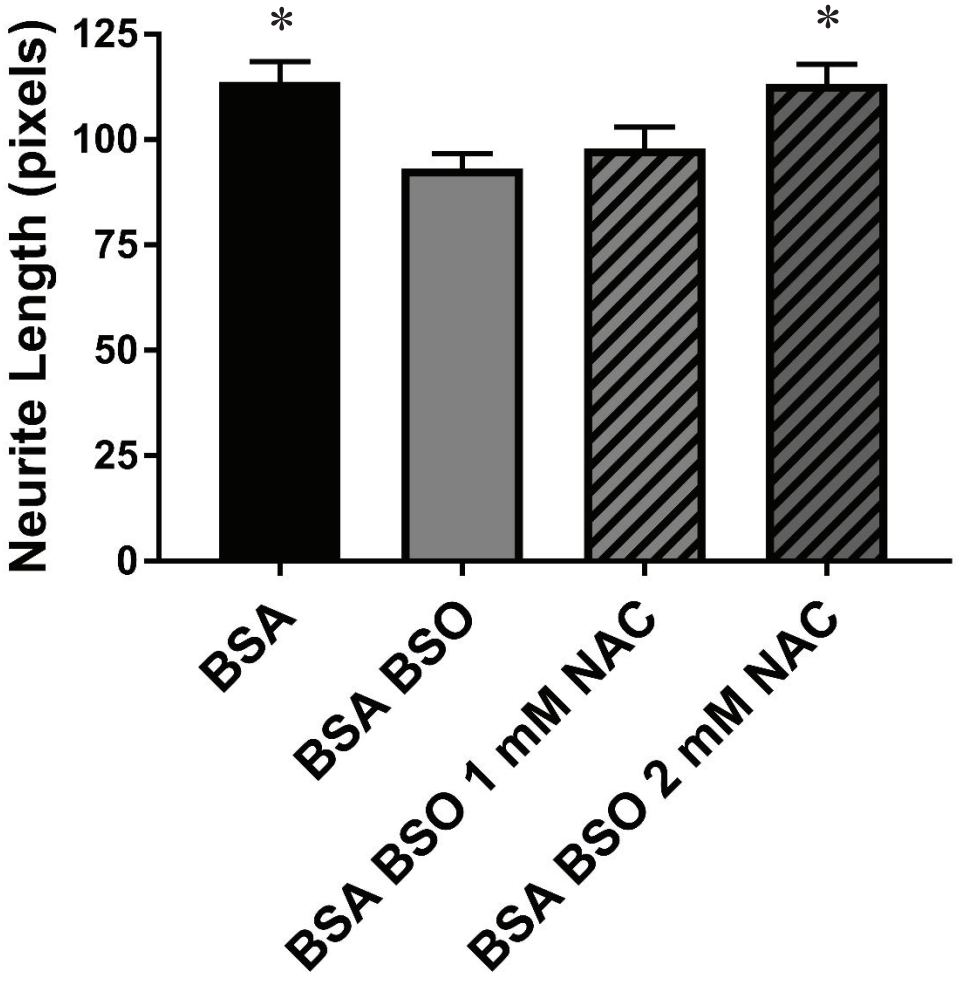

Figure 2.6 BSO treatment induces neurite loss and 2 mM NAC pre-treatment confers protection. Following differentiation, 1000 μM BSO was added to media for 72 hours with 1-2 mM NAC. After the 72-hour treatment, 5 mg/mL BSA was added along with replenishment of BSO and NAC. Data were analyzed by one-way ANOVA with Dunnett's post-hoc analysis from 4 independent experiments. At least 170 neurites were analyzed per treatment group. Bars with an * are significantly different ($p < 0.05$) from the BSA BSO group.

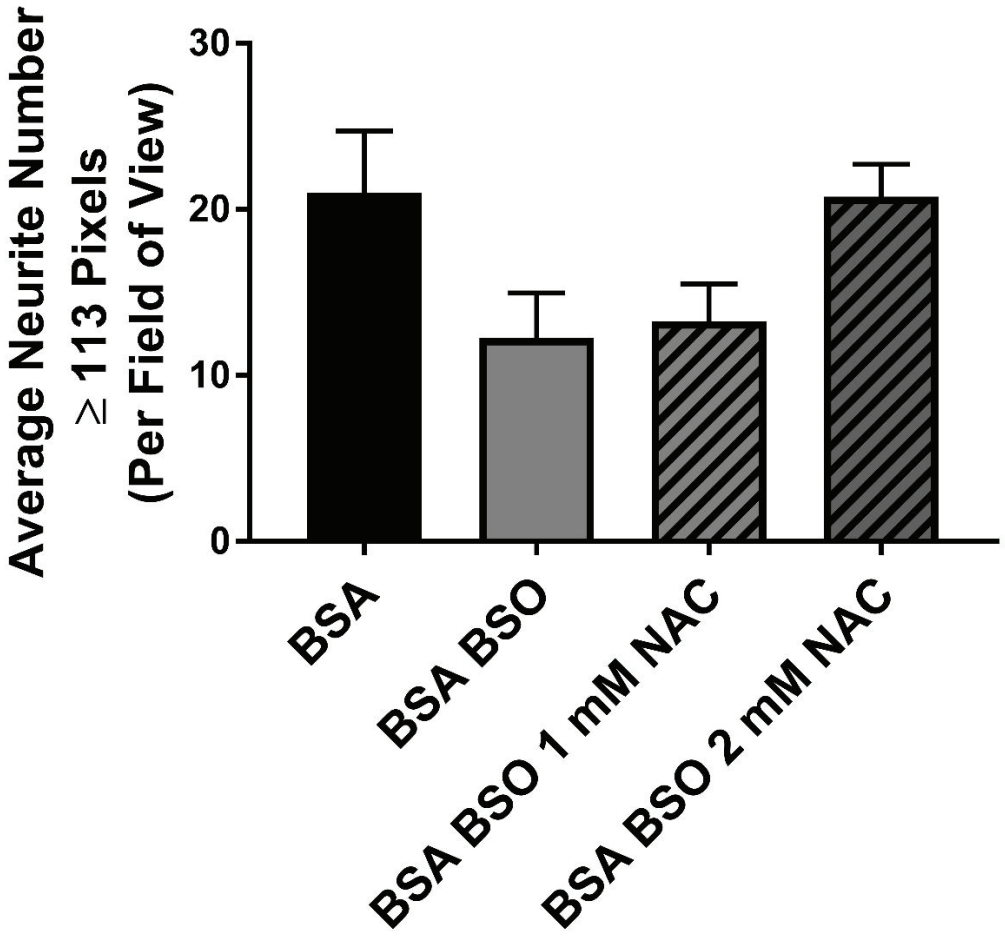

Figure 2.7 BSO treatment has no significant impact on number of long neurites

Following differentiation, 1000 μM BSO was added to media for 72 hours with 1-2 mM NAC. After the 72-hour treatment, 5 mg/mL BSA was added along with replenishment of BSO and NAC. Data were analyzed by one-way ANOVA with Tukey's post-hoc analysis from 4 independent experiments. At least 170 neurites were analyzed per treatment group. Bars with superscript letters different from each other are significantly different ($p < 0.05$).

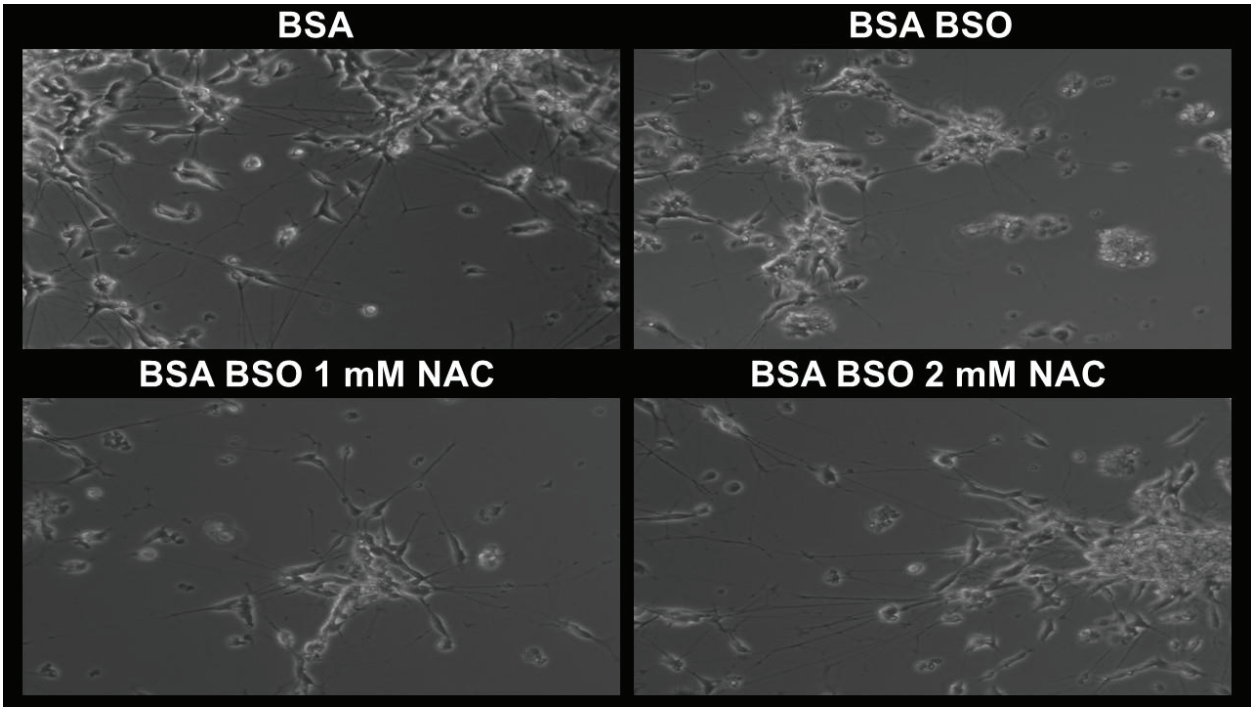

Figure 2.8 BSO treatment induces neurite loss and 2 mM NAC confers protection.

Following differentiation, 1000 μM BSO was added to media for 72 hours with 1-2 mM NAC. After the 72-hour treatment, 5 mg/mL BSA was added along with replenishment of BSO and NAC. Images are representative samples of each treatment group and are captured at 10X.

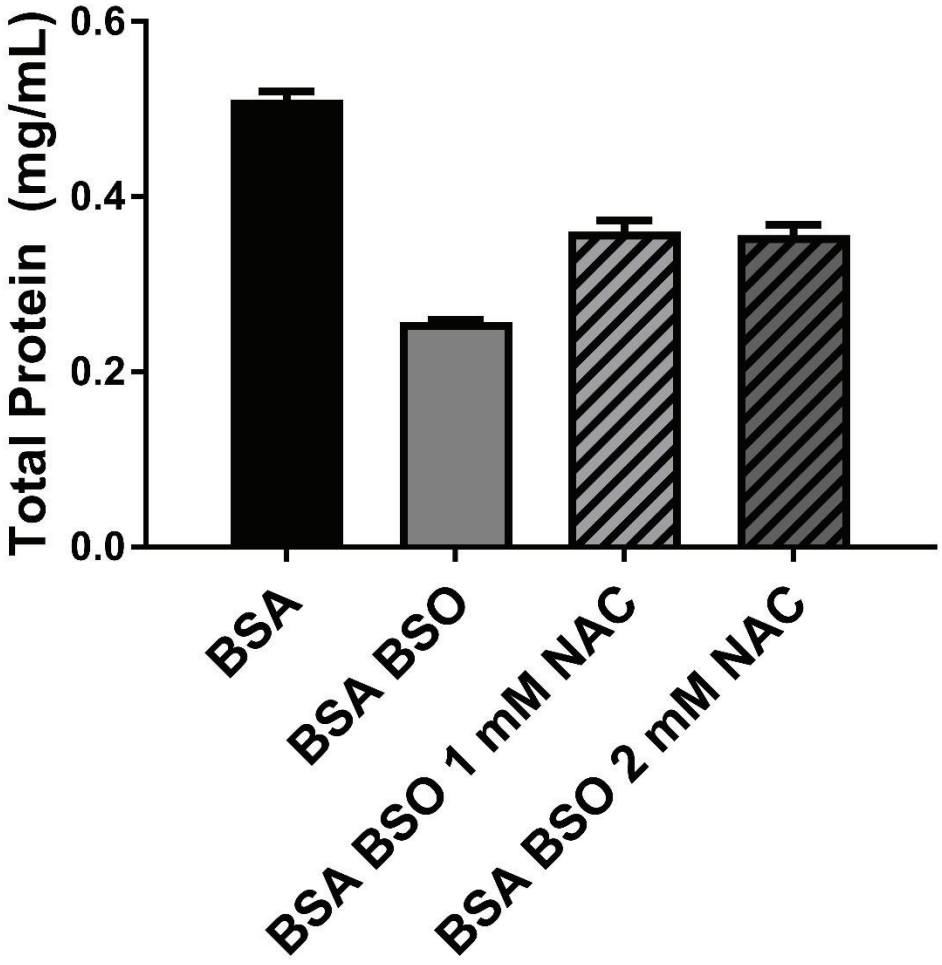

Figure 2.9 BSO treatment decreases viability and NAC pre-treatment confers partial protection.

Following differentiation, 1000 μM BSO was added to media for 72 hours with 1-2 mM NAC. After the 72-hour treatment, 5 mg/mL BSA was added along with replenishment of BSO and NAC. Data were analyzed by one-way ANOVA with Tukey's post-hoc analysis from 3 independent experiments. Bars with superscript letters different from each other are significantly different ($p < 0.05$).

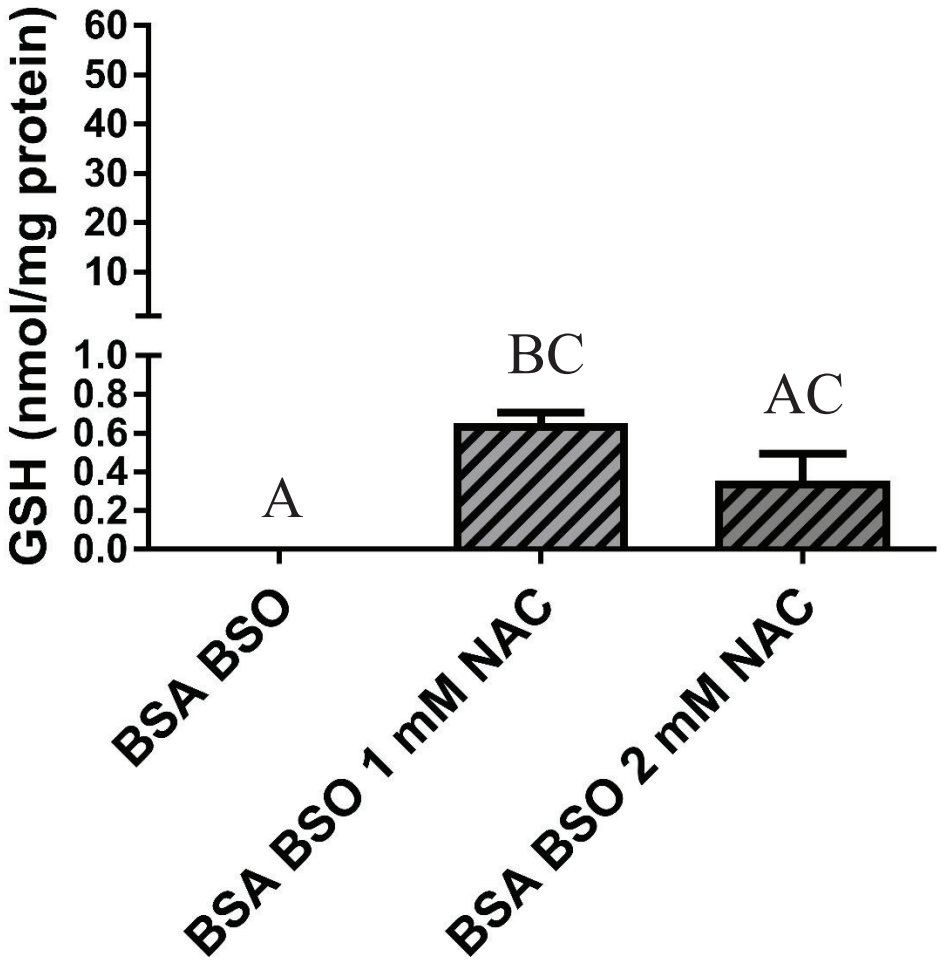

Figure 2.10 NAC does not restore GSH with BSO treatment.

Following differentiation, 1000 μM BSO was added to media for 72 hours with 1-2 mM NAC. After the 72-hour treatment, 5 mg/mL BSA was added along with replenishment of BSO and NAC. GSH concentrations were normalized to total protein. Data were analyzed by one-way ANOVA with Tukey's post-hoc analysis from 3 independent experiments. Bars not joined by a common superscript letter are significantly different from each other ($p < 0.05$).

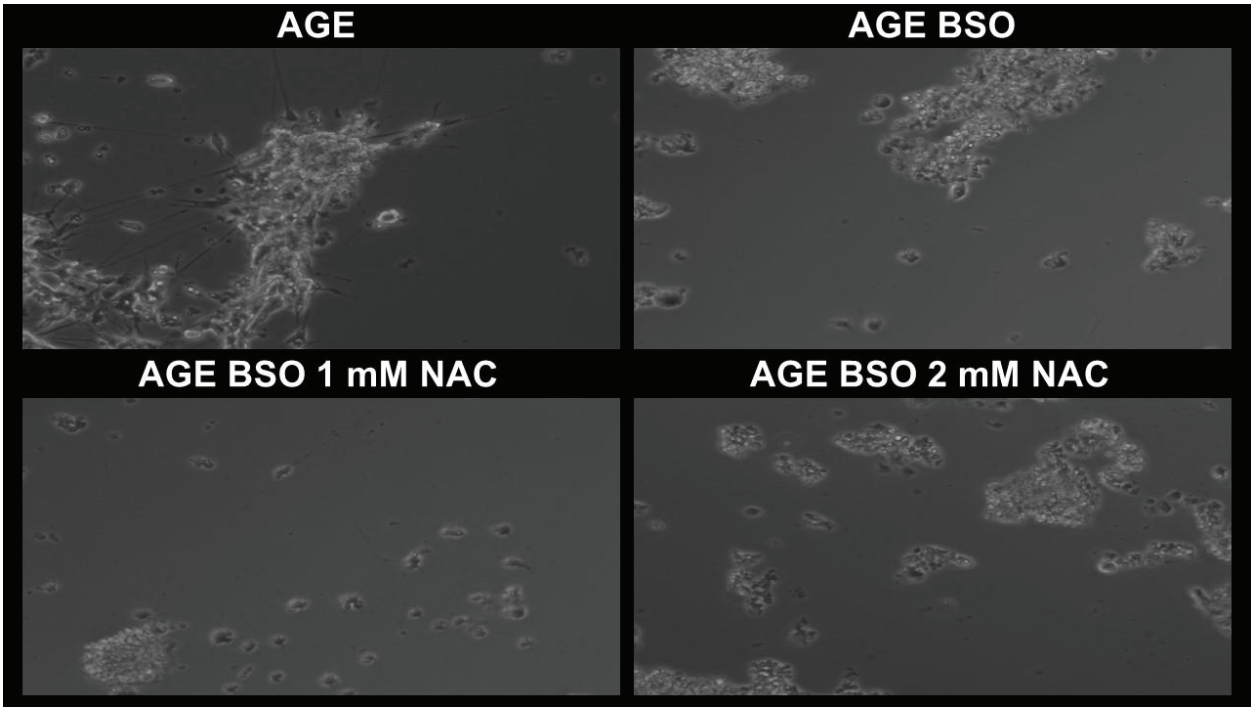

Figure 2.11 NAC does not confer protection against AGE-induced neurite retraction following BSO treatment.

Following differentiation, 1000 μM BSO was added to media for 72 hours with 1-2 mM NAC. After the 72-hour treatment, 5 mg/mL AGE was added along with replenishment of BSO and NAC. Images are representative samples of each treatment group and are captured at 10X.

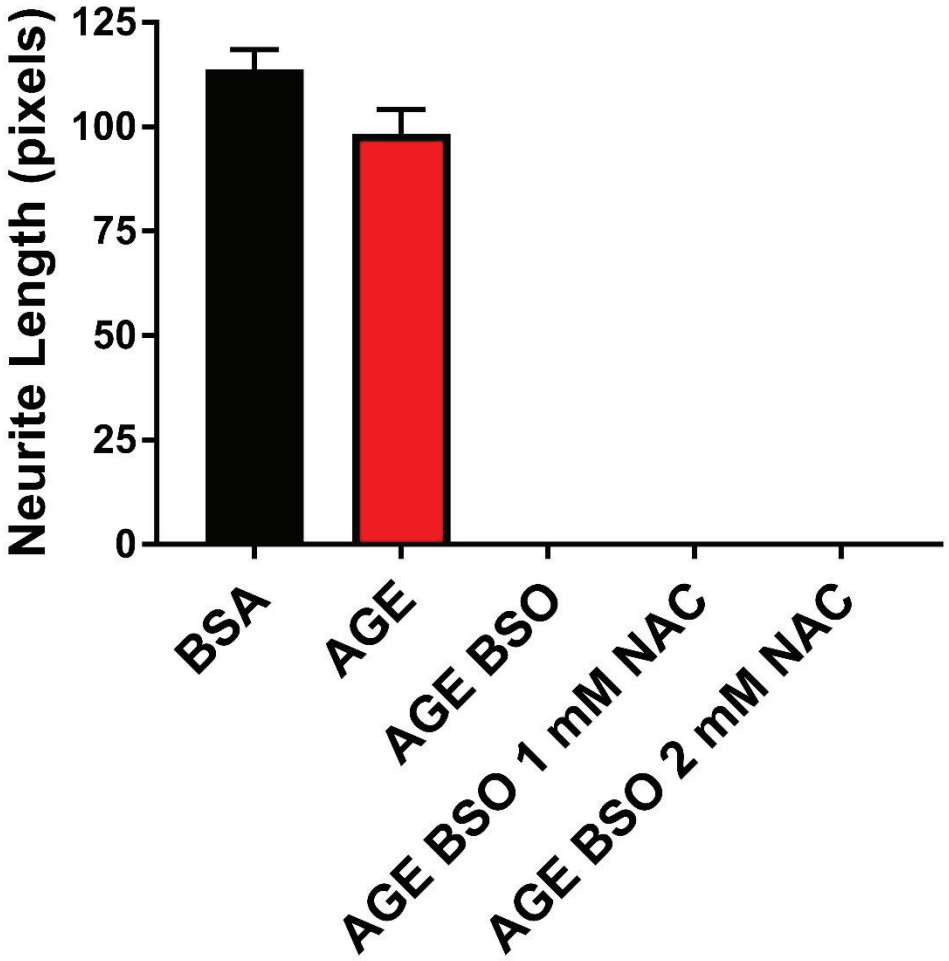

Figure 2.12 NAC does not confer protection against AGE-induced neurite retraction following BSO treatment.

Following differentiation, 1000 μM BSO was added to media for 72 hours with 1-2 mM NAC. After the 72-hour treatment, 5 mg/mL AGE was added along with replenishment of BSO and NAC. Data were analyzed by one-way ANOVA with Tukey's post-hoc analysis from 4 independent experiments. Bars with superscript letters different from each other are significantly different ($p < 0.05$).

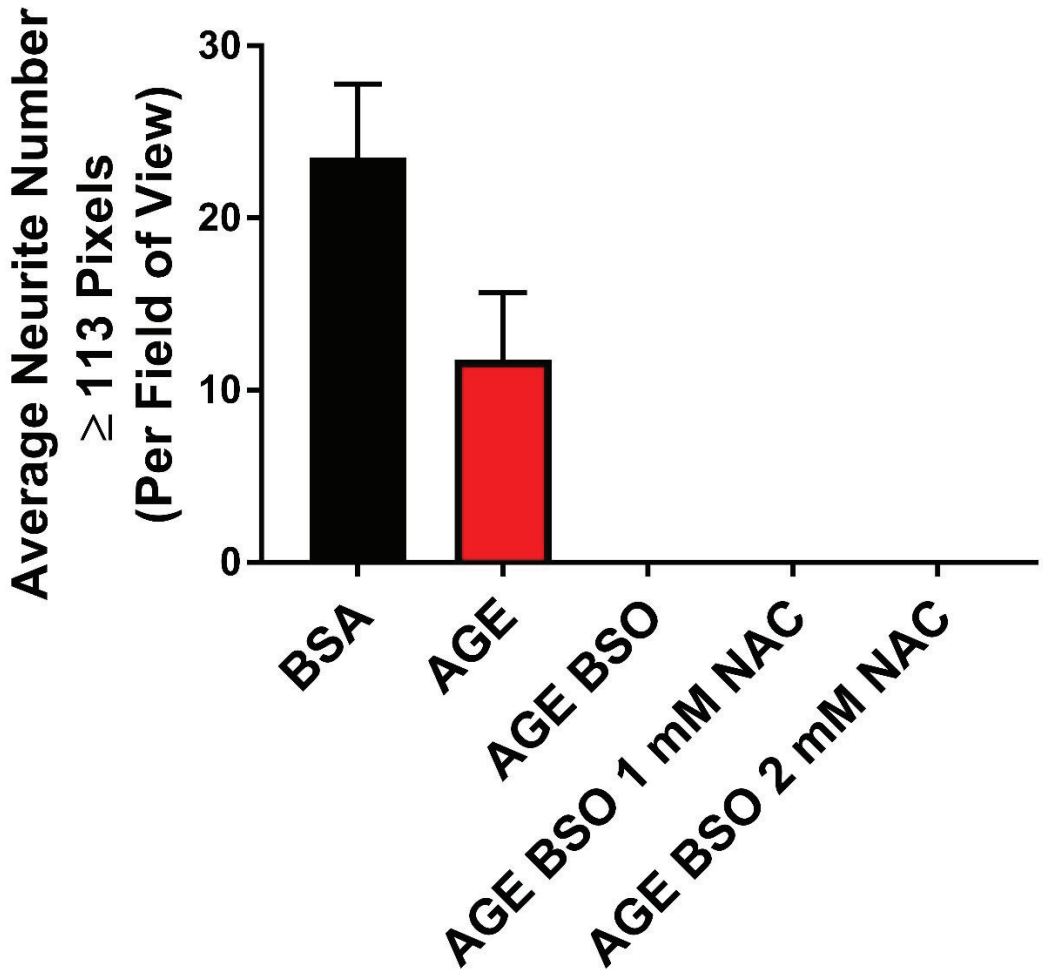

Figure 2.13 NAC does not confer protection against AGE-induced long neurite loss following BSO treatment.

Following differentiation, 1000 μM BSO was added to media for 72 hours with 1-2 mM NAC. After the 72-hour treatment, 5 mg/mL AGE was added along with replenishment of BSO and NAC. Data were analyzed by one-way ANOVA with Tukey's post-hoc analysis from 4 independent experiments. Bars with superscript letters different from each other are significantly different ($p < 0.05$).

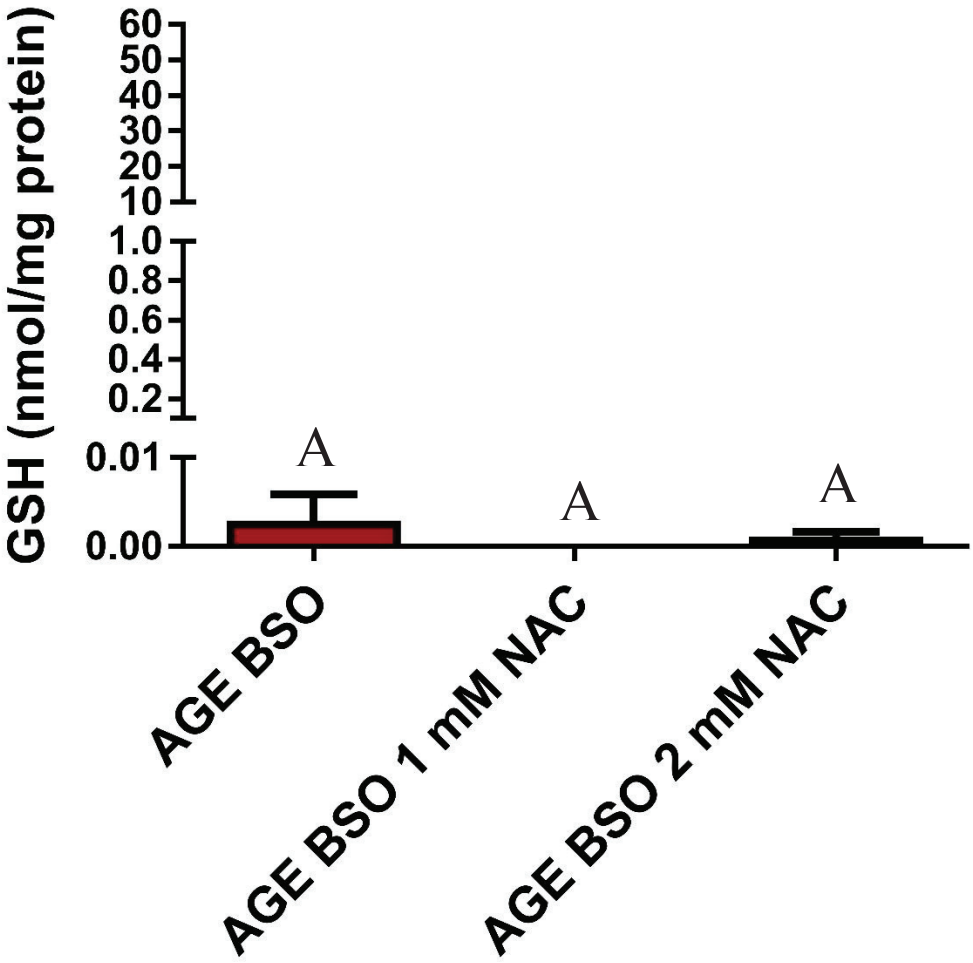

Figure 2.14 NAC pre-treatment does not restore GSH after AGE-BSO treatment.

Following differentiation, 1000 μM BSO was added to media for 72 hours with 1-2 mM NAC. After the 72-hour treatment, 5 mg/mL AGE was added along with replenishment of BSO and NAC. GSH concentrations were normalized to total protein. Data were analyzed by one-way ANOVA with Tukey's post-hoc analysis from 3 independent experiments. Bars with superscript letters different from each other are significantly different ($p < 0.05$).

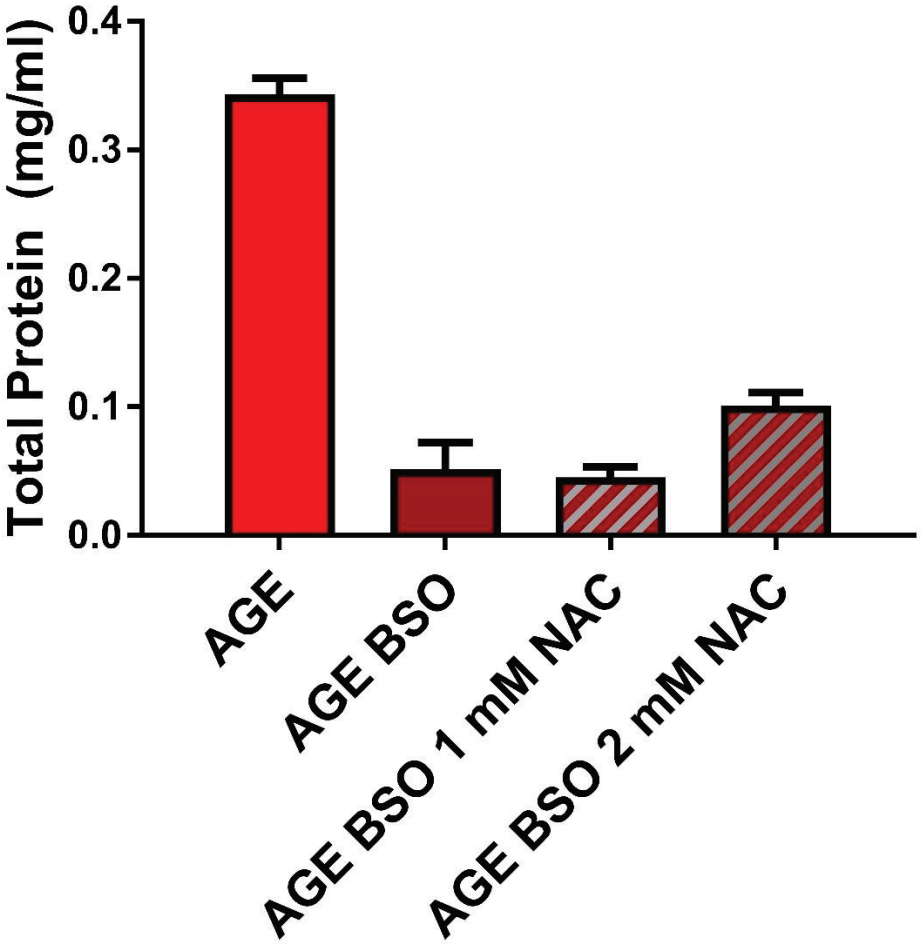

Figure 2.15 NAC does not confer protection against AGE-BSO-induced viability loss.

Following differentiation, 1000 μM BSO was added to media for 72 hours with 1-2 mM NAC. After the 72-hour treatment, 5 mg/mL AGE was added along with replenishment of BSO and NAC. Data were analyzed by one-way ANOVA with Tukey's post-hoc analysis from 3 independent experiments. Bars with superscript letters different from each other are significantly different ($p < 0.05$).

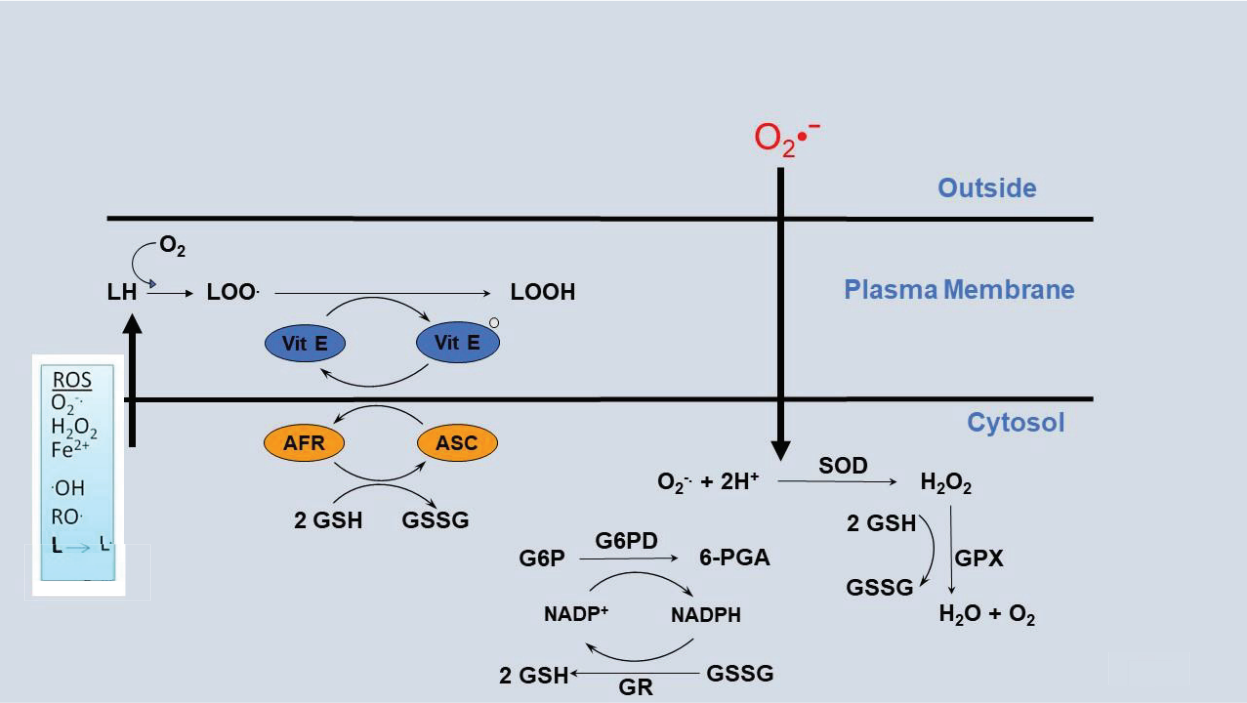

Figure 2.16 Synergistic role of GSH in the endogenous antioxidant defense system.

Lipid (LH); lipid peroxyl radical (LOO·); lipid hydroperoxide (LOOH); α-tocopherol (Vit E); tocopheryl radical (Vit E°); ascorbate (ASC); ascorbate free radical (AFR); glucose-6-phosphate dehydrogenase (G6PD); glucose-6-phosphate (G6P); 6-phosphogluconate (6-PGA); glutathione reductase (GR); glutathione peroxidase (GPX); superoxide dismutase (SOD). Vit E reduces reactive LOO· to LOOH to protect/prevent against a chain reaction of phospholipid fatty acid oxidation. This process generates Vit E°, which is then reduced back to Vit E by ASC. ASC is maintained in its reduced state by a GSH-dependent enzymatic reaction. GPX reduces hydrogen peroxide at the expense of GSH. Pro-oxidative conditions will lead to depletion of GSH and a buildup of GSSG. GR reduces GSSG to GSH at the expense of NADPH. G6PD is the major cellular generator of NADPH.

2.6 References

[1] A.L. Jones, Mechanism of action and value of N-acetylcysteine in the treatment of early and late acetaminophen poisoning: a critical review., J. Toxicol. Clin. Toxicol. 36 (1998) 277–85. http://www.ncbi.nlm.nih.gov/pubmed/9711192 (accessed April 18, 2018).

[2] J.T. Slattery, J.M. Wilson, T.F. Kalhorn, S.D. Nelson, Dose-dependent pharmacokinetics of acetaminophen: Evidence of glutathione depletion in humans, Clin. Pharmacol. Ther. 41 (1987) 413–418. doi:10.1038/clpt.1987.50.

[3] M.B. Reid, D.S. Stokić, S.M. Koch, F.A. Khawli, A.A. Leis, N-acetylcysteine inhibits muscle fatigue in humans., J. Clin. Invest. 94 (1994) 2468–74. doi:10.1172/JCI117615.

[4] I. Medved, M.J. Brown, A.R. Bjorksten, K.T. Murphy, A.C. Petersen, S. Sostaric, X. Gong, M.J. McKenna, *N* -acetylcysteine enhances muscle cysteine and glutathione availability and attenuates fatigue during prolonged exercise in endurance-trained individuals, J. Appl. Physiol. 97 (2004) 1477–1485. doi:10.1152/japplphysiol.00371.2004.

[5] C.A. Haber, T.K.T. Lam, Z. Yu, N. Gupta, T. Goh, E. Bogdanovic, A. Giacca, I.G. Fantus, N-acetylcysteine and taurine prevent hyperglycemia-induced insulin resistance in vivo: possible role of oxidative stress., Am. J. Physiol. Endocrinol. Metab. 285 (2003) E744-53. doi:10.1152/ajpendo.00355.2002.

[6] S. Neri, S.S. Signorelli, B. Torrisi, D. Pulvirenti, B. Mauceri, G. Abate, L. Ignaccolo, F. Bordonaro, D. Cilio, S. Calvagno, C. Leotta, Effects of antioxidant supplementation on postprandial oxidative stress and endothelial dysfunction: a single-blind, 15-day clinical trial in patients with untreated type 2 diabetes, subjects with impaired glucose tolerance, and healthy controls., Clin. Ther. 27 (2005) 1764–73. doi:10.1016/j.clinthera.2005.11.006.

[7] V. Martina, A. Masha, V.R. Gigliardi, L. Brocato, E. Manzato, A. Berchio, P. Massarenti, F. Settanni, L. Della Casa, S. Bergamini, A. Iannone, Long-term N-acetylcysteine and L-arginine administration reduces endothelial activation and systolic blood pressure in hypertensive patients with type 2 diabetes., Diabetes Care. 31 (2008) 940–4. doi:10.2337/dc07-2251.

[8] S.C. De Rosa, M.D. Zaretsky, J.G. Dubs, M. Roederer, M. Anderson, A. Green, D. Mitra, N. Watanabe, H. Nakamura P, I. Tjioe, S.C. Deresinski, W.A. Moore, S.W. Ela, D. Parks, L.A. Herzenberg, L.A. Herzenberg, N-acetylcysteine replenishes glutathione in HIV infection, Eur. J. Clin. Invest. 30 (2000) 915–929. doi:10.1046/j.1365-2362.2000.00736.x.

[9] S.S. Kamboj, R.K. Vasishta, R. Sandhir, N-acetylcysteine inhibits hyperglycemia-induced oxidative stress and apoptosis markers in diabetic neuropathy., J. Neurochem. 112 (2010) 77–91. doi:10.1111/j.1471-4159.2009.06435.x.

[10] M. Arakawa, Y. Ito, N-acetylcysteine and neurodegenerative diseases: Basic and clinical pharmacology, The Cerebellum. 6 (2007) 308–314. doi:10.1080/14734220601142878.

[11] D. Marmolino, M. Manto, Past, present and future therapeutics for cerebellar ataxias., Curr. Neuropharmacol. 8 (2010) 41–61. doi:10.2174/157015910790909476.

[12] J.D. Rothstein, L.A. Bristol, B. Hosler, R.H. Brown, R.W. Kuncl, Chronic inhibition of superoxide dismutase produces apoptotic death of spinal neurons, Proc. Natl. Acad. Sci. 91 (1994) 4155–4159. doi:10.1073/PNAS.91.10.4155.

[13] K.R. Atkuri, J.J. Mantovani, L.A. Herzenberg, L.A. Herzenberg, N-Acetylcysteine--a safe antidote for cysteine/glutathione deficiency., Curr. Opin. Pharmacol. 7 (2007) 355–9. doi:10.1016/j.coph.2007.04.005.

[14] A. Dhar, I. Dhar, K.M. Desai, L. Wu, Methylglyoxal scavengers attenuate endothelial dysfunction induced by methylglyoxal and high concentrations of glucose., Br. J. Pharmacol. 161 (2010) 1843–56. doi:10.1111/j.1476-5381.2010.01017.x.

[15] C.Y. Yan, G. Ferrari, L.A. Greene, N-acetylcysteine-promoted survival of PC12 cells is glutathione-independent but transcription-dependent., J. Biol. Chem. 270 (1995) 26827–32. doi:10.1074/JBC.270.45.26827.

[16] I.A. Cotgreave, N-acetylcysteine: pharmacological considerations and experimental and clinical applications., Adv. Pharmacol. 38 (1997) 205–27. http://www.ncbi.nlm.nih.gov/pubmed/8895810 (accessed April 27, 2018).

[17] R. Pazdro, J.R. Burgess, Differential effects of α-tocopherol and N-acetyl-cysteine on advanced glycation end product-induced oxidative damage and neurite degeneration in SH-SY5Y cells., Biochim. Biophys. Acta. 1822 (2012) 550–6. doi:10.1016/j.bbadis.2012.01.003.

[18] R. Pazdro, J.R. Burgess, The antioxidant 3H-1,2-dithiole-3-thione potentiates advanced glycation end-product-induced oxidative stress in SH-SY5Y cells., Exp. Diabetes Res. 2012 (2012) 137607. doi:10.1155/2012/137607.

[19] N.G. Hattangady, M.S. Rajadhyaksha, A brief review of in vitro models of diabetic neuropathy., Int. J. Diabetes Dev. Ctries. 29 (2009) 143–9. doi:10.4103/0973-3930.57344.

[20] E.L. Feldman, K.-A. Nave, T.S. Jensen, D.L.H. Bennett, New Horizons in Diabetic Neuropathy: Mechanisms, Bioenergetics, and Pain, Neuron. 93 (2017) 1296–1313. doi:https://doi.org/10.1016/j.neuron.2017.02.005.

[21] A.M. Vincent, L. Perrone, K. a Sullivan, C. Backus, A.M. Sastry, C. Lastoskie, E.L. Feldman, Receptor for advanced glycation end products activation injures primary sensory neurons via oxidative stress., Endocrinology. 148 (2007) 548–58. doi:10.1210/en.2006-0073.

[22] I.K. Lukic, P.M. Humpert, P.P. Nawroth, A. Bierhaus, The RAGE pathway: activation and perpetuation in the pathogenesis of diabetic neuropathy., Ann. N. Y. Acad. Sci. 1126 (2008) 76–80. doi:10.1196/annals.1433.059.

[23] R. Wada, S. Yagihashi, Role of advanced glycation end products and their receptors in development of diabetic neuropathy., Ann. N. Y. Acad. Sci. 1043 (2005) 598–604. doi:10.1196/annals.1338.067.

[24] H. Vlassara, The AGE-receptor in the pathogenesis of diabetic complications., Diabetes. Metab. Res. Rev. 17 (2001) 436–43. http://www.ncbi.nlm.nih.gov/pubmed/11757079 (accessed September 23, 2014).

[25] T. Sato, M. Iwaki, N. Shimogaito, X. Wu, S.-I. Yamagishi, M. Takeuchi, TAGE (toxic AGEs) theory in diabetic complications., Curr. Mol. Med. 6 (2006) 351–8. http://www.ncbi.nlm.nih.gov/pubmed/16712480 (accessed September 23, 2014).

[26] M. Jack, D. Wright, Role of advanced glycation endproducts and glyoxalase I in diabetic peripheral sensory neuropathy., Transl. Res. 159 (2012) 355–65. doi:10.1016/j.trsl.2011.12.004.

[27] M. Nitti, A.L. Furfaro, N. Traverso, P. Odetti, D. Storace, D. Cottalasso, M.A. Pronzato, U.M. Marinari, C. Domenicotti, PKC delta and NADPH oxidase in AGE-induced neuronal death, Neurosci. Lett. 416 (2007) 261–265. doi:10.1016/j.neulet.2007.02.013.

[28] M. Nitti, C. d'Abramo, N. Traverso, D. Verzola, G. Garibotto, A. Poggi, P. Odetti, D. Cottalasso, U.M. Marinari, M.A. Pronzato, C. Domenicotti, Central role of PKCδ in glycoxidation-dependent apoptosis of human neurons, Free Radic. Biol. Med. 38 (2005) 846–856. doi:10.1016/j.freeradbiomed.2004.12.002.

[29] F.J. Romero, E. Monsalve, C. Hermenegildo, F.J. Puertas, V. Higueras, E. Nies, J. Segura-Aguilar, J. Romá, Oxygen toxicity in the nervous tissue: comparison of the antioxidant defense of rat brain and sciatic nerve., Neurochem. Res. 16 (1991) 157–61. http://www.ncbi.nlm.nih.gov/pubmed/1908956 (accessed November 2, 2014).

[30] I. Rahman, A. Kode, S.K. Biswas, Assay for quantitative determination of glutathione and glutathione disulfide levels using enzymatic recycling method, Nat. Protoc. 1 (2007) 3159–3165. doi:10.1038/nprot.2006.378.

[31] J.L. Edwards, A.M. Vincent, H.T. Cheng, E.L. Feldman, Diabetic neuropathy: mechanisms to management., Pharmacol. Ther. 120 (2008) 1–34. doi:10.1016/j.pharmthera.2008.05.005.

[32] M. Sinnreich, B. V. Taylor, P.J.B. Dyck, Diabetic Neuropathies, Neurologist. 11 (2005) 63–79. doi:10.1097/01.nrl.0000156314.24508.ed.

[33] A.K. Naik, S.K. Tandan, S.P. Dudhgaonkar, S.H. Jadhav, M. Kataria, V.R. Prakash, D. Kumar, Role of oxidative stress in pathophysiology of peripheral neuropathy and modulation by N-acetyl-l-cysteine in rats, Eur. J. Pain. 10 (2006) 573–573. doi:10.1016/j.ejpain.2005.08.006.

[34] C.H. Lillig, C. Berndt, A. Holmgren, Glutaredoxin systems, Biochim. Biophys. Acta - Gen. Subj. 1780 (2008) 1304–1317. doi:10.1016/j.bbagen.2008.06.003.

[35] A.P. Fernandes, A. Holmgren, Glutaredoxins: Glutathione-Dependent Redox Enzymes with Functions Far Beyond a Simple Thioredoxin Backup System, Antioxid. Redox Signal. 6 (2004) 63–74. doi:10.1089/152308604771978354.

[36] J. Lu, A. Holmgren, The thioredoxin antioxidant system, Free Radic. Biol. Med. 66 (2014) 75–87. doi:10.1016/J.FREERADBIOMED.2013.07.036.

[37] B. Carletti, C. Passarelli, M. Sparaco, G. Tozzi, A. Pastore, E. Bertini, F. Piemonte, Effect of protein glutathionylation on neuronal cytoskeleton: a potential link to neurodegeneration, Neuroscience. 192 (2011) 285–294. doi:10.1016/j.neuroscience.2011.05.060.

[38] A.J. Cooper, B.S. Kristal, Multiple roles of glutathione in the central nervous system., Biol. Chem. 378 (1997) 793–802. http://www.ncbi.nlm.nih.gov/pubmed/9377474 (accessed May 25, 2018).

[39] O.W. Griffith, A. Meister, Potent and specific inhibition of glutathione synthesis by buthionine sulfoximine (S-n-butyl homocysteine sulfoximine)., J. Biol. Chem. 254 (1979) 7558–60. http://www.ncbi.nlm.nih.gov/pubmed/38242 (accessed May 25, 2018).

[40] M.E. Gegg, J.B. Clark, S.J.R. Heales, Determination of glutamate-cysteine ligase (gamma-glutamylcysteine synthetase) activity by high-performance liquid chromatography and electrochemical detection., Anal. Biochem. 304 (2002) 26–32. doi:10.1006/abio.2001.5607.

[41] D. Marmolino, M. Manto, Past, present and future therapeutics for cerebellar ataxias., Curr. Neuropharmacol. 8 (2010) 41–61. doi:10.2174/157015910790909476.

[42] A.. Hart, G. Terenghi, J.-O. Kellerth, M. Wiberg, Sensory neuroprotection, mitochondrial preservation, and therapeutic potential of n-acetyl-cysteine after nerve injury, Neuroscience. 125 (2004) 91–101. doi:10.1016/j.neuroscience.2003.12.040.

CHAPTER 3. D3T POTENTIATES ADVANCED GLYCATION END PRODUCT INDUCED OXIDATIVE STRESS IN A CELL CULTURE MODEL OF DIABETIC PERIPHERAL NEUROPATHY

3.1 Abstract

Diabetes mellitus is one of the most common chronic diseases and peripheral neuropathy (PN) affects at least 50% of diabetic patients. Medications available for patients ameliorate symptoms (pain), but do not protect against cellular damage and come with severe side effects leading to discontinued use. In our lab we use differentiated SH-SY5Y cells treated with advanced glycation end products (AGE) as a model to mimic diabetic conditions and to study the mechanisms of oxidative stress (OS) mediated cell damage and antioxidant protection. N-acetylcysteine (NAC), a common supplement, was previously shown in our lab to fully protect against AGE-induced damage. Our lab has also shown that 3H-1,2-dithiole-3-thione (D3T), a cruciferous vegetable constituent and potent inducer of nuclear factor (erythroid-derived 2)- like (Nrf2), can significantly increase cellular GSH concentrations and protect against H_2O_2–induced cell death. Paradoxically, D3T conferred no protection against AGE-induced cell death or neurite degeneration. In the present study we show that D3T in combination with AGE increased reactive oxygen species (ROS) generation, depleted GSH, and increased glucose-6-phosphate dehydrogenase (G6PD) expression, suggesting its role as an NADPH generating agent may promote OS rather than provide protection under these conditions. D3T further contributed to depletion of GSH in combination with AGE challenge by significantly depressing glutathione reductase activity. Inhibition of NADPH generation via G6PD, the protein product of a Nrf2-responsive gene, with dehydroepiandrosterone was found to protect against AGE-induced ROS generation, loss of viability, and neurite degeneration. These results suggest that using a strategy

to protect against oxidative stress by upregulation of the endogenous antioxidant defense system via Nrf2 may backfire and promote further damage if the products of upregulation contribute to ROS generation.

3.2 Introduction

Diabetes mellitus, a disease hallmarked by hyperglycemia, is one of the most common chronic diseases worldwide with new diagnoses on an upward trajectory. By some estimates, 30.3 million Americans live with diabetes[1]. The high incidence of diabetes poses both a public health as well as a financial concern. Direct annual medical costs for diabetes treatment in recent years has reached $176 billion[2]. Therefore, there has been growing interest in identifying new and easily accessible preventive compounds that may alleviate diabetic health complications.

Peripheral neuropathy (PN) is one of the most common health complications in type 1 and 2 diabetics, with oxidative stress implicated as a major contributor to diabetes-induced PN[3]. An underlying cause of oxidative stress-induced complications in diabetes, including PN, is the accumulation of Advanced Glycation End Products (AGEs) in circulation and tissues [4–8]. The products of non-enzymatic glycation of proteins, AGEs accumulate in peripheral nerves of diabetic patients [9]. Through binding the receptor for AGE (RAGE) in target tissues, AGEs stimulate oxidative stress through downstream activation of NADPH oxidase in a PKCδ-dependent manner [10,11]. The resulting increase in reactive oxygen species (ROS) facilitates damage in peripheral neurons [4]. Given the above mechanism of AGE-induced PN, dietary compounds with antioxidant properties have been proposed as potential remediating agents.

Dietary compounds with antioxidant properties may provide benefit through a variety of mechanisms [12–14]. Some compounds including ascorbate, N-acetylcysteine (NAC) or alpha-tocopherol have intrinsic antioxidant potential. These compounds can either directly neutralize

ROS and free radicals, or in the case of NAC, provide the necessary substrate for synthesis of essential cellular antioxidants such as glutathione (GSH). Other compounds, including 3H-1,2-dithiole-3-thione (D3T), generate an antioxidant effect through stimulating endogenous cellular antioxidant defenses. In the case of D3T, the antioxidant response involves activation of Nuclear factor (erythroid-derived 2)-like 2 (Nrf2) through several potential mechanisms [15–18]. Nrf2, a transcription factor, controls expression of a wide array of target genes including glutathione synthesizing enzymes, quinone reductases, glutathione reductase (GR), as well as NADPH generating enzymes such as glucose-6-phosphate dehydrogenase (G6PD) [14,19–21]. Reduced NADPH resulting from G6PD upregulation serves as a cofactor for GR mediated recycling of oxidized glutathione (GSSG) back to its reduced form (GSH). However, NADPH oxidases (a major source of AGE-induced oxidative stress) [4,9] may also potentially utilize reduced NADPH generated through Nrf2 activation to increase ROS production, stressing the importance of mechanistic context when assessing the benefit of individual antioxidant and phytochemical compounds.

The variable mechanism of action of different antioxidants suggests some compounds may be more suitable than others in protection against diabetic PN. In particular, previous studies from our laboratory demonstrated variable effects of antioxidant compounds on AGE-induced oxidative stress and neurite morphology in the differentiated SH-SY5Y cell model. NAC offered protection from neurite loss as well as protection from DNA and protein oxidation [22]. On the other hand, D3T, a potent Nrf2 inducer, had a paradoxical impact on redox balance in SH-SY5Y cells exposed to AGE. D3T co-treatment promoted AGE-induced ROS formation, did not maintain GSH levels (compared to BSA control group), and did not protect from AGE-induced neurite loss [23]. In the present studies, the mechanism underlying D3T's paradoxical effect on

oxidative stress in the presence of AGEs was investigated. It was hypothesized that D3T mediated induction of NADPH generating antioxidant enzyme G6PD promotes AGE-induced oxidative damage.

3.3 Methods

3.3.1 Materials

Dulbecco's Modified Medium (DMEM), Ham's F12 Medium, penicillin-streptomycin, and fetal bovine serum (FBS) were purchased from Invitrogen (Waltham, MO). All standard cell culture flasks and plates were purchased from ThermoFisher Scientific (Waltham, MO). Black 24-well culture plates for fluorescence analysis were purchased from Cellvis (Sunnyvale, CA). All reagents such as retinoic acid (RA), dehydroepiandrosterone (DHEA), bovine serum albumin (BSA), NAC, D3T, and reagents for GSH, ROS, and GR activity analysis were purchased from Sigma-Aldrich (St. Louis, MO) unless otherwise stated.

3.3.2 Cell Culture

SH-SY5Y cells were purchased from ATCC (Manassas, VA) and were cultured initially in growth media (DMEM, 10% FBS, 1% penicillin-streptomycin, 8 mM glucose) for 24 hours to allow for adherence. Following adherence, growth media was replaced with differentiating media (1:1 DMEM: F12, 1% FBS, 8 mM glucose, 10 μM retinoic acid) for five days to allow for neuronal cell phenotype development. Treatments for all experiments took place following the five-day differentiation period. Cells treated with NAC or D3T had 1 mM NAC (<1% PBS) or 100 μM D3T (<1% DMSO) added to the media 24 hours prior to 5 mg/mL BSA or AGE treatment. This treatment was then replenished in BSA and AGE treatment groups for 24 hours.

For DHEA treated cells, 100 μM DHEA (< 1% DMSO) was added to the media 24 hours prior to BSA or AGE treatment and replenished during the 24-hour BSA or AGE treatment.

3.3.3 Preparation of AGE-BSA and BSA Concentration

AGE-BSA was prepared as was previously reported in our lab [23]. Briefly, 5 mg/mL BSA in PBS was incubated with 33 mM glycolaldehyde dimer for 20 hours at 37°C. Control BSA was treated in the same manner, but without the addition of glycolaldehyde. Both control and glycated BSA were then concentrated via ammonium sulfate precipitation. Ammonium sulfate was added to glycated BSA and control solutions (80% ammonium sulfate solution), and then centrifuged at 10,000g for 30 minutes. Precipitated proteins were resuspended with the minimal amount of PBS required for resuspension. Solutions were then dialyzed in PBS for three days, with daily replacement of PBS. Following dialysis, solutions were sterile filtered. The final concentrations of both glycated and control BSA were approximately 15 mg/mL.

3.3.4 GSH Assay

Reduced GSH, as well as its oxidized form GSSG, were quantified using a colorimetric based assay as described by Rahman *et al*. [24]. SH-SY5Y cells were plated in 6-well plates (9 cm^2) at a concentration of .4 x 10^6. Each well was then pretreated with either NAC, D3T, or vehicle (<1% DMSO or PBS) for 24 hours followed by co-treatment and addition of AGE-BSA or BSA-control for an additional 24 hours. Absorption was measured using a Bio-Tek Powerwave X200 (Winooski, VT) spectrophotometer (abs. 412nm). All values were normalized to protein content using a BCA assay kit (Pierce, Rockford, IL).

3.3.5 ROS Assay

ROS assay was conducted as described previously[25]. Briefly, SH-SY5Y cells were plated on black coated 24-well plates (1.9 cm^2) at a concentration of .08 x $10^6/cm^2$. After differentiation, each well was pre-treated with indicated compounds for 24 hours. followed by an additional 24-hour co-treatment and addition of either AGEs or BSA control. At the end of 48 hours, media was gently removed and 200 µl of 20 µM 2′,7′-dichlorofluorescin diacetate (DCFH-DA) in PBS was added to each well. Intracellular ROS was measured after a 20-minute incubation at 37°C and 5% CO_2 using a Synergy H1 Multi-Mode Reader (ex/em. 485/530). Fluorescence units were further normalized to viable cell number using a 3-(4,5-dimethylthiazol-2-yl)-2,5-diphenyltetrazolium bromide (MTT) assay (Sigma-Aldrich, St. Louis, MO).

3.3.6 Glutathione Reductase Activity

GR activity was measured as described by Mannervik [26]. Briefly, SH-SY5Y cells were plated in 6-well plates (9 cm^2) at a concentration of .4 x 10^6. Each well was then pretreated with either NAC, D3T, or vehicle (<1% DMSO or PBS) for 24 hours followed by co-treatment and addition of AGE-BSA or BSA-control for an additional 24 hours. Absorption was measured using an Agilent Cary 60 (Santa Clara, CA) spectrophotometer (abs. 340 nm) at 30°C over a five-minute period. Activity for each sample was normalized to total DNA. DNA content was measured with 1µL of sample using a Thermo Scientific NanoDrop 2000 (Waltham, MA) spectrophotometer (abs. 260 & 280 nm). Activity is reported as % of BSA control.

3.3.7 Cell Viability Assay

Cell viability was assessed after indicated treatment and duration using MTT, according to the manufacturer's instructions. Briefly, SH-SY5Y cells were plated and differentiated in 24-well plates. At the end of the specified time point, cell media was removed and replaced with

serum free media containing 500ug/mL MTT. Cells were incubated for 2 hours. Formazan product was dissolved using DMSO and quantified using Bio-Tek Powerwave X200 spectrophotometer (abs. 540nm).

3.3.8 Western Blotting

All Western blots were run using a Mini-PROTEAN Tetra Cell system (Bio-rad, Hercules, CA). Both 10% and 4-20% gradient polyacrylamide gels were used. For gel electrophoresis, the running buffer was made up of 25 mM Tris, 192 mM glycine, and .1% (w/v) SDS at pH 8.3. Gels were run at constant voltage (200v) for 30-50 minutes. For protein transfer to nitrocellulose membranes, transfer buffer was made up of 25 mM Tris, .2 M glycine, and 20% methanol at pH 8.5. A constant voltage (90v) for 60 minutes was maintained for transfers. The transfer buffer was refrigerated prior to use, and the entire apparatus was kept cold (approx. 4°C) during protein transfer. Following transfer, blots were incubated based on antibody manufacturer recommendations. For G6PD, GR, and β-actin quantification, blots were incubated for 12 hours on a plate shaker at 4°C with a polyclonal rabbit antibody (1:1000) (Cell Signaling, Danvers, MA) for G6PD, monoclonal mouse antibody (2 µg/mL) (Sigma-Aldrich, St. Louis, MO) for GR, and monoclonal rabbit (1:1000) (Cell Signaling, Danvers, MA) for β-actin. Both anti-rabbit and anti-mouse secondary antibodies (1:1000) were HRP-linked, and an HRP-detection kit followed by photo-development was used (Cell Signaling, Danvers, MA). All G6PD and GR bands were normalized to their corresponding β-actin bands and results reported as % of β-actin.

3.3.9 Neurite Quantification

At the completion of experiments, photos were taken to document morphological changes of differentiated SH-SY5Y cells. Images were captured at 10x magnification using a Zeiss Axio Vert. A1 microscope (Oberkochen, Germany). A Zeiss AxioCam ICm1 camera was used to take

photos using Zeiss Zen2 imaging software. All images were 1388 x 1038 pixels, and exposure time for all photos was 32.03 ms. Images were then analyzed using ImageJ (NIH) software with NeuronJ (ImageScience) plugin. Individual neurites were traced, and neurite length was reported as length in pixels. Neurites present in the field of view were quantified from three to four independent experiments for each treatment group. Exclusion criteria included counting only neurites with clearly defined start and end locations. Neurites that were shorter than the width of the cell body were not counted. For each treatment group, a minimum of 100 total neurites was quantified. To quantify the impact of treatments on the longest neurites, the number of neurites greater than or equal to the average length of neurites in the BSA control group (115 pixels) was calculated for each treatment group.

3.3.10 Statistical Methods

Values are presented as mean ±S.E.M. Comparison of means was conducted using analysis of variance (ANOVA) followed by multiple comparisons of means (Dunnett or Tukey HSD), with $P<0.05$ considered statistically significant.

3.4 Results

3.4.1 Impact of D3T and NAC on GSH status

Previously, Pazdro and Burgess demonstrated that both NAC and D3T increase total GSH in the absence of AGEs, while only NAC exerted a protective effect on GSH in the presence of AGEs [22,23]. To further evaluate this variable effect in SH-SY5Y cells, reduced GSH and its oxidized form GSSG were measured in cells treated with NAC or D3T and AGE challenge or BSA control. Both NAC and D3T significantly increased total GSH in BSA and AGE groups (Fig. 3.1). In addition, NAC and D3T increased reduced GSH levels by 241% and

444%, respectively (Fig. 3.2). Importantly, D3T treatment significantly increased reduced GSH in the absence of AGEs to a greater extent than NAC. This is consistent with the mechanism of action of D3T through Nrf2 induction, where both GSH synthesis and NADPH-dependent recycling of GSSG via GR are upregulated [27]. Hence reduced GSH, in response to D3T, is increased not only through increased synthesis, but also through increased recycling of oxidized GSSG back to its reduced form. In contrast, NAC provides antioxidant protection primarily through providing cysteine as substrate for GSH synthesis [28], independent of NADPH-mediated recycling of GSSG. Consistent with this mechanism, GSSG levels were upregulated in the absence of AGE with NAC treatment while D3T treatment did not significantly increase GSSG under the same conditions (Fig. 3.3). When challenged with AGE, D3T treated SH-S5Y5 cells showed no significant increase in GSH (Fig. 3.2) but a drastic increase in GSSG (Fig. 3.3), showing a pro-oxidative effect of D3T specific to AGE challenge conditions. The 3-fold increase in GSSG with D3T treatment (compared to AGE control group) suggests that GR-mediated recycling of GSSG back to GSH may be impaired under AGE-D3T treated conditions. NAC treatment, on the other hand demonstrated a significant increase in both reduced GSH and GSSG in the presence of AGEs, consistent with AGE-mediated pro-oxidative effect and the protective role of NAC (Fig. 3.2 & 3.3).

3.4.2 Impact of D3T on Cell Viability and ROS Generation

To further assess the paradoxical effect of D3T upon AGE treatment, cell viability after vehicle or D3T and AGE challenge was assessed. SH-SY5Y cells treated with AGEs alone had a significant decrease in cell viability (Fig. 3.4). While D3T had no effect on cell viability in the absence of AGEs, treatment of SH-SY5Y cells with AGEs and D3T resulted in a potentiated effect of AGEs on decreased cell viability (Fig. 3.4). Intracellular ROS levels were further

measured to specifically investigate the potentiation effect of D3T on AGE-induced oxidative stress. Consistent with cell viability data, AGE treatment alone significantly increased intracellular ROS while D3T treatment amplified that effect (Fig. 3.5).

3.4.3 The Effect of D3T on G6PD

Given the potentiation effect of D3T on AGE-induced oxidative stress, and the mechanism of action of AGE through activation of NADPH oxidase, it was hypothesized that D3T promotes AGE-induced oxidative stress through increased generation of reduced NADPH. G6PD, the rate-limiting enzyme of the pentose phosphate pathway, is one of the major contributors to the cellular reduced NADPH pool. It is further a Nrf2 target gene, suggesting that D3T may upregulate G6PD via its Nrf2-mediated mechanism of action. To assess the effect of D3T on G6PD, G6PD protein expression was measured after a D3T treatment in AGE challenge or BSA control conditions. D3T significantly increased G6PD protein expression under BSA control conditions. Interestingly, AGE treatment alone also upregulated G6PD expression relative to BSA-control. Finally, D3T and AGE treatment demonstrated an additive effect on G6PD expression (Fig. 3.6). These findings were consistent with the hypothesis that D3T potentiates AGE-induced oxidative stress via increased G6PD-mediated generation of NADPH that feeds NADPH oxidase and sustains its generation of ROS.

3.4.4 The effect of D3T on Glutathione Reductase

Reducing potential generated by G6PD in the form of NADPH may be utilized by NADPH oxidase or GR, among other enzymes. The potentiation impact of D3T on AGE-induced oxidative stress may therefore result from both upregulating NADPH generation as well as hindering other enzymes that would normally utilize NADPH. To explore this possibility, the impact of D3T treatment on GR was investigated, since GR is a major NADPH utilizing enzyme

in the context of antioxidant defense. D3T treatment under BSA control conditions increased GR protein expression (Fig. 3.7), likely due to its Nrf2 inducing properties and consistent with the profound increase in reduced GSH resulting from D3T treatment in the absence of AGEs. AGE treatment alone also increased GR protein expression, and co-treatment with D3T resulted in no further change (Fig. 3.7). Interestingly, GR activity did not correlate with protein expression in cells challenged with AGE and treated with D3T. In this scenario, D3T treatment unexpectedly resulted in a significant decrease in GR activity (Fig. 3.8). The impact of D3T on GR activity under AGE challenge conditions sheds further light on the mechanism for the D3T paradox. Upregulation of G6PD via D3T helps explain the mechanism for increased ROS generation under AGE challenge, but theoretically this mechanism would also provide more reducing equivalents for GR to maintain GSH. Therefore, the increase in GSSG (3-fold) between AGE and AGE-D3T groups remained perplexing. Our data provide an answer for this apparent disconnect. Treatment with D3T under AGE challenge conditions not only exacerbates ROS generation, but also disrupts GR activity, a critical enzyme necessary for maintaining redox balance, leaving the cells highly susceptible to oxidative damage.

3.4.5 The Effect of DHEA on Cell Viability and ROS Generation

To test the relationship between G6PD and oxidative stress under AGE treatment, DHEA was utilized. DHEA is an uncompetitive inhibitor of G6PD [29]. Treatment of SH-SY5Y cells with AGEs in the presence of DHEA reversed the effect of AGEs on ROS (Fig. 3.9). Furthermore, DHEA treatment reversed the effect of D3T on potentiating AGE-induced ROS. Cell viability was additionally measured in response to D3T and AGE treatment in the presence or absence of DHEA. As confirmed previously (Fig. 3.3), D3T potentiated the effect of AGE on cell viability (Fig. 3.10). Co-treatment with DHEA rescued SH-SY5Y cells from AGE-induced

and AGE-D3T-induced decrease in cell viability (Fig. 3.10). Collectively these studies confirmed the importance of G6PD in AGE-induced oxidative stress. They further implicated G6PD in the potentiation effect of D3T on the pro-oxidative outcomes of AGE treatment.

3.4.6 The Effect of DHEA on Neurite Morphology

To assess the importance of G6PD in AGE-mediated neurite functional outcomes, neurite length and average number of neurites per field of view were analyzed in the presence and absence of DHEA. Consistent with previous studies, AGE treatment compromised neurite morphology as measured by average neurite length (Fig. 3.11) and average neurite number per field of view (Fig. 3.12). While D3T did not further potentiate the effect of AGE on neurite morphology, it is possible a ceiling effect was approached with AGE treatment alone. Interestingly, inhibition of G6PD via DHEA rescued SH-SY5Y cells from AGE-induced neurite damage (Figs. 3.11-3.13), demonstrating the importance of G6PD-mediated generation of NADPH in the AGE-mediated mechanism of PN.

3.5 Discussion

In the diabetic state there is a significant increase AGE synthesis, as well as AGE accumulation in peripheral nerves [5,9]. To elucidate the mechanism of action of the AGE-RAGE axis, the Vincent *et al.* group isolated dorsal root ganglia (DRG) from Sprague Dawley rats. RAGE was shown to be localized throughout the entire neurons, and neurons that were treated with the RAGE ligand S100 had a significant increase in ROS generation. Inhibition of RAGE with an antibody led to near complete inhibition of S100 induced ROS generation, thus further establishing the importance of AGE-RAGE interaction in ROS generation[4]. Our laboratory has focused on this pathway and strategies to ameliorate the effects of excess ROS

production in differentiated SH-SY5Y cells. It was found that RAGE is abundantly expressed in differentiated SY-SY5Y cells and that multiple treatments do not impact protein expression (data not shown).

The present studies evaluated the mechanisms responsible for the potentiation effect of D3T on AGE-induced oxidative stress. Pazdro and Burgess have previously shown that treatment with NAC was able to protect both viability and morphology of SH-SY5Y cells stressed with AGEs [22]. It was hypothesized that NAC conferred protection by maintaining intracellular GSH. However, treating with D3T led to potentiation of damage under AGE stress even though under control conditions a significant increase in GSH was observed [23]. The critical observation from the Pazdro and Burgess study, that D3T potentiated ROS generation only under AGE-challenged conditions, led us to explore this mechanism in greater detail.

G6PD emerged as a key enzyme responsible for D3T-mediated potentiation of oxidative stress induced by AGEs, due to its role as a major generator of NADPH. Depending on context, increased expression and activity of G6PD has been shown to increase NADPH concentration and NADPH oxidase-mediated superoxide generation [30]. In our cell culture model, oxidative stress is induced by AGE-mediated activation of NADPH oxidase [22,23], and hence an increase in NADPH concentration would provide more reducing equivalents for superoxide generation. Furthermore, D3T has been shown to be a potent Nrf2 inducer [31] and G6PD is a Nrf2 responsive gene [32]. By inhibiting G6PD with DHEA, we were able to completely reverse both the effect of AGE and AGE-D3T treatment on ROS generation, viability, and morphology. These data bring to light the critical role of G6PD in AGE-mediated ROS generation and add further complexity to the relationship between oxidative stress and endogenous antioxidant defenses.

Traditionally, Nrf2 activation is expected to protect against oxidative stress through its coordinated regulation of metabolic and antioxidant enzyme expression. In particular, the downstream upregulation of pentose phosphate pathway enzymes is critical for production of NADPH to maintain antioxidants such as GSH, thioredoxin, and glutaredoxin [33]. In the liver, the major detoxification organ, Nrf2-null mice are prone to oxidative stress induced liver injury [34]. Keap1-hepatocyte knockout mice (Keap1-HKO), a model for increased liver Nrf2 activation, have been shown to be more resistant to acetaminophen hepatotoxicity [35]. Keap1-HKO mice had significantly higher G6PD mRNA expression which corresponded to a significant increase in liver NADPH concentration [19]. These observations suggest that Nrf2-induced increase in NADPH generation enzymes lead to protection by reduction of oxidative stress [19]. In our model of PN, however, potent Nrf2 inducer D3T promoted an increase in oxidative stress under AGE challenge (Fig. 3.5). Under control conditions, treatment with D3T led to a significant increase in GSH and had no effect on GSSG (Figs. 3.2 & 3.3). Upregulation of antioxidant enzymes with D3T treatment allows for increased intracellular GSH and maintenance of glutathione in its reduced form by GR. This scenario reverses in the AGE-challenge group. D3T treatment no longer leads to increased GSH, and there is a dramatic increase in GSSG compared to the BSA control group. Under AGE conditions, treatment with D3T promotes further increase in G6PD (Fig. 3.6). By increasing G6PD there is a likely increase in NADPH generation that can provide reducing equivalents for NADPH oxidase, leading to the rise in ROS generation that is observed (Fig. 3.5). GSH stores can then be depleted by antioxidant enzymes such as glutathione peroxidase (Gpx), and GSSG concentrations will begin to rise. Due to suppression of GR activity, redox balance is no longer maintained, and cell morphology and viability deteriorate (Fig. 3.14).

The pathogenesis of PN has been strongly linked with excess production of ROS and the disruption of the redox state [36], leading to complications such as axonal degeneration [37]. Previously in our laboratory, Pazdro and Burgess quantified loss of neurite number in RA differentiated SH-SY5Y cells after AGE challenge as a marker of neurite deterioration [22,23]. We expanded on this method, and quantified neurite length and long neurite number. This was done to observe the effects of antioxidants on protection against neurite retraction and protection of long neurites upon AGE-challenge. We focused on the long neurites, neurites equal to or longer than the average neurite length in the control BSA group, because in PN the longest neurons are generally the first to get damaged [36,37]. AGE-challenged cells showed significant deterioration of neurite structure, with mean neurite length dropping from 115 to 76 pixels (Fig. 3.11). D3T treatment under AGE-challenge had no further effect, potentially due to a floor effect where the extent of neurite damage in our model is maximized. However, G6PD inhibition with DHEA was able to completely rescue neurite length under both AGE and AGE-D3T challenge (Fig. 3.11). An even more dramatic change was observed with AGE and AGE-D3T challenge on the average number of long neurites. The BSA control group contained an average of 21 long neurites per field of view, and this number dropped significantly to 6.8 and 3.3 for AGE and AGE-D3T groups, respectively (Fig. 3.12). Again, DHEA treatment completely protected neurites in both groups (Fig. 3.12). These results in differentiated SH-SY5Y cells bring to light the potentially critical role of G6PD and NADPH in potentiation of AGE-mediated neuronal degeneration. Strategies aimed at increasing expression of Nrf2 target antioxidant enzymes such as G6PD may need to be revaluated within the context of AGE-induced PN.

AGE and AGE-D3T-challenge conditions lead to neurite degeneration (Fig. 11&12), and research in our laboratory is ongoing to establish the mechanism responsible for this effect. Of

interest is the accumulation of GSSG in stressed conditions. Exogenous application of GSSG in differentiated NSC34 cells led to tubulin glutathionylation and significant neurite retraction [38]. A similar mechanism may be at play in our cell culture model. The accumulation of GSSG (Fig. 3) may initiate glutathionylation of neurite structural proteins, as GSSG can react with cysteine residues to form mixed disulfides [39,40]. With depletion of glutathione stores (Fig. 2), activity of glutaredoxin-1, the major enzyme responsible for reducing mixed disulfides [39], would be suppressed and glutathionylated proteins would accumulate. Confirming this mechanism in future studies will be crucial in establishing why maintaining GSH is critical for neurite protection.

In conclusion, results of this study continue to support previous data from our laboratory that GSH is critical for maintaining neurites in differentiated SH-SY5Y cells. We show that under AGE-challenge conditions, D3T further disrupts redox balance and potentiates ROS generation. This potentiation effect is due to upregulation of the Nrf2 responsive gene G6PD, and a decrease in the activity of GR. Botanical Nrf2 inducers, such as D3T, are seen as protective against diseases with an oxidative stress component [36]. However, the results suggest that Nrf2 inducing phytochemicals may exacerbate AGE-mediated neuronal degeneration. Further studies in different cell lines and animal models will need to be conducted before phytochemicals such as D3T can be recommended or advised against for patients suffering with diabetic PN.

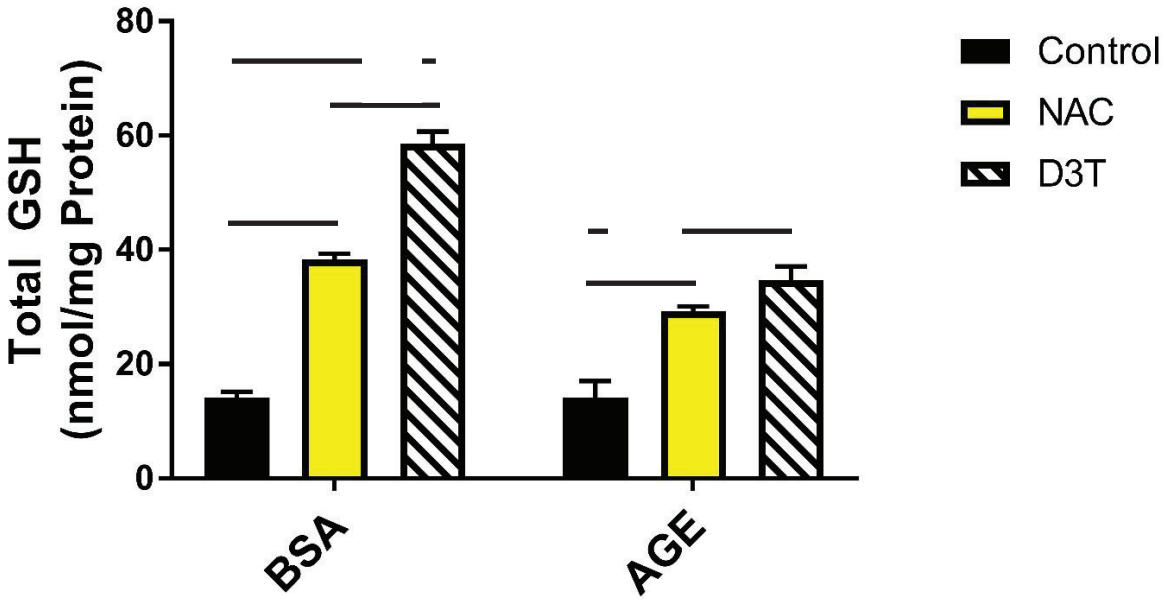

Figure 3.1 NAC and D3T treatment increases total GSH.

Differentiated cells were treated with 1 mM NAC or 100 μM D3T for 24 hours prior to 5 mg/mL BSA or AGE treatment. NAC and D3T were replenished during BSA and AGE treatment. GSH concentrations were normalized to total protein. Data were analyzed by two-way ANOVA with Tukey's post-hoc analysis from 3 independent experiments. Bars linked with an * are significantly different ($p < 0.05$).

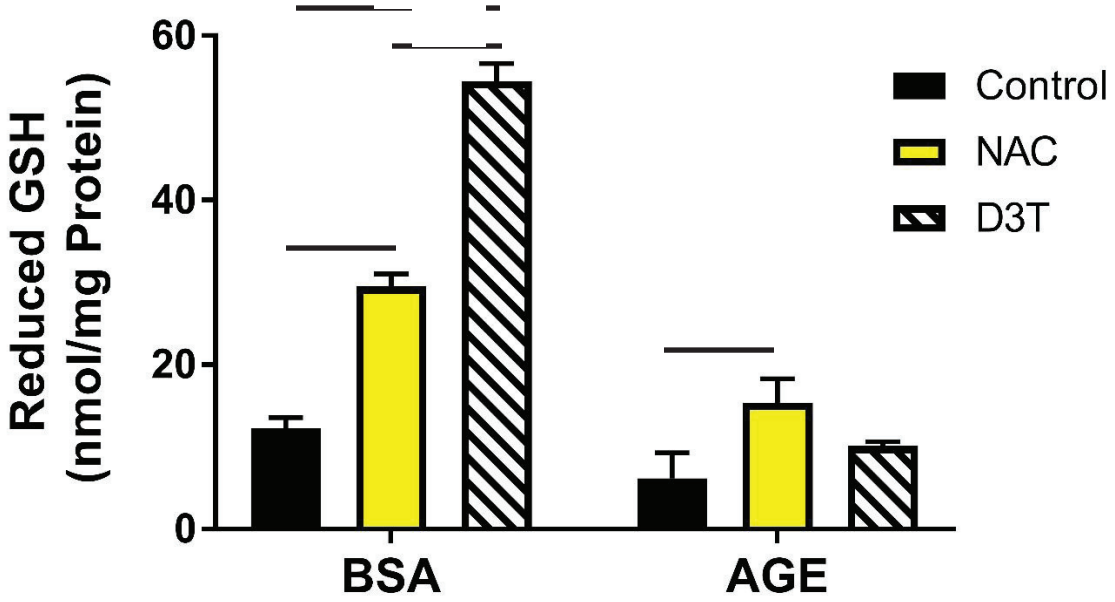

Figure 3.2 D3T does not protect reduced GSH under AGE-treated conditions.

Differentiated cells were treated with 1 mM NAC or 100 μM D3T for 24 hours prior to 5 mg/mL BSA or AGE treatment. NAC and D3T were replenished during BSA and AGE treatment. Reduced GSH was calculated by subtracting 2x GSSG from total GSH. Data were analyzed by two-way ANOVA with Tukey's post-hoc analysis from 3 independent experiments. Bars linked with an * are significantly different ($p < 0.05$).

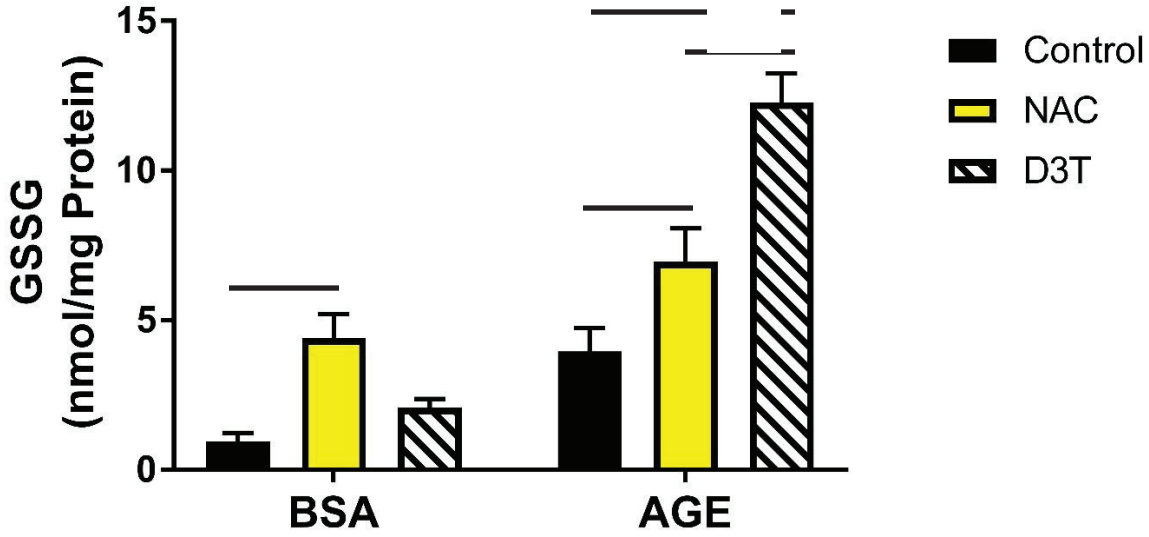

Figure 3.3 D3T exacerbates AGE-induced GSSG increase.

Differentiated cells were treated with 1 mM NAC or 100 μM D3T for 24 hours prior to 5 mg/mL BSA or AGE treatment. NAC and D3T were replenished during BSA and AGE treatment. GSSG concentrations were normalized to total protein. Data were analyzed by two-way ANOVA with Tukey's post-hoc analysis from 3 independent experiments. Bars linked with an * are significantly different ($p < 0.05$).

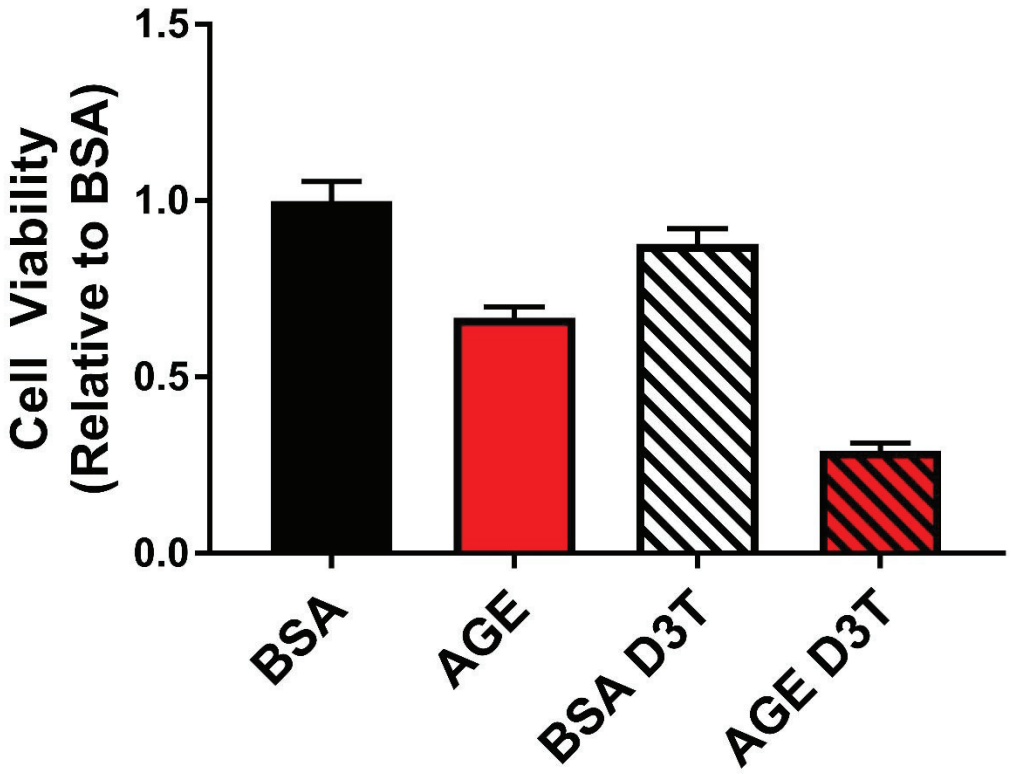

Figure 3.4 D3T exacerbates AGE-induced viability loss.

Differentiated cells were treated with 100 μM D3T for 24 hours prior to 5 mg/mL BSA or AGE treatment. D3T was replenished during BSA and AGE treatment. Viability was assessed using an MTT assay and results are presented as values relative to control (BSA) group. Data were analyzed by one-way ANOVA with Tukey's post-hoc analysis from 4-5 independent experiments. Bars with superscript letters different from each other are significantly different ($p < 0.05$).

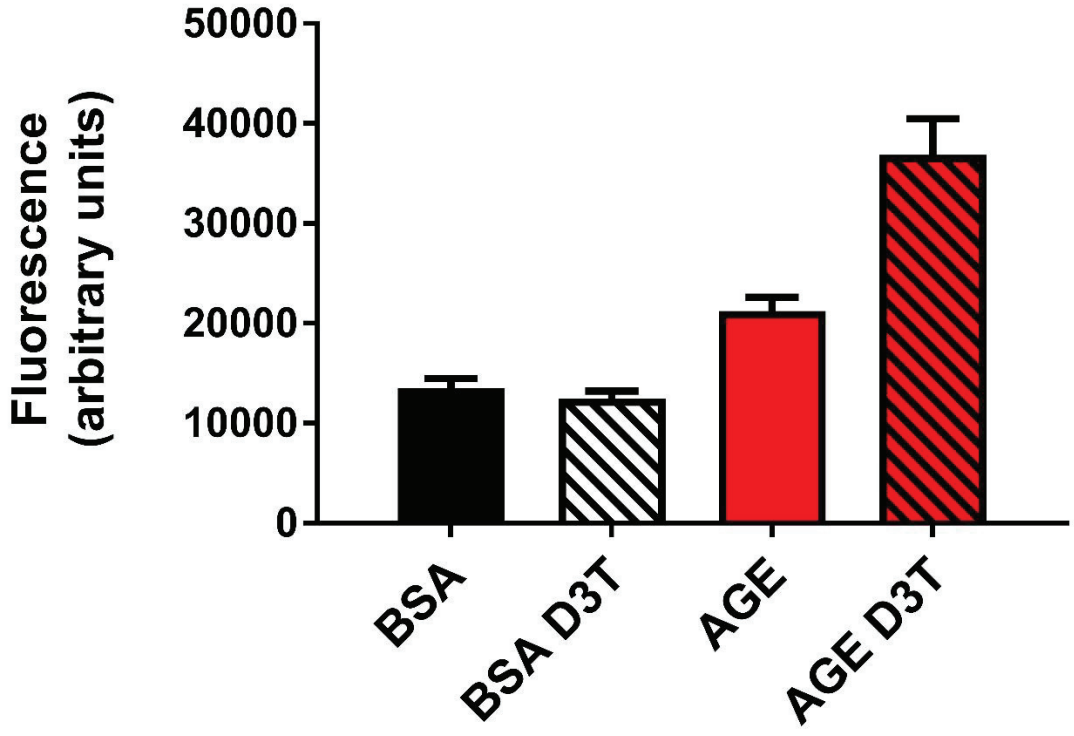

Figure 3.5 D3T exacerbates AGE-induced ROS generation.

Differentiated cells were treated with 100 μM D3T for 24 hours prior to 5 mg/mL BSA or AGE treatment. D3T was replenished during BSA and AGE treatment. Data were analyzed by one-way ANOVA with Tukey's post-hoc analysis from 4-5 independent experiments. Bars with superscript letters different from each other are significantly different ($p < 0.05$).

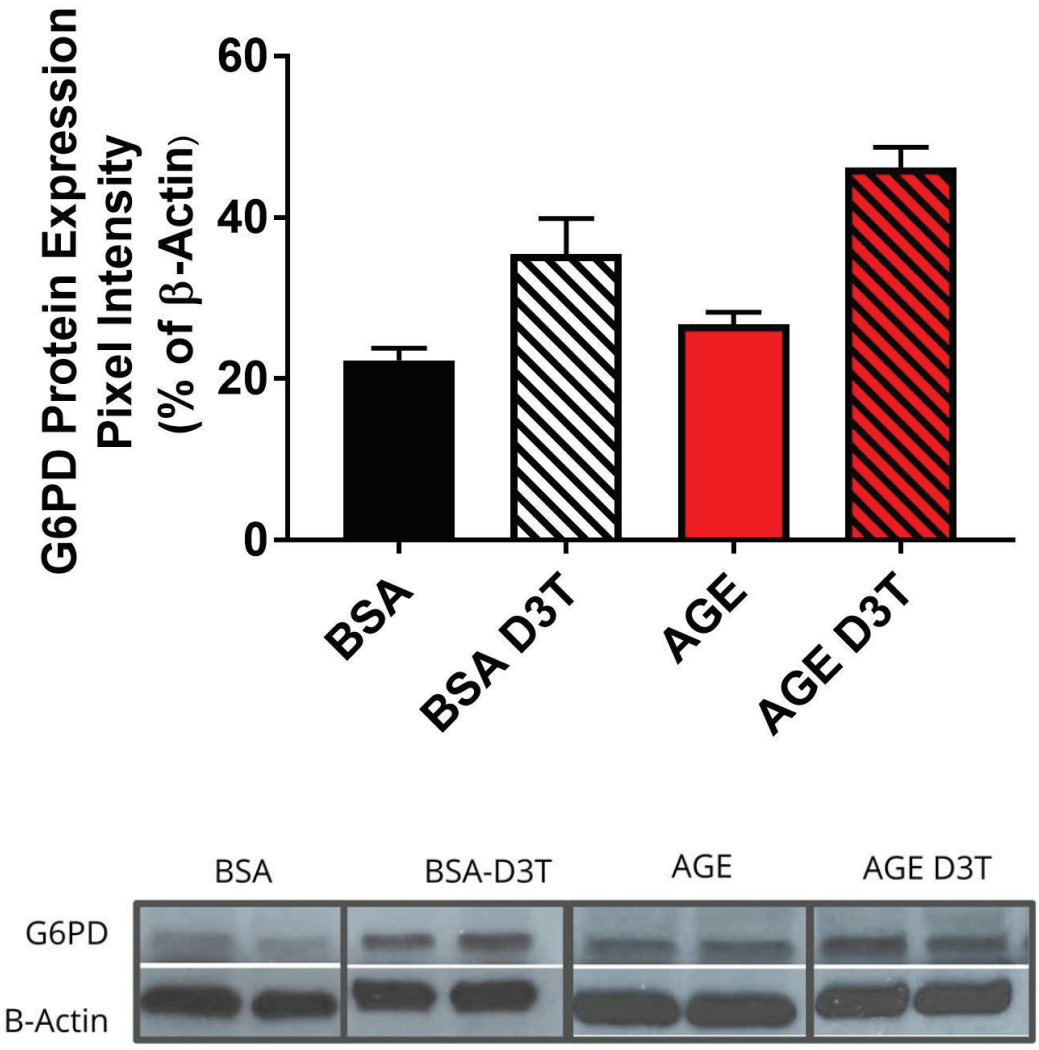

Figure 3.6 D3T treatment results in increased G6PD protein expression.

Differentiated cells were treated with 100 μM D3T for 24 hours prior to 5 mg/mL BSA or AGE treatment. D3T was replenished during BSA and AGE treatment. Blots shown are representative samples of each group. Data were analyzed by one-way ANOVA with Tukey's post-hoc analysis from 3 independent experiments. Bars not linked by a superscript letter are significantly different from each other ($p < 0.05$).

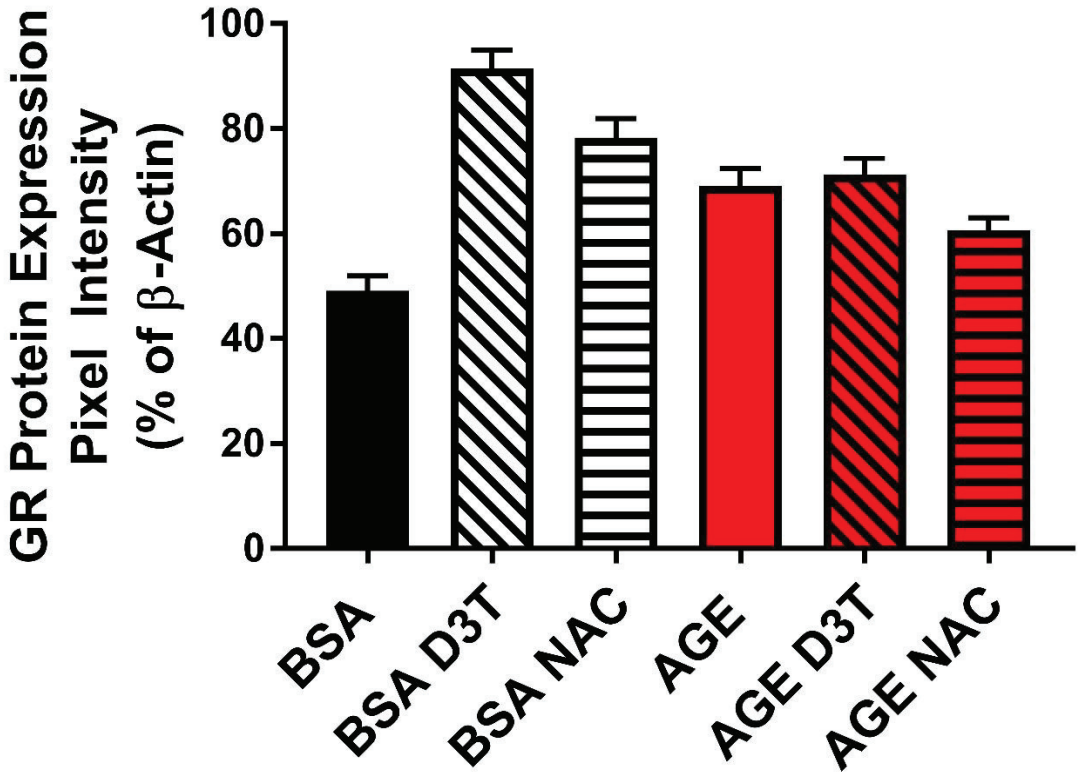

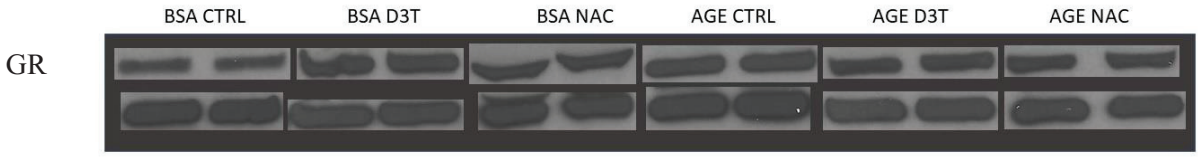

Figure 3.7 Impact of NAC and D3T treatment on GR protein expression.

Differentiated cells were treated with 1 mM NAC or 100 μM D3T for 24 hours prior to 5 mg/mL BSA or AGE treatment. NAC and D3T were replenished during BSA and AGE treatment. Blots shown are representative samples of each group. Data were analyzed by one-way ANOVA with Tukey's post-hoc analysis from 3 independent experiments. Bars not linked by a superscript letter are significantly different from each other ($p < 0.05$).

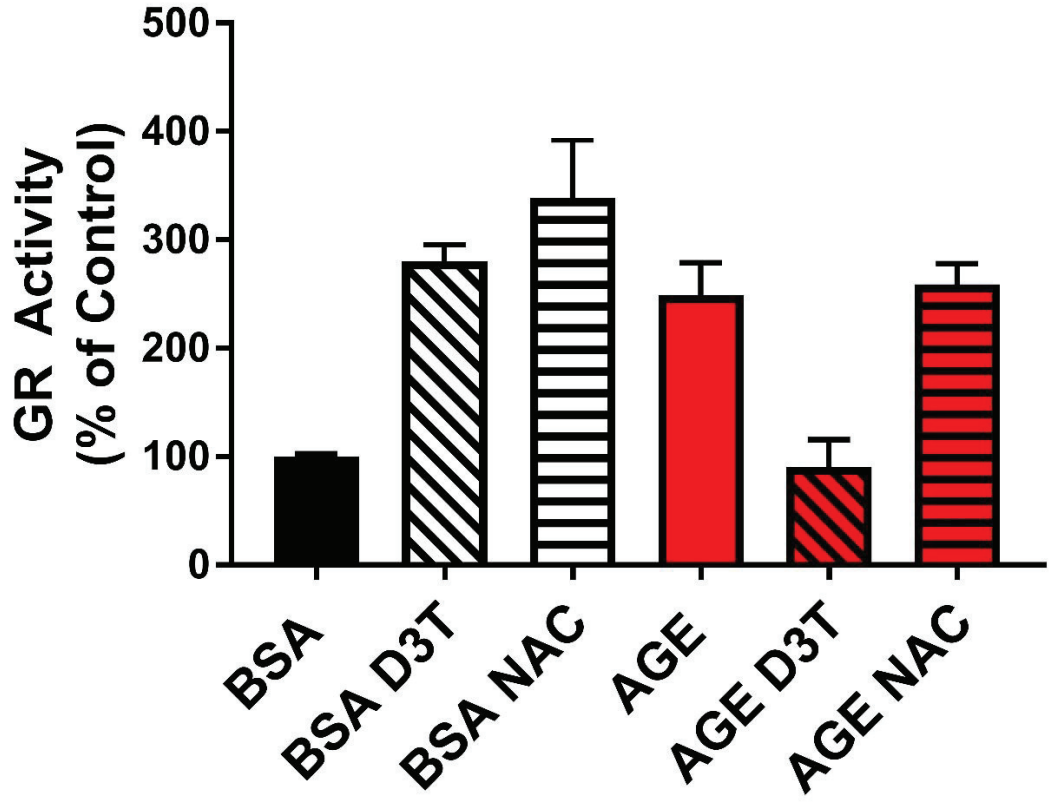

Figure 3.8 D3T treatment reduces GR activity in AGE-challenged cells.

Differentiated cells were treated with 1 mM NAC or 100 μM D3T for 24 hours prior to 5 mg/mL BSA or AGE treatment. NAC and D3T were replenished during BSA and AGE treatment. Results are presented as a % of the control (BSA) group. Data were analyzed by one-way ANOVA with Tukey's post-hoc analysis from 3 independent experiments. Bars with superscript letters different from each other are significantly different ($p < 0.05$).

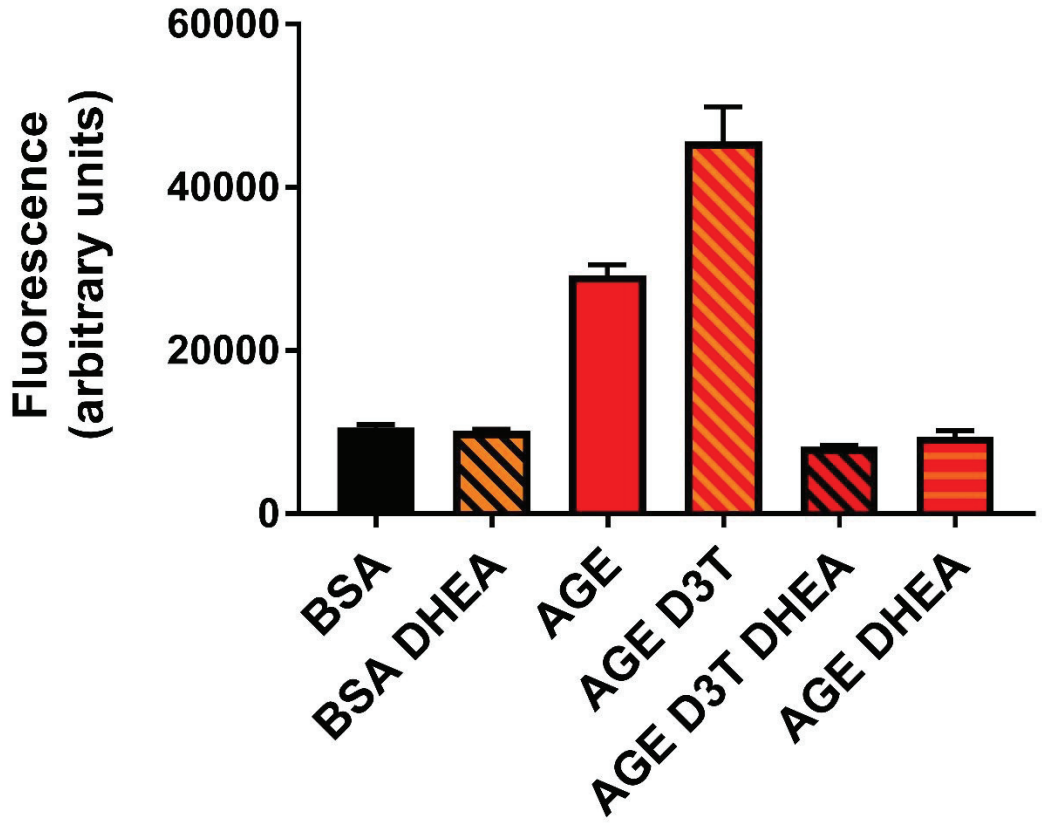

Figure 3.9 DHEA inhibits AGE and D3T-induced ROS generation.

Differentiated cells were treated with 100 μM D3T and/or 100 μM DHEA for 24 hours prior to 5 mg/mL BSA or AGE treatment. D3T and DHEA were replenished during BSA and AGE treatment. Data were analyzed by one-way ANOVA with Tukey's post-hoc analysis from 3-4 independent experiments. Bars with superscript letters different from each other are significantly different ($p < 0.05$).

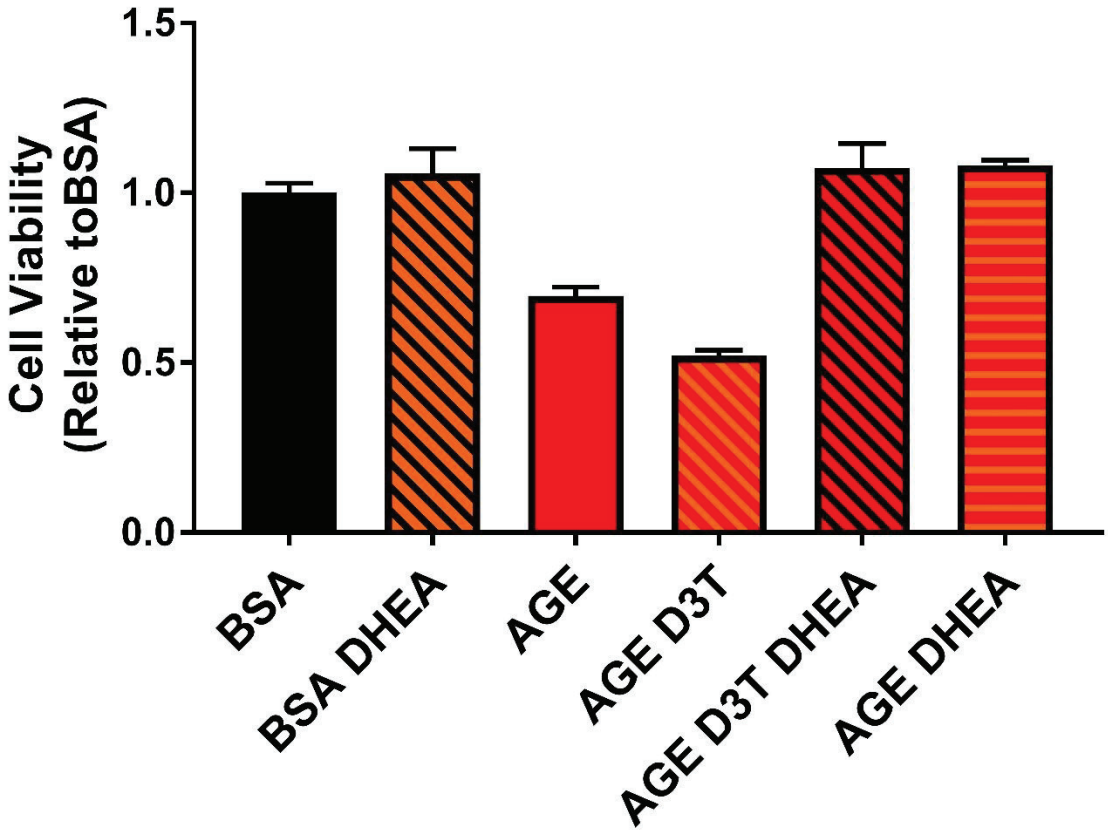

Figure 3.10 G6PD inhibition protects against AGE and D3T-induced viability loss.

Differentiated cells were treated with 100 μM D3T and/or 100 μM DHEA for 24 hours prior to 5 mg/mL BSA or AGE treatment. D3T and DHEA were replenished during BSA and AGE treatment. Data were analyzed by one-way ANOVA with Tukey's post-hoc analysis from 3-4 independent experiments. Bars with superscript letters different from each other are significantly different ($p < 0.05$).

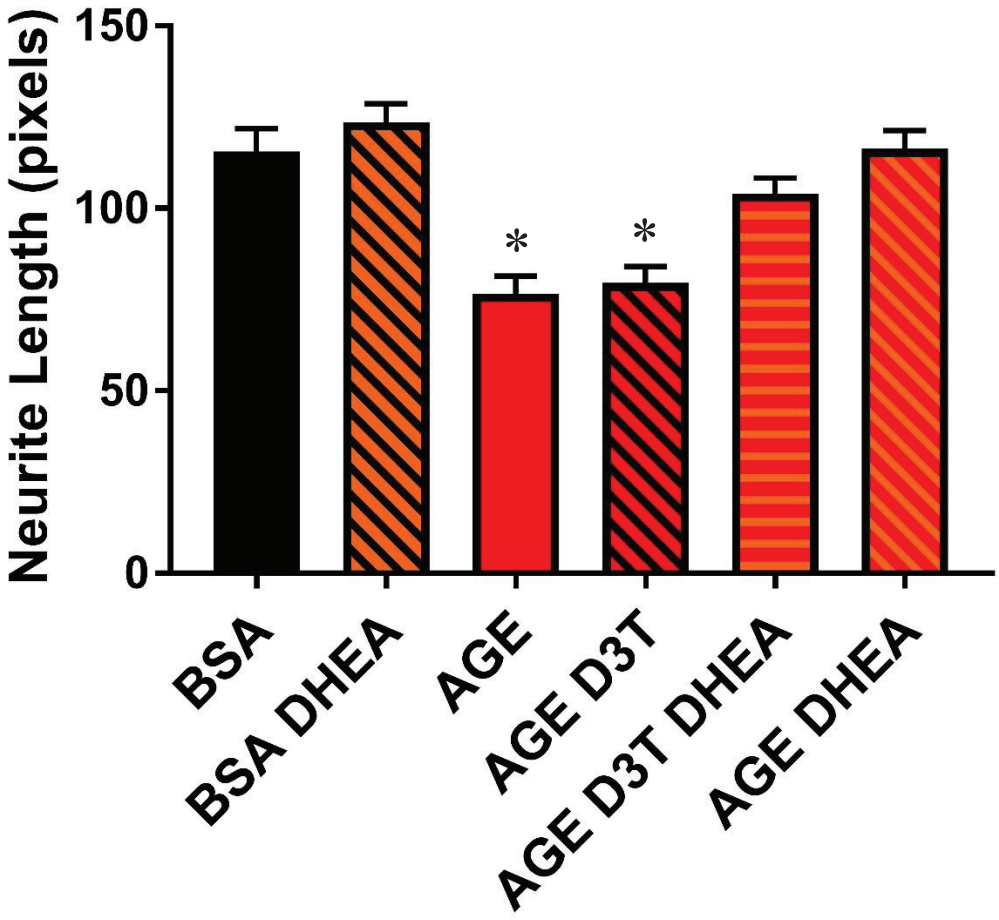

Figure 3.11 DHEA protects against AGE-induced neurite retraction.

Differentiated cells were treated with 100 μM D3T and/or 100 μM DHEA for 24 hours prior to 5 mg/mL BSA or AGE treatment. D3T and DHEA were replenished during BSA and AGE treatment. A minimum of 100 neurites per group were analyzed. Neurite length in 10x images was quantified using Image J software with NeuronJ plugin. Data were analyzed by one-way ANOVA with Dunnett's post-hoc analysis. Bars with an * are significantly different ($p < 0.05$) compared to control (BSA).

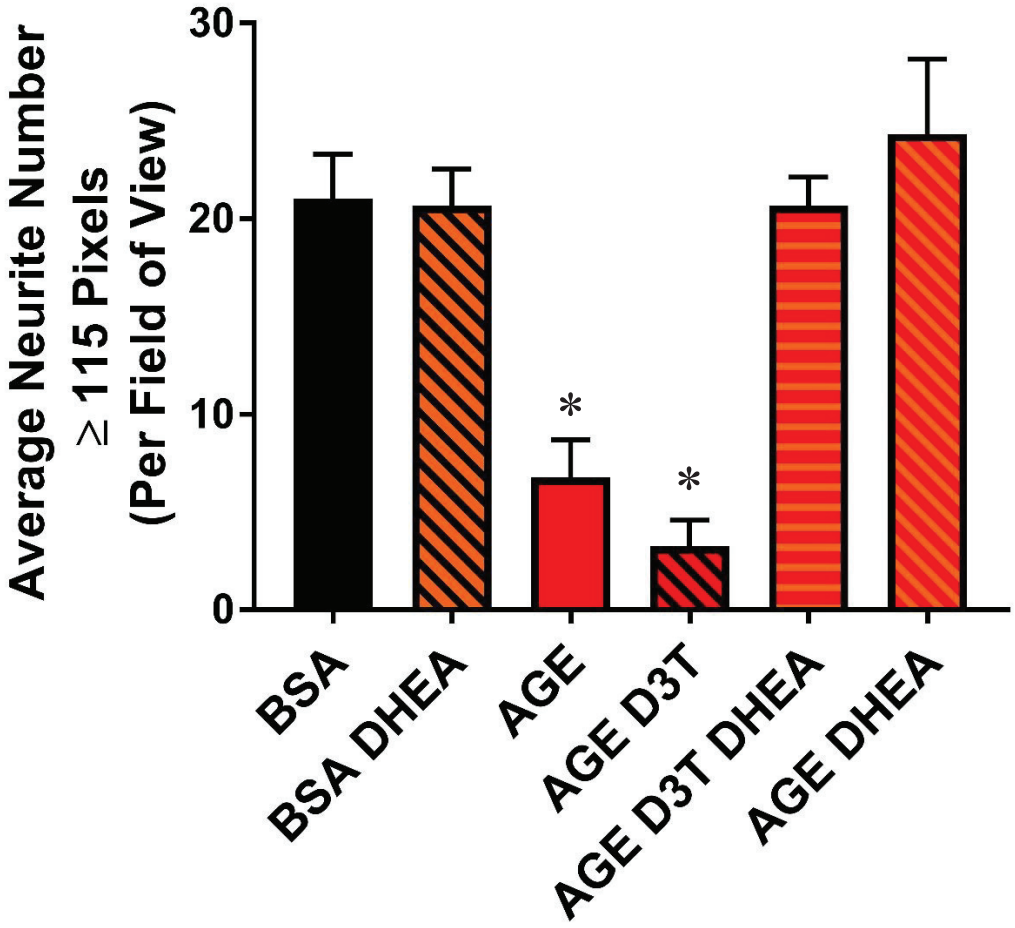

Figure 3.12 DHEA protects against AGE-induced loss of long neurites.

Differentiated cells were treated with 100 μM D3T and/or 100 μM DHEA for 24 hours prior to 5 mg/mL BSA or AGE treatment. D3T and DHEA were replenished during BSA and AGE treatment. A minimum of 100 neurites per group were analyzed. Long neurite number in 10x images was quantified using Image J software with NeuronJ plugin. Data were analyzed by one-way ANOVA with Dunnett's post-hoc analysis. Bars with an * are significantly different ($p < 0.05$) compared to control (BSA).

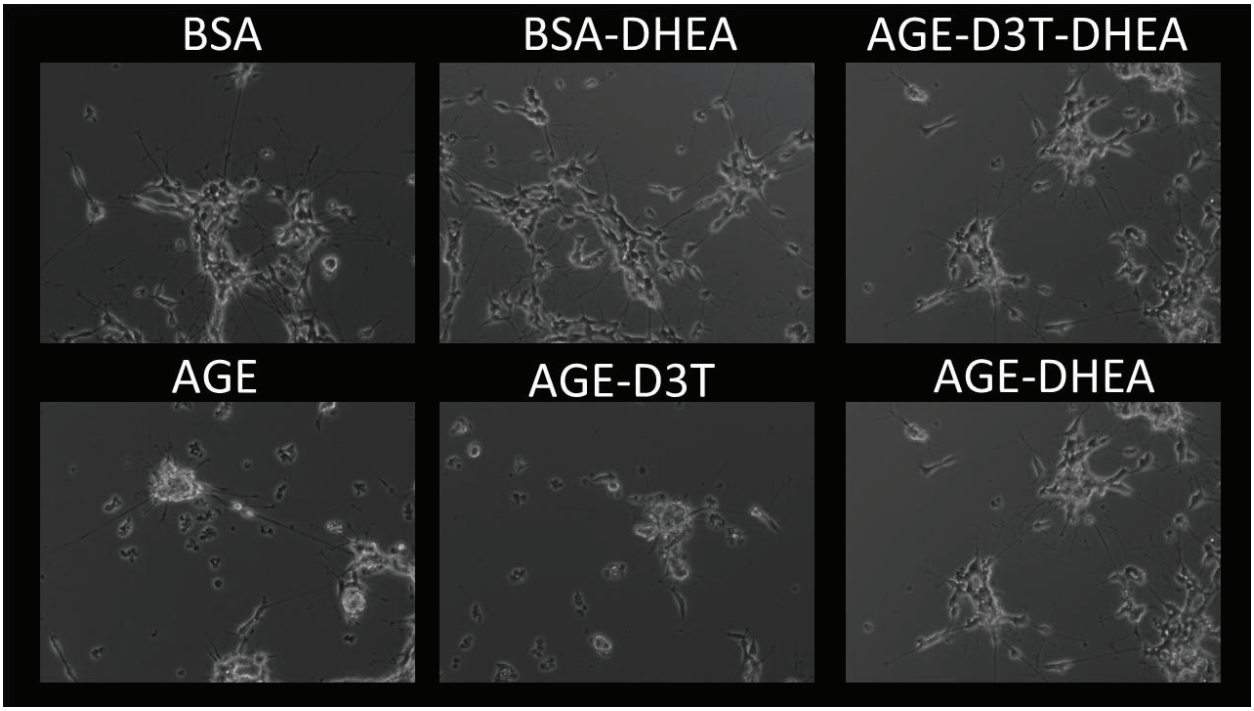

Figure 3.13 DHEA protects against AGE-induced loss of long neurites and retraction.

Differentiated cells were treated with 100 μM D3T and/or 100 μM DHEA for 24 hours prior to 5 mg/mL BSA or AGE treatment. D3T and DHEA were replenished during BSA and AGE treatment. Representative 10x images of those quantified using Image J software with NeuronJ plugin.

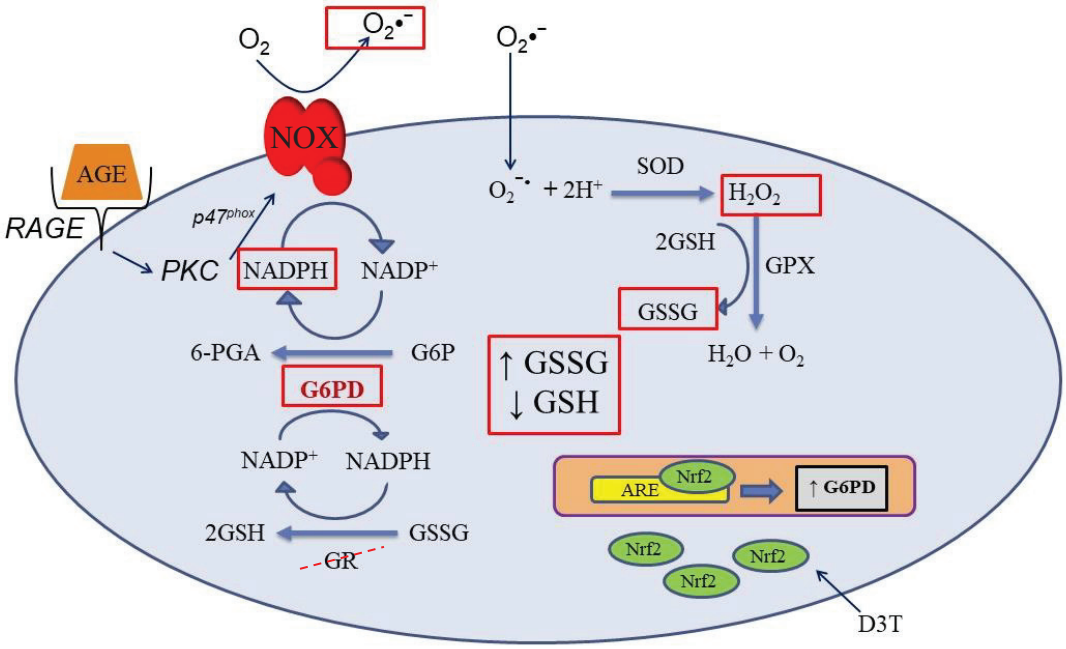

Figure 3.14 Mechanism of the D3T paradox.

Receptor for advanced glycation end products (RAGE); advanced glycation end product (AGE); NADPH oxidase (NOX); glucose-6-phosphate dehydrogenase (G6PD); glucose-6-phosphate (G6P); 6-phosphogluconate (6-PGA); glutathione reductase (GR); glutathione peroxidase (GPX); superoxide dismutase (SOD); antioxidant response element (ARE); nuclear factor (erythroid-derived 2)-like 2 (Nrf2); 3H-1,2-dithiole-3-thione (D3T). AGE-challenge results in activation of RAGE, downstream activation of NOX, and generation of superoxide. Superoxide enters the cells and undergoes dismutation to hydrogen peroxide. Hydrogen peroxide is reduced to water and molecular oxygen at the expense of GSH by GPX. These conditions result in the observed increase in GSSG and decrease in GSH. Addition of D3T further exacerbates this condition by upregulation of G6PD, leading to increased production of reducing equivalents (NADPH) that are then used by NOX to generate more superoxide. Furthermore, D3T blunts upregulation of GR activity, which leads to depletion of GSH, promotes build-up of GSSG, and disrupts redox balance.

3.6 References

[1] Centers for Disease Control and Prevention, National Diabetes Statistics Report Centers for Disease Control and Prevention, ; 2017., Atlanta, GA, 2017.

[2] Economic costs of diabetes in the U.S. in 2012. Diabetes Care 2013;36:1033–1046, Diabetes Care. 36 (2013) 1797 LP-1797.

[3] E.L. Feldman, K.-A. Nave, T.S. Jensen, D.L.H. Bennett, New Horizons in Diabetic Neuropathy: Mechanisms, Bioenergetics, and Pain, Neuron. 93 (2017) 1296–1313. doi:https://doi.org/10.1016/j.neuron.2017.02.005.

[4] A.M. Vincent, L. Perrone, K. a Sullivan, C. Backus, A.M. Sastry, C. Lastoskie, E.L. Feldman, Receptor for advanced glycation end products activation injures primary sensory neurons via oxidative stress., Endocrinology. 148 (2007) 548–58. doi:10.1210/en.2006-0073.

[5] I.K. Lukic, P.M. Humpert, P.P. Nawroth, A. Bierhaus, The RAGE pathway: activation and perpetuation in the pathogenesis of diabetic neuropathy., Ann. N. Y. Acad. Sci. 1126 (2008) 76–80. doi:10.1196/annals.1433.059.

[6] R. Wada, S. Yagihashi, Role of advanced glycation end products and their receptors in development of diabetic neuropathy., Ann. N. Y. Acad. Sci. 1043 (2005) 598–604. doi:10.1196/annals.1338.067.

[7] H. Vlassara, The AGE-receptor in the pathogenesis of diabetic complications., Diabetes. Metab. Res. Rev. 17 (2001) 436–43. http://www.ncbi.nlm.nih.gov/pubmed/11757079 (accessed September 23, 2014).

[8] T. Sato, M. Iwaki, N. Shimogaito, X. Wu, S.-I. Yamagishi, M. Takeuchi, TAGE (toxic AGEs) theory in diabetic complications., Curr. Mol. Med. 6 (2006) 351–8. http://www.ncbi.nlm.nih.gov/pubmed/16712480 (accessed September 23, 2014).

[9] M. Jack, D. Wright, Role of advanced glycation endproducts and glyoxalase I in diabetic peripheral sensory neuropathy., Transl. Res. 159 (2012) 355–65. doi:10.1016/j.trsl.2011.12.004.

[10] M. Nitti, A.L. Furfaro, N. Traverso, P. Odetti, D. Storace, D. Cottalasso, M.A. Pronzato, U.M. Marinari, C. Domenicotti, PKC delta and NADPH oxidase in AGE-induced neuronal death, Neurosci. Lett. 416 (2007) 261–265. doi:10.1016/j.neulet.2007.02.013.

[11] M. Nitti, C. d'Abramo, N. Traverso, D. Verzola, G. Garibotto, A. Poggi, P. Odetti, D. Cottalasso, U.M. Marinari, M.A. Pronzato, C. Domenicotti, Central role of PKCδ in glycoxidation-dependent apoptosis of human neurons, Free Radic. Biol. Med. 38 (2005) 846–856. doi:10.1016/j.freeradbiomed.2004.12.002.

[12] M.T. Lee, W.C. Lin, B. Yu, T.T. Lee, Antioxidant capacity of phytochemicals and their potential effects on oxidative status in animals - A review., Asian-Australasian J. Anim. Sci. 30 (2017) 299–308. doi:10.5713/ajas.16.0438.

[13] S. Chikara, L.D. Nagaprashantha, J. Singhal, D. Horne, S. Awasthi, S.S. Singhal, Oxidative stress and dietary phytochemicals: Role in cancer chemoprevention and treatment, Cancer Lett. 413 (2018) 122–134. doi:10.1016/J.CANLET.2017.11.002.

[14] H. Kumar, I.-S. Kim, S.V. More, B.-W. Kim, D.-K. Choi, Natural product-derived pharmacological modulators of Nrf2/ARE pathway for chronic diseases, Nat. Prod. Rep. 31 (2014) 109–139. doi:10.1039/C3NP70065H.

[15] K.-R. Li, S.-Q. Yang, Y.-Q. Gong, H. Yang, X.-M. Li, Y.-X. Zhao, J. Yao, Q. Jiang, C. Cao, 3H-1,2-dithiole-3-thione protects retinal pigment epithelium cells against Ultra-violet radiation via activation of Akt-mTORC1-dependent Nrf2-HO-1 signaling., Sci. Rep. 6 (2016) 25525. doi:10.1038/srep25525.

[16] J. Dong, D. Yan, S. Chen, Stabilization of Nrf2 Protein by D3T Provides Protection against Ethanol-Induced Apoptosis in PC12 Cells, PLoS One. 6 (2011) e16845. doi:10.1371/journal.pone.0016845.

[17] Z. Jia, H. Zhu, M.A. Trush, H.P. Misra, Y. Li, Generation of superoxide from reaction of 3H-1,2-dithiole-3-thione with thiols: implications for dithiolethione chemoprotection., Mol. Cell. Biochem. 307 (2008) 185–91. doi:10.1007/s11010-007-9598-z.

[18] M. Kobayashi, L. Li, N. Iwamoto, Y. Nakajima-Takagi, H. Kaneko, Y. Nakayama, M. Eguchi, Y. Wada, Y. Kumagai, M. Yamamoto, The antioxidant defense system Keap1-Nrf2 comprises a multiple sensing mechanism for responding to a wide range of chemical compounds., Mol. Cell. Biol. 29 (2009) 493–502. doi:10.1128/MCB.01080-08.

[19] K.C. Wu, J.Y. Cui, C.D. Klaassen, Beneficial Role of Nrf2 in Regulating NADPH Generation and Consumption, Toxicol. Sci. 123 (2011) 590–600. doi:10.1093/toxsci/kfr183.

[20] L. Baird, A.T. Dinkova-Kostova, The cytoprotective role of the Keap1-Nrf2 pathway., Arch. Toxicol. 85 (2011) 241–72. doi:10.1007/s00204-011-0674-5.

[21] Y. Zhang, G.B. Gordon, A strategy for cancer prevention: stimulation of the Nrf2-ARE signaling pathway., Mol. Cancer Ther. 3 (2004) 885–93. http://www.ncbi.nlm.nih.gov/pubmed/15252150 (accessed March 21, 2018).

[22] R. Pazdro, J.R. Burgess, Differential effects of α-tocopherol and N-acetyl-cysteine on advanced glycation end product-induced oxidative damage and neurite degeneration in SH-SY5Y cells., Biochim. Biophys. Acta. 1822 (2012) 550–6. doi:10.1016/j.bbadis.2012.01.003.

[23] R. Pazdro, J.R. Burgess, The antioxidant 3H-1,2-dithiole-3-thione potentiates advanced glycation end-product-induced oxidative stress in SH-SY5Y cells., Exp. Diabetes Res. 2012 (2012) 137607. doi:10.1155/2012/137607.

[24] I. Rahman, A. Kode, S.K. Biswas, Assay for quantitative determination of glutathione and glutathione disulfide levels using enzymatic recycling method, Nat. Protoc. 1 (2007) 3159–3165. doi:10.1038/nprot.2006.378.

[25] T. Wilmanski, X. Zhou, W. Zheng, A. Shinde, S.S. Donkin, M. Wendt, J.R. Burgess, D. Teegarden, Inhibition of Pyruvate Carboxylase by 1α,25-Dihydroxyvitamin D Promotes Oxidative Stress in Early Breast Cancer Progression, Cancer Lett. (2017). doi:10.1016/j.canlet.2017.09.045.

[26] B. Mannervik, Measurement of Glutathione Reductase Activity, Curr. Protoc. Toxicol. 00 (1999) 7.2.1-7.2.4. doi:10.1002/0471140856.tx0702s00.

[27] Z. Jia, H. Zhu, Y. Li, H.P. Misra, Cruciferous nutraceutical 3H-1,2-dithiole-3-thione protects human primary astrocytes against neurocytotoxicity elicited by MPTP, MPP(+), 6-OHDA, HNE and acrolein., Neurochem. Res. 34 (2009) 1924–34. doi:10.1007/s11064-009-9978-8.

[28] D. Marmolino, M. Manto, Past, present and future therapeutics for cerebellar ataxias., Curr. Neuropharmacol. 8 (2010) 41–61. doi:10.2174/157015910790909476.

[29] G. Gordon, M.C. Mackow, H.R. Levy, On the Mechanism of Interaction of Steroids with Human Glucose 6-Phosphate Dehydrogenase, Arch. Biochem. Biophys. 318 (1995) 25–29. doi:10.1006/abbi.1995.1199.

[30] R.S. Gupte, V. Vijay, B. Marks, R.J. Levine, H.N. Sabbah, M.S. Wolin, F.A. Recchia, S.A. Gupte, Upregulation of glucose-6-phosphate dehydrogenase and NAD(P)H oxidase activity increases oxidative stress in failing human heart., J. Card. Fail. 13 (2007) 497–506. doi:10.1016/j.cardfail.2007.04.003.

[31] M.K. Kwak, K. Itoh, M. Yamamoto, T.R. Sutter, T.W. Kensler, Role of transcription factor Nrf2 in the induction of hepatic phase 2 and antioxidative enzymes in vivo by the cancer chemoprotective agent, 3H-1, 2-dimethiole-3-thione., Mol. Med. 7 (2001) 135–45. http://www.ncbi.nlm.nih.gov/pubmed/11471548 (accessed March 14, 2018).

[32] R.K. Thimmulappa, K.H. Mai, S. Srisuma, T.W. Kensler, M. Yamamoto, S. Biswal, Identification of Nrf2-regulated genes induced by the chemopreventive agent sulforaphane by oligonucleotide microarray., Cancer Res. 62 (2002) 5196–203. http://www.ncbi.nlm.nih.gov/pubmed/12234984 (accessed May 23, 2014).

[33] A.S. Veskoukis, N. V. Margaritelis, A. Kyparos, V. Paschalis, M.G. Nikolaidis, Spectrophotometric assays for measuring redox biomarkers in blood and tissues: the NADPH network, Redox Rep. 23 (2018) 47–56. doi:10.1080/13510002.2017.1392695.

[34] L.M. Aleksunes, J.E. Manautou, Emerging role of Nrf2 in protecting against hepatic and gastrointestinal disease., Toxicol. Pathol. 35 (2007) 459–73. doi:10.1080/01926230701311344.

[35] H. Okawa, H. Motohashi, A. Kobayashi, H. Aburatani, T.W. Kensler, M. Yamamoto, Hepatocyte-specific deletion of the keap1 gene activates Nrf2 and confers potent resistance against acute drug toxicity, Biochem. Biophys. Res. Commun. 339 (2006) 79–88. doi:10.1016/j.bbrc.2005.10.185.

[36] J.L. Edwards, A.M. Vincent, H.T. Cheng, E.L. Feldman, Diabetic neuropathy: mechanisms to management., Pharmacol. Ther. 120 (2008) 1–34. doi:10.1016/j.pharmthera.2008.05.005.

[37] M. Sinnreich, B. V. Taylor, P.J.B. Dyck, Diabetic Neuropathies, Neurologist. 11 (2005) 63–79. doi:10.1097/01.nrl.0000156314.24508.ed.

[38] B. Carletti, C. Passarelli, M. Sparaco, G. Tozzi, A. Pastore, E. Bertini, F. Piemonte, Effect of protein glutathionylation on neuronal cytoskeleton: a potential link to neurodegeneration, Neuroscience. 192 (2011) 285–294. doi:10.1016/j.neuroscience.2011.05.060.

[39] A.P. Fernandes, A. Holmgren, Glutaredoxins: Glutathione-Dependent Redox Enzymes with Functions Far Beyond a Simple Thioredoxin Backup System, Antioxid. Redox Signal. 6 (2004) 63–74. doi:10.1089/152308604771978354.

[40] C.H. Lillig, C. Berndt, A. Holmgren, Glutaredoxin systems, Biochim. Biophys. Acta - Gen. Subj. 1780 (2008) 1304–1317. doi:10.1016/j.bbagen.2008.06.003.

CHAPTER 4. EFFECT OF DISRUPTING THE THIOL REDOX STATE ON NEURITE DEGENERATION

4.1 Abstract

Peripheral neuropathy is one of the most common health complications in diabetic patients with a significant impact on quality of life. Oxidative stress plays a major role in the development of diabetic peripheral neuropathy, therefore reducing or increasing protection against oxidative stress should be a key focus for ameliorating diabetic complications. In our laboratory we use differentiated SH-SY5Y cells as a model system to study the mechanisms of oxidative stress mediated cell damage and antioxidant protection in diabetic peripheral neuropathy. Previously, we have shown that disruption of the thiol redox state results in loss of cell viability and the dying-back (degeneration) of neurites. Treatment with N-acetylcysteine (NAC), a common antioxidant, protected intracellular glutathione levels and conferred protection against neurite retraction under pro-oxidative conditions. In the present studies, the effects of glutathione-mediated oxidative damage were investigated. Exogenous treatment of differentiated SH-SY5Y cells resulted in significant neurite degeneration. Further disruption of the thiol redox state via inhibition of glutathione reductase and glutaredoxin-1 exacerbated neurite damage, resulting in a dramatic increase of thinning neurites and a loss of long neurites. The significant impact observed of glutathione reductase and glutaredoxin-1 inhibition suggested protein glutathionylation of structural proteins as a mechanism for neurite degeneration. Treating SH-SY5Y cells with advanced glycation end products (AGE) to mimic diabetic conditions resulted in significant protein glutathionylation. NAC treatment conferred complete protection against AGE-induced protein glutathionylation. Future studies using glutaredoxin-1 knockdown cells will need to be conducted to elucidate the role of glutathionylation in neurite degeneration.

Establishing mechanisms for neurite degeneration has the potential to help with the development of a targeted approach to protect peripheral neurons of diabetic patients.

4.2 Introduction

Peripheral neuropathy (PN) is one of the most common health complications in diabetic patients, affecting up to 66% of type 1 diabetics and 59% of type 2 diabetics [1]. Oxidative stress is implicated as a major contributor to development of diabetes-induced PN [2]. The diabetic condition results in increased non-enzymatic glycation of proteins, known as advanced glycation end products (AGE) [3]. Increases in hemoglobin A1c, an AGE, are commonly used as a diagnostic criterion for both prediabetes and diabetes [3]. In the diabetic state, AGEs accumulate in peripheral nerves [4] which can lead to binding to the receptor for advanced glycation end products (RAGE) that is localized in the axons of peripheral neurons [5]. Binding of RAGE results in increased oxidative stress via downstream activation of NADPH oxidase in a PKCδ-dependent manner [6,7]. In our laboratory, we use differentiated SH-SY5Y cells stressed with AGEs as a model of diabetic PN [8,9]. In chapter 3 of this dissertation we show that cells stressed with AGEs experience increased oxidative stress, as evidenced by increased reactive oxygen species (ROS) generation, as well as disruption in the thiol redox state, as evidenced by a decrease in reduced glutathione (GSH) and an increase in oxidized glutathione (GSSG). Furthermore, AGE treatment resulted in loss of viability and the dying-back (retraction or degeneration) of neurites. We focused on two dietary compounds with antioxidant properties, 3H-1,2-dithiole-3-thione (D3T), and N-acetylcysteine (NAC), as potential protective agents against AGE-induced damage.

Initial studies from our laboratory linked neurite protection with maintenance of GSH [8,9]. Both α-tocopherol and D3T did not confer protection against AGE-induced neurite loss,

and neither of these antioxidants protected against AGE-induced GSH depletion [8,9]. In fact, in chapter 3 we show that D3T paradoxically exacerbates AGE-induced viability loss, generation of ROS, and increased GSSG concentrations. For a full review of the D3T paradox, please see chapter 3. In summary, D3T treatment in the presence of AGE led to further disruption of redox balance by inhibition of glutathione reductase (GR) activity and increased ROS generation via upregulation of glucose-6-phosphate dehydrogenase (G6PD). On the other hand, NAC treatment was able to maintain GSH in AGE-treated cells and conferred complete protection against AGE-induced damage. These results clearly implicate the critical role that GSH plays in neurite maintenance and health under stressed conditions. Our results from chapter 2 further implicate the importance of GSH under baseline conditions, as simple inhibition of GSH synthesis resulted in neurite retraction.

Our previous studies suggest that glutathione-mediated oxidative damage could be responsible for the neurite retraction observed in AGE-challenged cells. Peripheral nerves have low GSH concentrations [10] and diabetes leads to high ROS levels in the axons [11]. PN often presents as axonal degeneration, where degeneration occurs in a distal-to-proximal manner but does not induce apoptosis of the parent cell body [1,11,12]. A potential explanation for this phenomenon could be that axons themselves have a much lower GSH content compared to the parent cell body [13]. GSSG accumulation in neuronal cells has been shown to induce oxidation of neurite cytoskeleton proteins such as tubulin, resulting in neurite damage and retraction [13]. In our present studies, the role of glutathione and the disruption of the thiol redox state are investigated in relation to the potential role they play in neurite degeneration.

4.3 Methods

4.3.1 Materials

Dulbecco's Modified Medium (DMEM), Ham's F12 Medium, penicillin-streptomycin, and fetal bovine serum (FBS) were purchased from Invitrogen (Waltham, MO). All standard cell culture flasks and plates were purchased from ThermoFisher Scientific (Waltham, MO). All reagents such as retinoic acid, bovine serum albumin (BSA), NAC, D3T, and 2-acetylamino-3-[4-(2-acetylamino-2-carboxyethylsulfanylthiocarbonylamino)phenylthiocarbamoylsulfanyl] propionic acid (AAPA) were purchased from Sigma-Aldrich (St. Louis, MO) unless otherwise stated. Oxidized glutathione methyl ester (GSSGme) was purchased from Peptide International (Louisville, KY).

4.3.2 Cell Culture

SH-SY5Y cells were purchased from ATCC (Manassas, VA) and were cultured initially in growth media (DMEM, 10% FBS, 1% penicillin-streptomycin, 8 mM glucose) in 6-well plates (9 cm^2) at a concentration of .4 x 10^6 for 24 hours to allow for adherence. Following adherence, growth media was replaced with differentiating media (1:1 DMEM: F12, 1% FBS, 8 mM glucose, 10 μM retinoic acid) for five days to allow for neuronal cell phenotype development. Treatments for all experiments took place following the five-day differentiation period. Cells treated with NAC or D3T had 1 mM NAC (<1% PBS) or 100 μM D3T (<1% DMSO) added to the media 24 hours prior to 5 mg/mL BSA or AGE treatment. This treatment was then replenished in BSA and AGE treatment groups for 24 hours. For GSSGme, AAPA, or GSSGme/AAPA combination treated cells, 200 μM GSSGme (<1% DMSO + PBS), 15 μM AAPA (<1% DMSO + PBS), or 200 μM GSSGme and 15 μM AAPA (<1% DMSO + PBS), respectively, was added to cells after the differentiation process.

4.3.3 Lentiviral Transduction

Low passage number SH-SY5Y cells were plated in 12 well plates (4 cm^2) at a density of 1 x 10^5 for 24 hours in growth media to allow for adherence. To calculate total transducing units needed, a multiplicity of infection of 10 was used. Total transducing units is calculated my multiplying the total number of cells per well by the desired multiplicity of infection. To increase cellular uptake of the virus, hexadimethrine bromide (polybrene) was used. SH-SY5Y cells are sensitive to polybrene, and concentrations above 4 µg/mL result in rapid viability loss. Lentiviral particles for stable knockdown of glutaredoxin-1 (GRX-1) as well as scramble control were obtained from Origene (Rockville, MD). Lentiviral particles also contained genes for green fluorescence protein and puromycin resistance. After adherence, cells were treated with the appropriate amount of total transducing units and 4 µg/mL polybrene for 20 hours. After lentiviral treatment, media was replaced with growth media containing no penicillin-streptomycin for 48 hours to allow for cells to recover. Following recovery, cells were split 1:5 in a new 12 well plate and allowed to adhere over a 24-hour period in penicillin-streptomycin free growth media. Next, media was replaced with .2µg/mL puromycin containing penicillin-streptomycin free growth media. After 3 days, the concentration of puromycin was increased to .5 µg/mL and then media with this concentration of puromycin was replaced every 3 days for an 18-day period (total of 21 days of puromycin treatment). After 21 days, a ≥ 90% transduction rate was achieved as noted by cells expressing green fluorescence.

4.3.4 Preparation of AGE-BSA and BSA Control

AGE-BSA was prepared as was previously reported in our lab [8]. Briefly, 5 mg/ML BSA in PBS was incubated with 33 mM glycolaldehyde dimer for 20 hours at 37°C. Control BSA was treated in the same manner, but without the addition of glycolaldehyde. Both control

and glycated BSA were then concentrated via ammonium sulfate precipitation. Ammonium sulfate was added to glycated BSA and control solutions (80% ammonium sulfate solution), and then centrifuged at 10,000g for 30 minutes. Precipitated proteins were resuspended with the minimal amount of PBS required for resuspension. Solutions were then dialyzed in PBS for three days, with daily replacement of PBS. Following dialysis, solutions were sterile filtered. The final concentrations of both glycated and control BSA were approximately 15 mg/mL.

4.3.5 Western Blotting

All Western blots were run using a Mini-PROTEAN Tetra Cell system (Bio-rad, Hercules, CA). Both 10% and 4-20% gradient polyacrylamide gels were used. Each sample contained 30 μg of protein. For gel electrophoresis, the running buffer was made up of 25 mM Tris, 192 mM glycine, and .1% (w/v) SDS at pH 8.3. Gels were run at constant voltage (200v) for 30-50 minutes. For protein transfer to nitrocellulose membranes, transfer buffer was made up of 25 mM Tris, .2 M glycine, and 20% methanol at pH 8.5. A constant voltage (90v) for 60 minutes was maintained for transfers. The transfer buffer was refrigerated prior to use, and the entire apparatus was kept cold (approx. 4°C) during protein transfer. Following transfer, blots were incubated based on antibody manufacturer recommendations. For GSH, GRX-1, and β-actin quantification, blots were incubated for 12 hours on a plate shaker at 4°C with a monoclonal mouse antibody (1:1000) (Abcam, Cambridge, MA) for GSH, polyclonal rabbit antibody (1:250) (Abcam, Cambridge, MA) for GRX-1, and monoclonal rabbit (1:1000) (Cell Signaling, Danvers, MA) for β-actin. Both anti-rabbit and anti-mouse secondary antibodies (1:1000) were HRP-linked, and an HRP-detection kit followed by photo-development was used (Cell Signaling, Danvers, MA). GRX-1 bands were normalized to their corresponding β-actin bands and results reported as % of β-actin.

4.3.6 Neurite Quantification

At the completion of experiments, photos were taken to document morphological changes of differentiated SH-SY5Y cells. Images were captured at 10x magnification using a Zeiss Axio Vert. A1 microscope (Oberkochen, Germany). A Zeiss AxioCam ICm1 camera was used to take photos using Zeiss Zen2 imaging software. All images were 1388 x 1038 pixels, and exposure time for all photos was 32.03 ms. Images were then analyzed using ImageJ (NIH) software with NeuronJ (ImageScience) plugin. Individual neurites were traced, and neurite length was reported as length in pixels. Neurites that expressed notable thinning across their length were counted in each treatment group. Neurites present in the field of view were quantified from 6 independent experiments for each treatment group. Exclusion criteria included counting only neurites with clearly defined start and end locations. Neurites that were shorter than the width of the cell body were not counted. For each treatment group, a minimum of 200 total neurites was quantified. To quantify the impact of treatments on the longest neurites, the number of neurites greater than or equal to the average length of neurites at time 0 was calculated for each treatment group.

4.3.7 Statistical Methods

Values are presented as group means ±S.E.M. Treatment effects were tested using a Student's t-test for two variables, or analysis of variance (ANOVA) for multiple variables. A significant ANOVA result was followed by a multiple comparisons of means test (Dunnett or Tukey HSD), with $P<0.05$ considered statistically significant.

4.4 Results

4.4.1 The Effect of GSSGme Treatment on Cell Morphology

The purpose of this study was to document the role of GSSG in the dying-back (retraction) of neurites when SH-SY5Y cells are exposed to pro-oxidative conditions. In order to evaluate the impact of GSSG on cell morphology, 200 μM GSSGme was added to the media for a period of 40 minutes. Photos of the cells were taken at 10x before and after treatment. 40-minute treatment with GSSGme induced significant neurite retraction, resulting in a 19% overall decrease in neurite length (Fig. 4.1). A visual representation of this retraction process is shown in Figure 4.2, where the blue arrows point to notable morphological changes over the 40-minute treatment. GSSGme treatment, however, did not significantly impact the average number of long neurites (Fig. 4.3) or neurite thinning (Fig. 4.4).

4.4.2 The Effect of AAPA Treatment on Cell Morphology

AAPA is a potent and irreversible inhibitor of both GR [14,15] and GRX-1 [16], and as such should significantly disrupt the thiol redox state. Treatment of differentiated cells with concentrations of AAPA above 15 μM induced significant lethality after 40 minutes. 15 μM AAPA treatment induced significant neurite retraction resulting in a 20% decrease in average neurite length (Fig. 4.5). Furthermore, AAPA had a dramatic impact on long neurites, leading to a 63% loss of long neurites in only 40 minutes of treatment (Fig. 4.6). In addition to neurite retraction, AAPA treatment resulted in a 3.3-fold increase in neurite breakdown (measured as neurite thinning) (Fig. 4.4). A 10x image of AAPA treated cells is shown in Figure 4.7, with blue arrows pointing to locations of neurite thinning.

4.4.3 The Effect of GSSGme and AAPA Combination on Cell Morphology

With AAPA inhibition of GR and GRX-1, addition of GSSGme was expected to further disrupt the thiol redox state. The combination treatment (200 μM GSSGme and 15 μM AAPA) for 40 minutes induced significant neurite retraction, resulting in a 29% decrease in average neurite length (Fig. 4.8). The 40-minute combination treatment also resulted in a 77% loss of long neurites (Fig. 4.9) and a 4-fold increase in the number of thinning neurites (Fig. 4.4).

4.4.4 The effect of AGE Treatment and Antioxidant Protection on Glutathionylation

Disruption of the thiol redox state and a buildup of intracellular GSSG can result in increased glutathionylation. Protein glutathionylation was measured via Western blot run under non-reducing conditions followed by incubation with an anti-GSH antibody. A weak band was detected in BSA treated cells with a molecular weight of approximately 55 kDa. AGE treated cells had a 2.6-fold higher intensity band at this molecular weight compared to control BSA cells. (Fig. 4.10). D3T treatment conferred no protection against AGE-induced glutathionylation (Fig. 4.10). However, treatment with NAC resulted in complete protection against AGE-induced glutathionylation.

4.4.5 Generation of Stable GRX-1 Knockdown SH-SY5Y Cells

To establish the role of GRX-1 in neurite protection, particularly under pro-oxidative conditions, GRX-1 knockdown was attempted via lentiviral transduction. Four unique target-specific shRNA containing lentiviral particles were used (TL312745VA, TL312745VB, TL312745VC, TL312745VD) along with a scramble control. Cell transduction efficiency, measured by cells expressing green fluoresce protein, was estimated to be ≥ 90%. GRX-1 knockdown, as measured by GRX-1 protein expression, was not successful for any of the

lentiviral variants (data not shown). A combination of all variants was attempted, but also proved unsuccessful (Fig. 4.11).

4.5 Discussion

A common pathophysiology of PN is the dying-back of neurons in a distal-proximal manner resulting in axonal degeneration [1]. In diabetic PN, neuronal cells undergo morphological changes and axonal degeneration but not cellular loss [11,17–21]. In rat dorsal root ganglia (DRG) cultures, neurons from STZ-diabetic rats showed significant accumulation of ROS in axons compared to non-diabetic controls [11]. Furthermore, 1-month treatment of diabetic rats with insulin did not protect against ROS buildup in peripheral neurons. In DRG cultures from diabetic rats, insulin treatment had no impact on the development of neurite degeneration [11]. Peripheral neurons can be particularly susceptible to hyperglycemia induced ROS generation due to expression of GLUT1 [22], which is not responsive to insulin, and overall low GSH concentrations [10].

Low levels of GSH coupled with increased axonal ROS generation can result in increased axonal structural protein modifications, such as glutathionylation [13]. As we have shown in chapter 3, stressed conditions result in an increase of GSSG concentrations. GSSG can react with free thiols on proteins to form a mixed disulfide (protein S-glutathionylation) via thiol/disulfide exchange reaction [23]. Glutathionylation can serve a protective role, as it is reversible and can protect proteins from irreversible oxidative damage. However, when redox balance becomes disrupted, particularly with depletion of GSH, the antioxidant systems responsible for maintaining reduced thiols (protein disulphide isomerase, thioredoxin, glutaredoxin) are no longer effective and proteins remain in their potentially inactive state [23–26]. Glutaredoxins are the major enzymes responsible for the reduction of glutathionylated proteins, as thioredoxins

show little to no activity with mixed disulfides [26]. Glutaredoxins are highly dependent on GSH levels, as they become glutathionylated upon reduction of mixed disulfides and are maintained in their reduced state by GSH [24,26].

In our study, we added exogenous membrane permeable GSSG (GSSGme) to differentiated SH-SY5Y cells for 40 minutes to disrupt redox balance and observe and quantify the effects on axons. As expected, GSSGme treatment led to a significant 19% decrease in neurite length. Average number of long neurites was also measured, as PN often presents in a "stocking- glove" distribution, where the longest neurons are damaged first and lead to sensory and motor nerve dysfunction in the extremities [27,28]. GSSGme treatment did not have a statistically significant effect on the number of long neurites and thinning neurites. These results suggested that when cells were stressed with GSSGme, the endogenous antioxidant defense system was still robust enough to confer protection. GR was of particular interest, as activity of this enzyme is critical for maintaining the thiol redox state due to its function of reducing GSSG to GSH [14]. To inhibit GR, differentiated cells were incubated with AAPA for 40 minutes. However, AAPA is not a specific inhibitor of GR (K_i 56μM, k_{inact} .1 min^{-1}) [14] and also inhibits GRX-1 (K_i 91.3μM, k_{inact} .127 min^{-1}) [16]. Human GRX-1 catalyzes the reduction of mixed disulfides and can therefore restore the structure/function of glutathionylated proteins [24]. Treatment with AAPA led to a dramatic decrease in long neurites (63% loss) and a 3.3-fold increase in neurite thinning. Combination treatment with AAPA and GSSGme resulted in 77% decrease in long neurites and 4-fold increase in the number of thinning neurites. The significant impact of GR and GRX-1 inhibition on neurite morphology suggests that disruption in the thiol redox state plays a critical role in neurite degeneration. Tubulin, a major cytoskeletal protein that makes up microtubules, is a likely target for glutathionylation due to 20 free thiol groups [13,29].

Tubulin cysteine oxidation has been shown to interfere with tubulin polymerization [13,30,31], and equilibrium between polymerized and depolymerized tubulin is essential for microtubule function and axon structure [13].

In chapter 3 of this dissertation, it was established that maintenance of GSH under stressed conditions is critical for neurite protection. Depletion of GSH and/or decreased activity of GR would promote protein glutathionylation [15], inactivation of GRX-1 [26], and induce neurite retraction [8,9]. We hypothesized that by maintaining GSH, NAC conferred protection against neurite retraction via protection against glutathionylation of neurite structural proteins. In this study we showed that AGE treatment induces significant glutathionylation of proteins at around the 55 kDa molecular weight. This could potentially correspond with α/β tubulin [32], but confirmation would require redox proteomics [33]. D3T treatment, which was not protective against AGE-induced GSH and neurite degeneration, did not confer protection against AGE-induced glutathionylation. Importantly, NAC treatment conferred complete protection against AGE-induced glutathionylation. To confirm the role of protein glutathionylation in neurite retraction, we attempted to knockdown GRX-1 in SH-SY5Y cells. We hypothesized that with GRX-1 inhibition, NAC would no longer confer protection against AGE-induced neurite retraction and glutathionylation regardless of cellular GSH status. These experiments would help establish a mechanism for GSH protection against neurite retraction. Unfortunately, the lentiviral constructs we used failed to knockdown GRX-1. New lentiviral constructs with modified target-specific shRNA will need to be developed to generate a stable GRX-1 knockdown SH-SY5Y cell line.

In conclusion, results from this study suggest that disruption of the thiol redox state plays a critical role in neurite degeneration. In particular, glutathionylation of structural proteins such

as tubulin may result in neurite damage and degeneration. We show that when cells are stressed with AGE, there is a significant increase in glutathionylation. Critically, NAC confers protection against this observed protein glutathionylation. Future studies using GRX-1 knockdown cells will need to be conducted to elucidate the role of glutathionylation in neurite degeneration and to establish the mechanism of GSH protection.

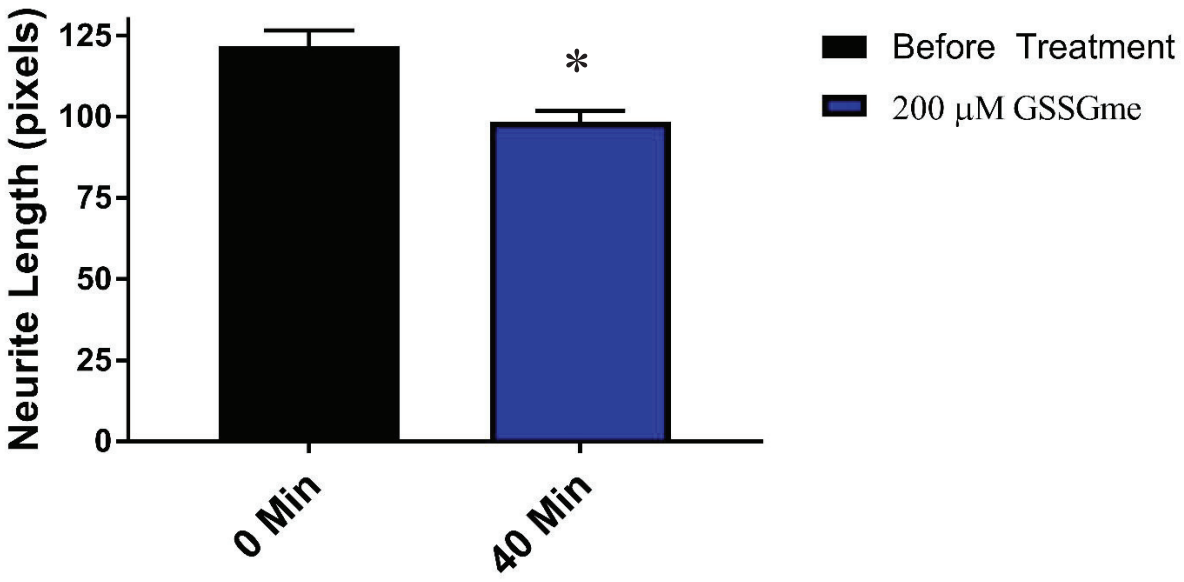

Figure 4.1 GSSGme treatment induces significant neurite retraction.

Following differentiation, cells were treated with 200 μM GSSGme for 40 minutes. Neurite length in 10x images was quantified before and after treatment using Image J with NeuronJ plugin. A minimum of 305 neurites per group were analyzed from 6 independent experiments. Data were analyzed via 2-tailed Student's t-test. Bars with an * are significantly different ($p < 0.05$) from the before treatment group.

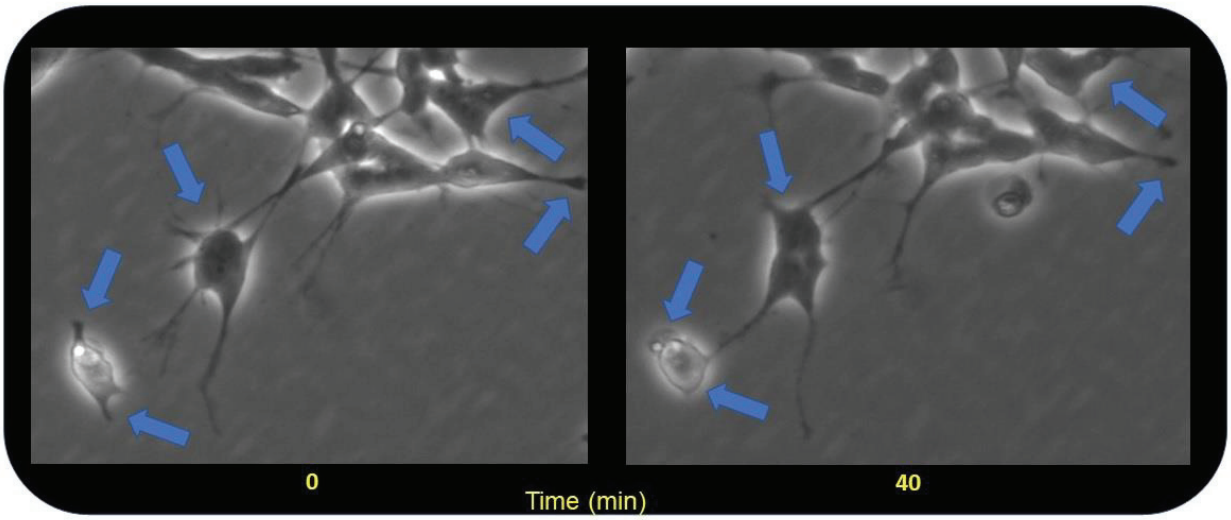

Figure 4.2 GSSGme induces neurite retraction.

Following differentiation, cells were treated with 200 μM GSSGme for 40 minutes. Images are captured at 10x in the same location at both time points. Blue arrows point to neurite outgrowth areas that diminish or disappear with GSSGme treatment.

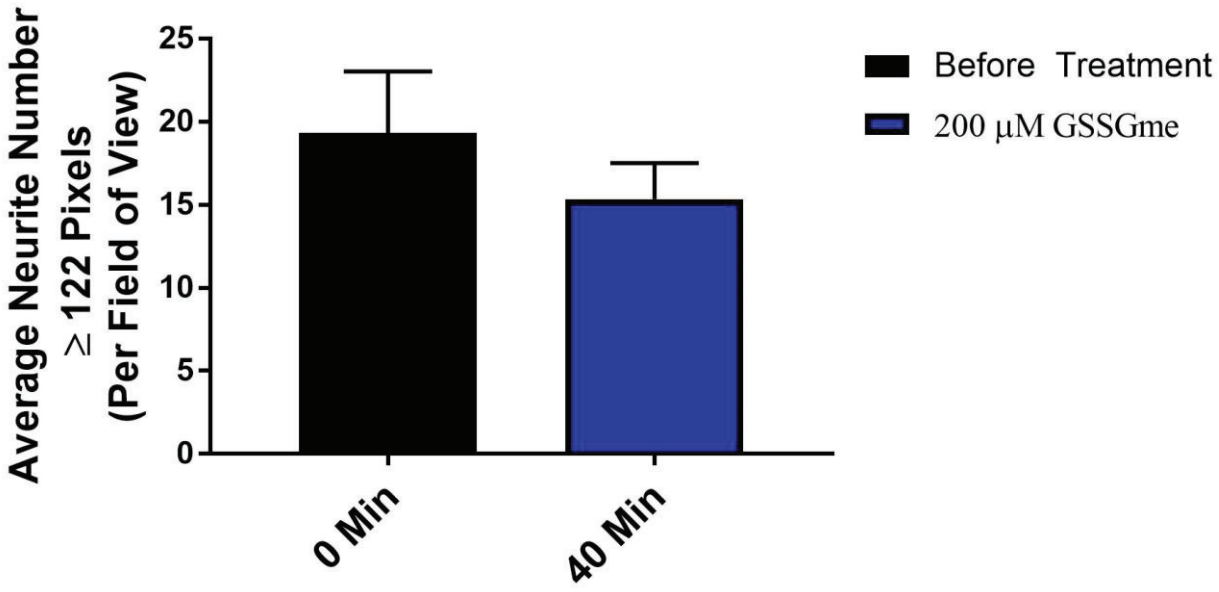

Figure 4.3 GSSGme treatment does not significantly induce loss of long neurites.

Following differentiation, cells were treated with 200 μM GSSGme for 40 minutes. Neurite length in 10x images was quantified before and after treatment using Image J with NeuronJ plugin. A minimum of 305 neurites per group were analyzed from 6 independent experiments. Data were analyzed via 2-tailed Student's t-test. Bars are not significantly different ($p > 0.05$) from each other.

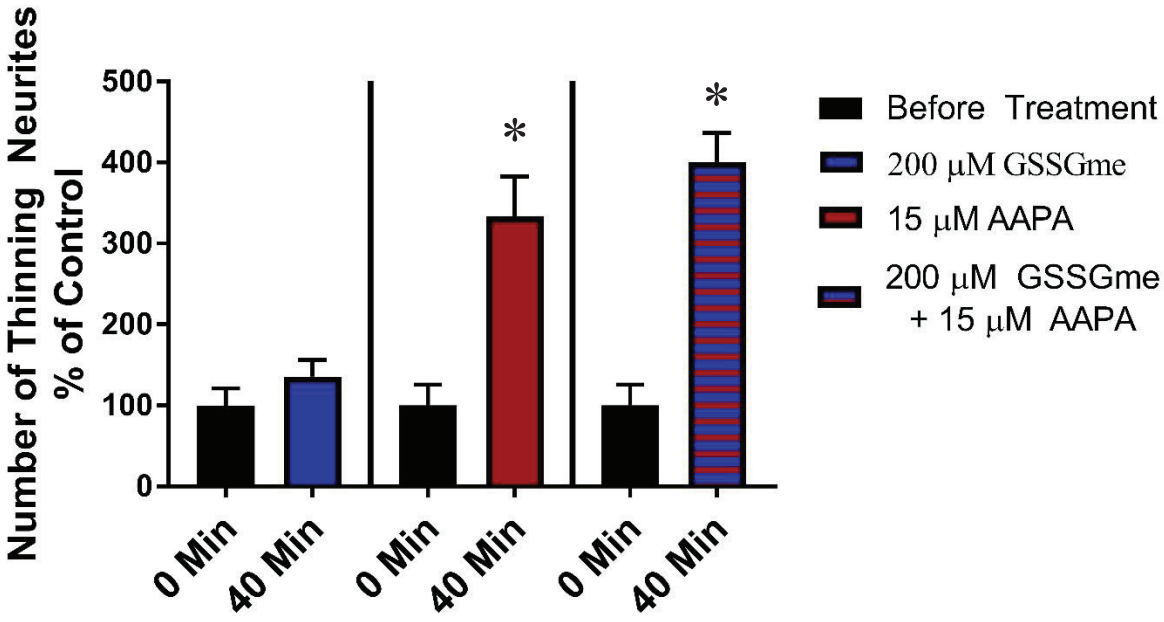

Figure 4.4 AAPA treatment results in significant neurite thinning.

Following differentiation, cells were treated with 200 μM GSSGme, 15 μM AAPA, or 200 μM GSSGme + 15 μM AAPA for 40 minutes. Neurite thinning in 10x images was quantified before and after treatment using Image J with NeuronJ plugin. A minimum of 214 neurites per group were analyzed from 6 independent experiments. Data were analyzed via 2-tailed Student's t-test. Bars with an * are significantly different ($p < 0.05$) from their respective before treatment group.

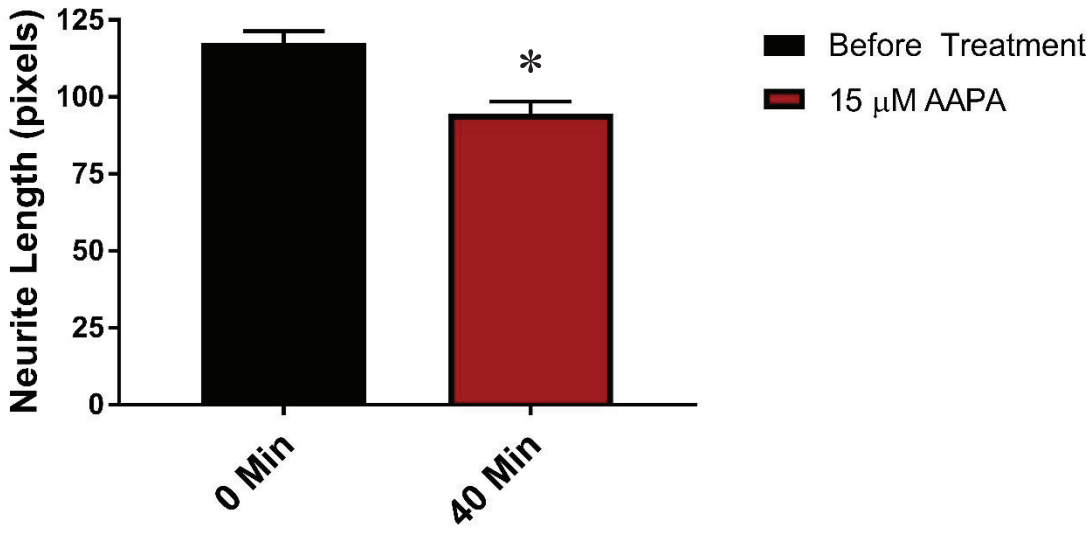

Figure 4.5 AAPA treatment results in significant neurite degeneration.

Following differentiation, cells were treated with 15 μM AAPA for 40 minutes. Neurite length in 10x images was quantified before and after treatment using Image J with NeuronJ plugin. A minimum of 238 neurites per group were analyzed from 6 independent experiments. Data were analyzed via 2-tailed Student's t-test. Bars with an * are significantly different ($p < 0.05$) from the before treatment group.

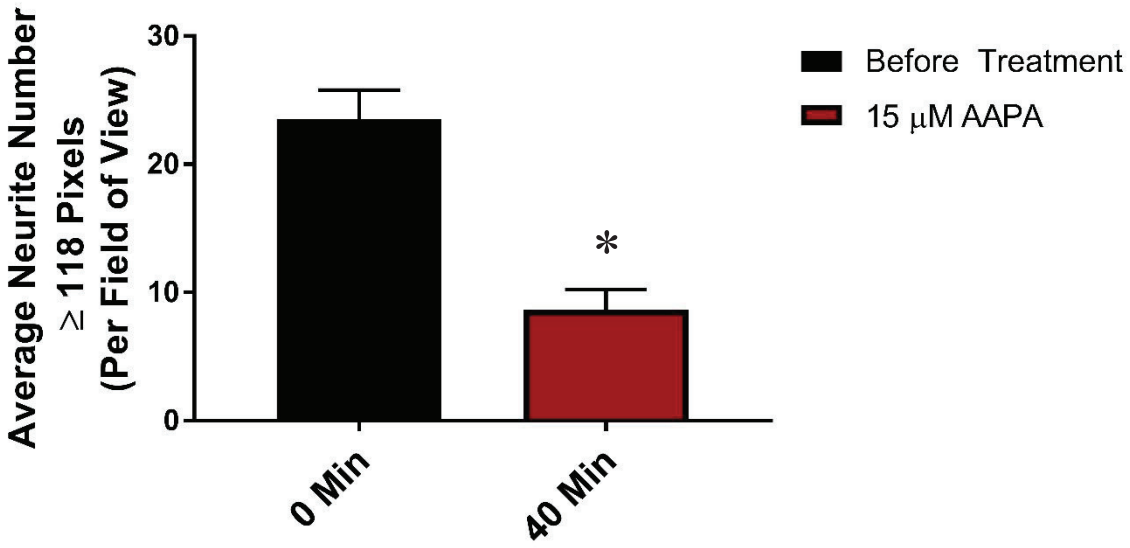

Figure 4.6 AAPA treatment results in significant loss of long neurites.

Following differentiation, cells were treated with 15 μM AAPA for 40 minutes. Neurite length in 10x images was quantified before and after treatment using Image J with NeuronJ plugin. A minimum of 238 neurites per group were analyzed from 6 independent experiments. Data were analyzed via 2-tailed Student's t-test. Bars with an * are significantly different ($p < 0.05$) from the before treatment group.

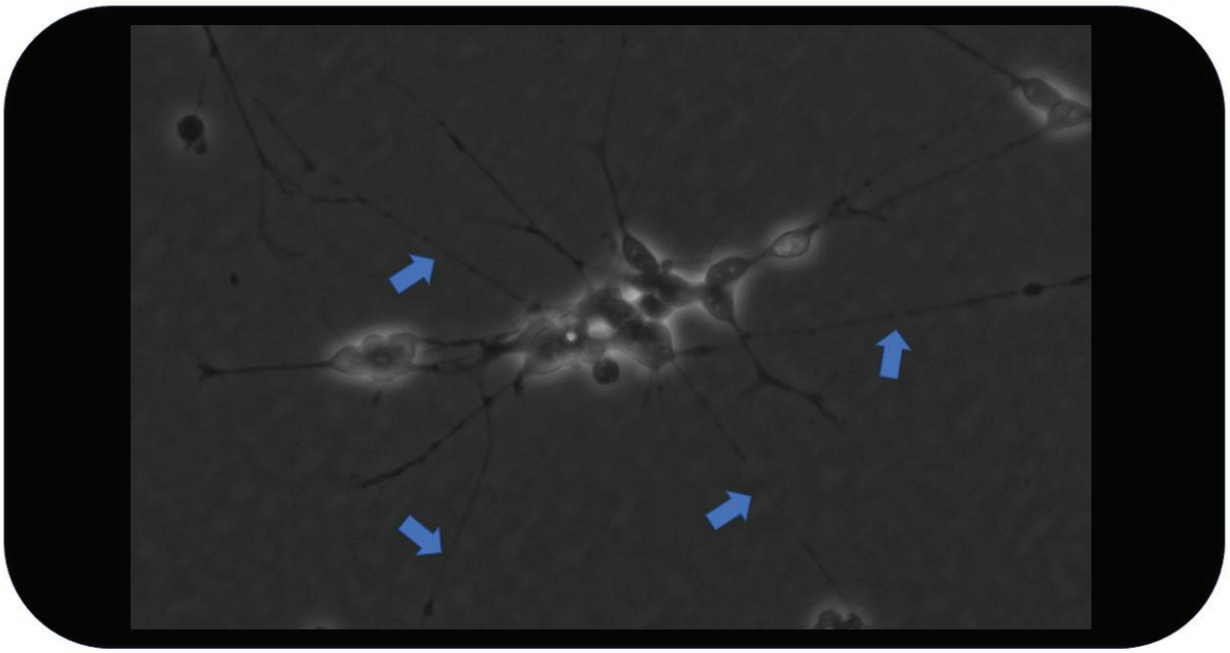

Figure 4.7 AAPA treatment results in neurite thinning.

Following differentiation, cells were treated with 15 µM AAPA for 40 minutes. Images are captured at 10x. Blue arrows point to neurites showing clear signs of thinning after a 40-minute treatment of AAPA.

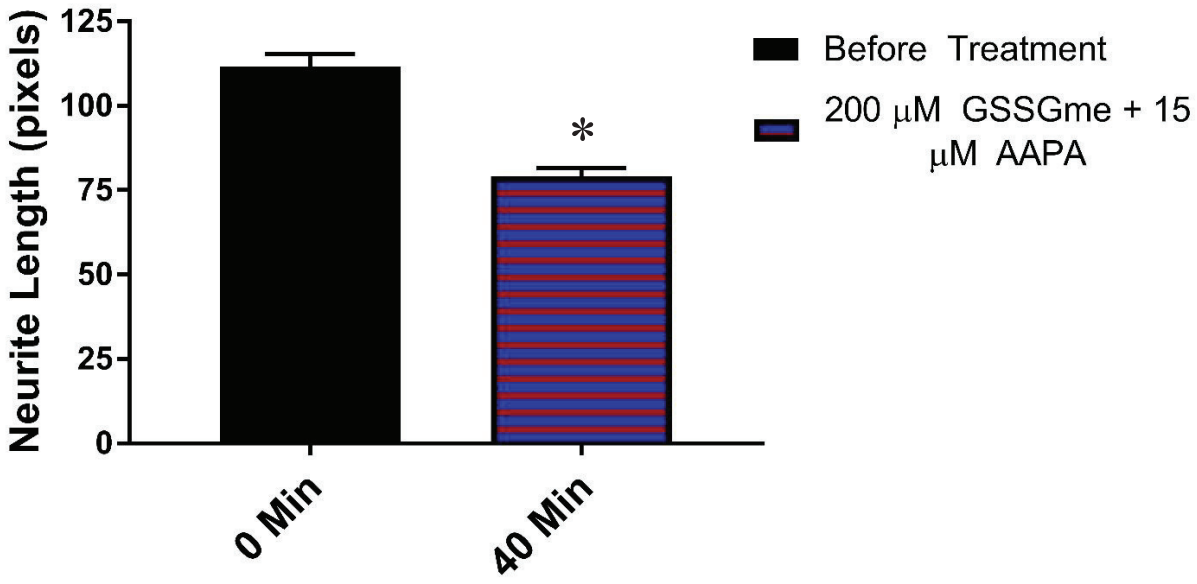

Figure 4.8 GSSGme and AAPA combination treatment results in neurite retraction.

Following differentiation, cells were treated with 200 μM GSSGme + 15 μM AAPA for 40 minutes. Neurite length in 10x images was quantified before and after treatment using Image J with NeuronJ plugin. A minimum of 214 neurites per group were analyzed from 6 independent experiments. Data were analyzed via 2-tailed Student's t-test. Bars with an * are significantly different ($p < 0.05$) from the before treatment group.

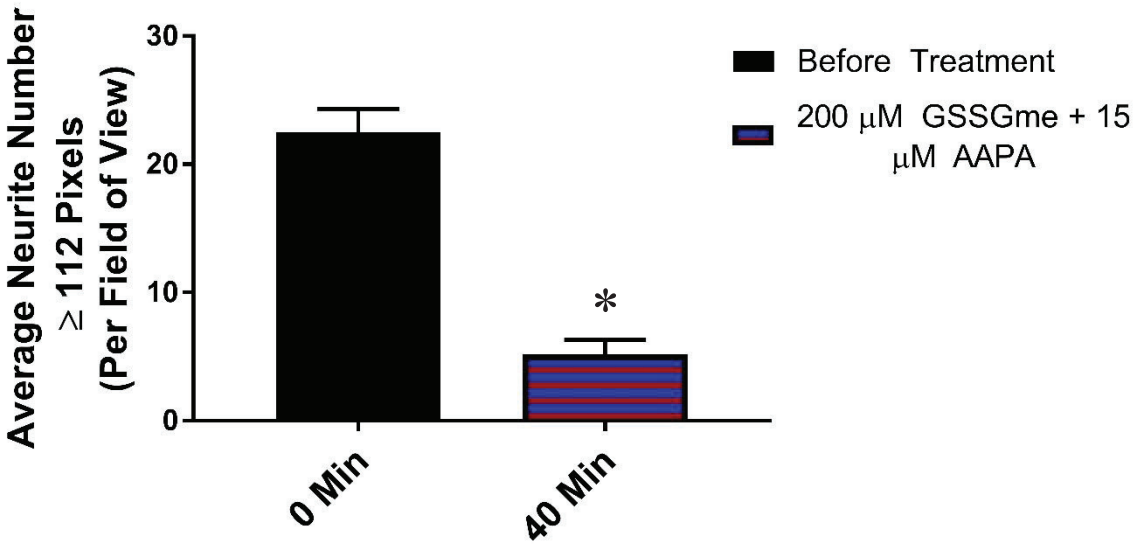

Figure 4.9 GSSGme and AAPA combination treatment results in dramatic loss of long neurites.

Following differentiation, cells were treated with 200 μM GSSGme + 15 μM AAPA for 40 minutes. Neurite length in 10x images was quantified before and after treatment using Image J with NeuronJ plugin. A minimum of 214 neurites per group were analyzed from 6 independent experiments. Data were analyzed via 2-tailed Student's t-test. Bars with an * are significantly different ($p < 0.05$) from the before treatment group.

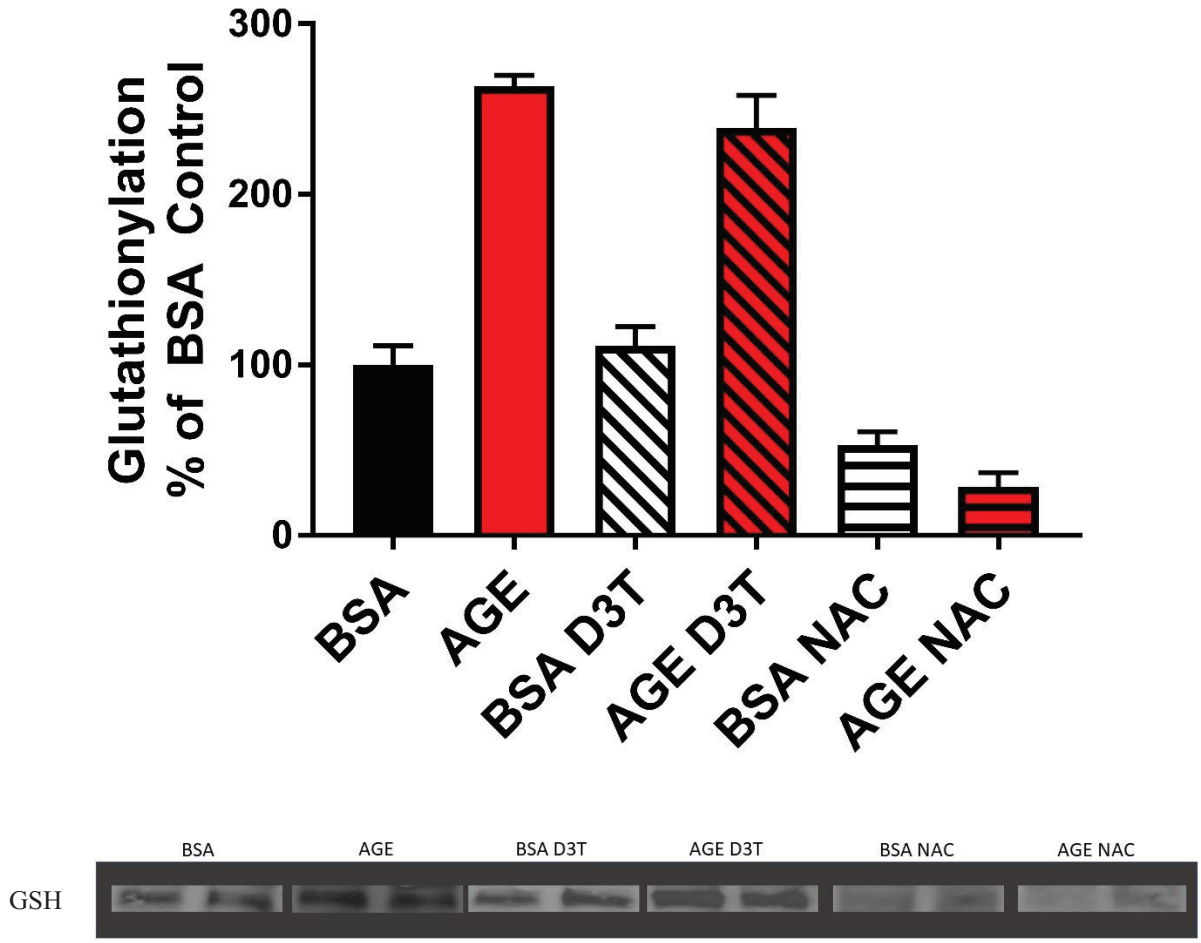

Figure 4.10 NAC treatment confers protection against AGE-induced glutathionylation.

Differentiated cells were treated with 1 mM NAC or 100 μM D3T for 24 hours prior to 5 mg/mL BSA or AGE treatment. NAC and D3T were replenished during the 24-hour BSA and AGE treatment. GSH band appears at a molecular weight of approximately 55 kDa. Data were analyzed by one-way ANOVA with Tukey's post-hoc analysis from 3 independent experiments. Bars not joined by a common superscript letter are significantly different from each other ($p < 0.05$).

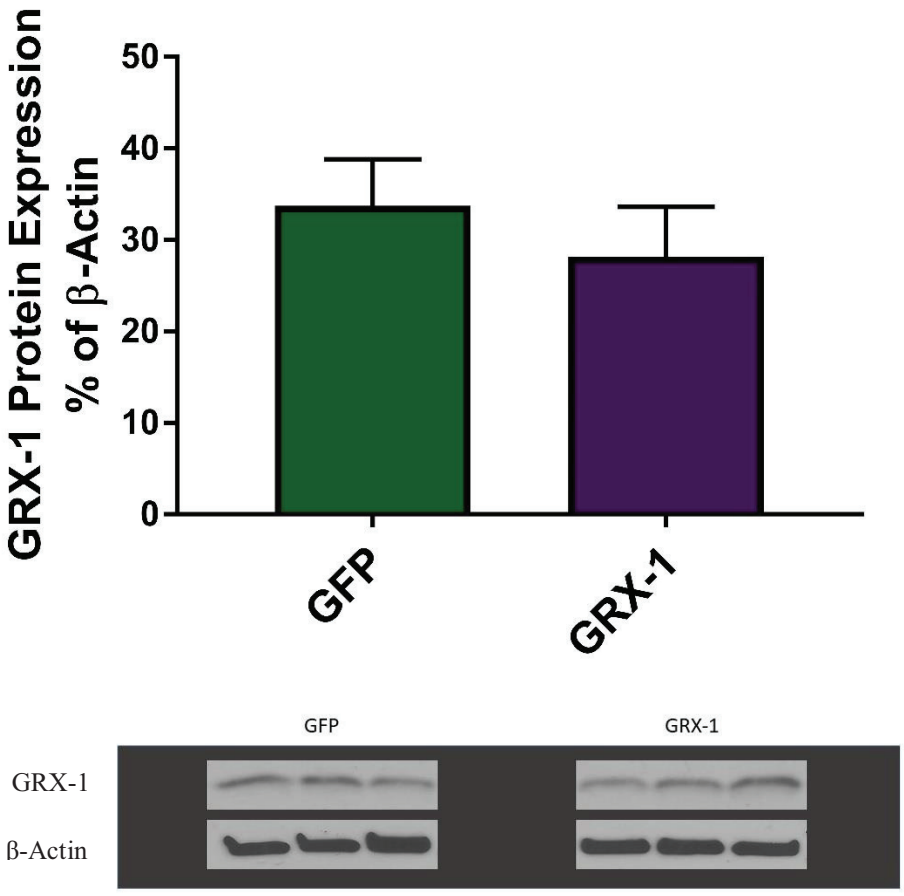

Figure 4.11 Lentiviral transduction does not knockdown GRX-1.

Green fluorescence protein (GFP) scramble control cells and GRX-1 knockdown cells expressed the same amount of GRX-1 protein. GRX-1 band appears at a molecular weight of approximately 10-12 kDa. Data were analyzed via 2-tailed Student's t-test from 3 independent experiments per group. Bars are not significantly different ($p > 0.05$) from each other.

4.6 References

[1] R. (Clevland C. for C.E. Shields, Peripheral Neuropathy, (2010). http://www.clevelandclinicmeded.com/medicalpubs/diseasemanagement/neurology/peripheral-neuropathy/.

[2] E.L. Feldman, K.-A. Nave, T.S. Jensen, D.L.H. Bennett, New Horizons in Diabetic Neuropathy: Mechanisms, Bioenergetics, and Pain, Neuron. 93 (2017) 1296–1313. doi:https://doi.org/10.1016/j.neuron.2017.02.005.

[3] T.J. Lyons, A. Basu, Biomarkers in diabetes: hemoglobin A1c, vascular and tissue markers., Transl. Res. 159 (2012) 303–12. doi:10.1016/j.trsl.2012.01.009.

[4] M. Jack, D. Wright, Role of advanced glycation endproducts and glyoxalase I in diabetic peripheral sensory neuropathy., Transl. Res. 159 (2012) 355–65. doi:10.1016/j.trsl.2011.12.004.

[5] I.G. Obrosova, Diabetes and the peripheral nerve., Biochim. Biophys. Acta. 1792 (2009) 931–40. doi:10.1016/j.bbadis.2008.11.005.

[6] M. Nitti, C. d'Abramo, N. Traverso, D. Verzola, G. Garibotto, A. Poggi, P. Odetti, D. Cottalasso, U.M. Marinari, M.A. Pronzato, C. Domenicotti, Central role of PKCδ in glycoxidation-dependent apoptosis of human neurons, Free Radic. Biol. Med. 38 (2005) 846–856. doi:10.1016/j.freeradbiomed.2004.12.002.

[7] M. Nitti, A.L. Furfaro, N. Traverso, P. Odetti, D. Storace, D. Cottalasso, M.A. Pronzato, U.M. Marinari, C. Domenicotti, PKC delta and NADPH oxidase in AGE-induced neuronal death, Neurosci. Lett. 416 (2007) 261–265. doi:10.1016/j.neulet.2007.02.013.

[8] R. Pazdro, J.R. Burgess, The antioxidant 3H-1,2-dithiole-3-thione potentiates advanced glycation end-product-induced oxidative stress in SH-SY5Y cells., Exp. Diabetes Res. 2012 (2012) 137607. doi:10.1155/2012/137607.

[9] R. Pazdro, J.R. Burgess, Differential effects of α-tocopherol and N-acetyl-cysteine on advanced glycation end product-induced oxidative damage and neurite degeneration in SH-SY5Y cells., Biochim. Biophys. Acta. 1822 (2012) 550–6. doi:10.1016/j.bbadis.2012.01.003.

[10] F.J. Romero, E. Monsalve, C. Hermenegildo, F.J. Puertas, V. Higueras, E. Nies, J. Segura-Aguilar, J. Romá, Oxygen toxicity in the nervous tissue: comparison of the antioxidant defense of rat brain and sciatic nerve., Neurochem. Res. 16 (1991) 157–61. http://www.ncbi.nlm.nih.gov/pubmed/1908956 (accessed November 2, 2014).

[11] E. Zherebitskaya, E. Akude, D.R. Smith, P. Fernyhough, Development of selective axonopathy in adult sensory neurons isolated from diabetic rats: role of glucose-induced oxidative stress., Diabetes. 58 (2009) 1356–64. doi:10.2337/db09-0034.

[12] L.R. Fischer, J.D. Glass, Oxidative stress induced by loss of Cu,Zn-superoxide dismutase (SOD1) or superoxide-generating herbicides causes axonal degeneration in mouse DRG cultures., Acta Neuropathol. 119 (2010) 249–59. doi:10.1007/s00401-009-0631-z.

[13] B. Carletti, C. Passarelli, M. Sparaco, G. Tozzi, A. Pastore, E. Bertini, F. Piemonte, Effect of protein glutathionylation on neuronal cytoskeleton: a potential link to neurodegeneration, Neuroscience. 192 (2011) 285–294. doi:10.1016/j.neuroscience.2011.05.060.

[14] T. Seefeldt, Y. Zhao, W. Chen, A.S. Raza, L. Carlson, J. Herman, A. Stoebner, S. Hanson, R. Foll, X. Guan, Characterization of a novel dithiocarbamate glutathione reductase inhibitor and its use as a tool to modulate intracellular glutathione., J. Biol. Chem. 284 (2009) 2729–37. doi:10.1074/jbc.M802683200.

[15] Y. Zhao, T. Seefeldt, W. Chen, X. Wang, D. Matthees, Y. Hu, X. Guan, Effects of glutathione reductase inhibition on cellular thiol redox state and related systems., Arch. Biochem. Biophys. 485 (2009) 56–62. doi:10.1016/j.abb.2009.03.001.

[16] S.S. Sadhu, E. Callegari, Y. Zhao, X. Guan, T. Seefeldt, Evaluation of a dithiocarbamate derivative as an inhibitor of human glutaredoxin-1, J. Enzyme Inhib. Med. Chem. 28 (2013) 456–462. doi:10.3109/14756366.2011.649267.

[17] R.A. Malik, S. Tesfaye, P.G. Newrick, D. Walker, S.M. Rajbhandari, I. Siddique, A.K. Sharma, A.J.M. Boulton, R.H.M. King, P.K. Thomas, J.D. Ward, Sural nerve pathology in diabetic patients with minimal but progressive neuropathy., Diabetologia. 48 (2005) 578–85. doi:10.1007/s00125-004-1663-5.

[18] S. Yagihashi, Pathology and pathogenetic mechanisms of diabetic neuropathy., Diabetes. Metab. Rev. 11 (1995) 193–225. http://www.ncbi.nlm.nih.gov/pubmed/8536541 (accessed June 14, 2018).

[19] S. Dronavalli, I. Duka, G.L. Bakris, The pathogenesis of diabetic nephropathy., Nat. Clin. Pract. Endocrinol. Metab. 4 (2008) 444–52. doi:10.1038/ncpendmet0894.

[20] R.E. Schmidt, D. Dorsey, C.A. Parvin, L.N. Beaudet, S.B. Plurad, K.A. Roth, Dystrophic axonal swellings develop as a function of age and diabetes in human dorsal root ganglia., J. Neuropathol. Exp. Neurol. 56 (1997) 1028–43. http://www.ncbi.nlm.nih.gov/pubmed/9291944 (accessed June 14, 2018).

[21] R.E. Schmidt, L.N. Beaudet, S.B. Plurad, D.A. Dorsey, Axonal cytoskeletal pathology in aged and diabetic human sympathetic autonomic ganglia., Brain Res. 769 (1997) 375–83. http://www.ncbi.nlm.nih.gov/pubmed/9374210 (accessed June 14, 2018).

[22] P. Magnani, P.V. Cherian, G.W. Gould, D.A. Greene, A.A.F. Sima, F.C.B. Iii, Glucose Transporters in Rat Peripheral Nerve : P a r a n o d a l Expression of GLUT1 and GLUT3, Metabolism. 45 (1996) 1466–1473.

[23] D. Giustarini, R. Rossi, A. Milzani, R. Colombo, I. Dalle-Donne, S-glutathionylation: from redox regulation of protein functions to human diseases., J. Cell. Mol. Med. 8 (n.d.) 201–12. http://www.ncbi.nlm.nih.gov/pubmed/15256068 (accessed June 13, 2018).

[24] C.H. Lillig, C. Berndt, A. Holmgren, Glutaredoxin systems, Biochim. Biophys. Acta - Gen. Subj. 1780 (2008) 1304–1317. doi:10.1016/j.bbagen.2008.06.003.

[25] J. Lu, A. Holmgren, The thioredoxin antioxidant system, Free Radic. Biol. Med. 66 (2014) 75–87. doi:10.1016/J.FREERADBIOMED.2013.07.036.

[26] A.P. Fernandes, A. Holmgren, Glutaredoxins: Glutathione-Dependent Redox Enzymes with Functions Far Beyond a Simple Thioredoxin Backup System, Antioxid. Redox Signal. 6 (2004) 63–74. doi:10.1089/152308604771978354.

[27] J.L. Edwards, A.M. Vincent, H.T. Cheng, E.L. Feldman, Diabetic neuropathy: mechanisms to management., Pharmacol. Ther. 120 (2008) 1–34. doi:10.1016/j.pharmthera.2008.05.005.

[28] M. Sinnreich, B. V. Taylor, P.J.B. Dyck, Diabetic Neuropathies, Neurologist. 11 (2005) 63–79. doi:10.1097/01.nrl.0000156314.24508.ed.

[29] P.J. Britto, L. Knipling, P. McPhie, J. Wolff, Thiol-disulphide interchange in tubulin: kinetics and the effect on polymerization., Biochem. J. 389 (2005) 549–58. doi:10.1042/BJ20042118.

[30] K. Huber, P. Patel, L. Zhang, H. Evans, A.D. Westwell, P.M. Fischer, S. Chan, S. Martin, 2-[(1-methylpropyl)dithio]-1H-imidazole inhibits tubulin polymerization through cysteine oxidation., Mol. Cancer Ther. 7 (2008) 143–51. doi:10.1158/1535-7163.MCT-07-0486.

[31] L.M. Landino, R. Hasan, A. McGaw, S. Cooley, A.W. Smith, K. Masselam, G. Kim, Peroxynitrite oxidation of tubulin sulfhydryls inhibits microtubule polymerization., Arch. Biochem. Biophys. 398 (2002) 213–20. doi:10.1006/abbi.2001.2729.

[32] S.R. Pfeffer, D.G. Drubin, R.B. Kelly, Identification of three coated vesicle components as alpha- and beta-tubulin linked to a phosphorylated 50,000-dalton polypeptide., J. Cell Biol. 97 (1983) 40–7. doi:10.1083/JCB.97.1.40.

[33] M. Fratelli, H. Demol, M. Puype, S. Casagrande, I. Eberini, M. Salmona, V. Bonetto, M. Mengozzi, F. Duffieux, E. Miclet, A. Bachi, J. Vandekerckhove, E. Gianazza, P. Ghezzi, Identification by redox proteomics of glutathionylated proteins in oxidatively stressed human T lymphocytes, Proc. Natl. Acad. Sci. 99 (2002) 3505–3510. doi:10.1073/pnas.052592699.

CHAPTER 5. SUMMARY AND FUTURE DIRECTIONS

5.1 Summary

Diabetes mellitus is one of the most common chronic diseases and PN affects at least 50% of diabetic patients [1,2]. Medications available to patients ameliorate symptoms (pain), but do not protect against cellular damage and come with severe side effects leading to discontinued use [3,4]. The lack of proper available treatment will continue to make PN a major public health concern, especially because it is estimated that 37% of US adults are currently classified as "prediabetic" [5]. Patients with prediabetes and metabolic syndrome are also at elevated risk for development of PN [2]. After development of PN, reversal is very difficult. Therefore, treatment and prevention strategies should also be focused on groups most susceptible to the development of PN. The most effective treatment or prevention strategy for PN is a return to normoglycemia [6,7]. Many times, however, this requires significant lifestyle modifications that include changes in both diet and exercise. For diabetic patients, additional comorbidities such as PN make this task more difficult to achieve. Establishing treatment and prevention strategies for PN should be of utmost priority. Prevention, slowing onset, or improvement of symptoms of PN can significantly improve the quality of life of prediabetic and diabetic patients and give them more tools to make difficult and dramatic lifestyle changes to combat diabetes.

Because oxidative stress is implicated as a major contributor to the development of diabetic PN [8], this dissertation focused on two easily assessible dietary compounds with antioxidant properties. In chapter 2 of this dissertation N-acetylcysteine (NAC), a thiol-containing compound known for its potent antioxidant properties, was studied. Differentiated SH-SY5Y cells were used as a model for peripheral neurons. In this cell culture model, diabetic conditions and the resulting induction of oxidative stress were mimicked by incubating cells with

advanced glycation end products (AGE). AGE treatment resulted in significant neurite degeneration, which was quantified by measuring neurite length and neurite number. The current studies confirmed previous results that NAC conferred complete protection against AGE-induced neurite degeneration. Because NAC can confer protection either as a free radical scavenger and/or through maintenance of glutathione, the mechanism of NAC protection was explored. Establishing this mechanism was of high importance, as the free radical scavenging properties of NAC are not observed in *in vivo* studies due to low bioavailability of native NAC due to metabolism [9,10]. By inhibiting glutathione synthesis, it was established that NAC conferred protection against AGE-induced neurite degeneration via a glutathione-mediated mechanism. With glutathione synthesis inhibited, NAC lost all protective effects. These studies further established the critical role of glutathione in neurite protection and maintenance. Inhibition of glutathione synthesis in differentiated SH-SY5Y cells under control conditions resulted in neurite degeneration quantified by a decrease in average neurite length and loss of long neurites.

Chapter 3 of this dissertation focused on 3H-1,2-dithole-3-thione (D3T), a compound/phytochemical found in cruciferous vegetables that generates its antioxidant effect through stimulating endogenous cellular antioxidant defenses. As a potent nuclear factor (erythroid-derived 2)- like (Nrf2) inducer, D3T was expected to confer protection against AGE-induced neurite degeneration. Paradoxically, D3T appeared to exacerbate AGE-induced damage [11]. In the present studies, D3T treatment exacerbated AGE-induced buildup of oxidized glutathione, further decreased cell viability, increased reactive oxygen species (ROS) generation, and conferred no neurite protection. D3T treatment increased glucose-6-phospahte dehydrogenase (G6PD) protein expression, a Nrf2 responsive gene. Inhibition of G6PD completely protected against AGE and AGE-D3T induced damage, suggesting its role as an

NADPH generating agent may promote oxidative stress rather than provide protection. This problem was compounded by another important discovery that when cells were stressed with AGE, D3T treatment reduced glutathione reductase activity. These results explained how D3T treatment further exacerbated AGE-induced glutathione buildup. In this manner, D3T inhibited the effectiveness of the endogenous antioxidant defense system and led to disruption of the thiol redox state. Results from chapter 3 suggest that using a strategy to protect against oxidative stress by upregulation of the endogenous antioxidant defense system via Nrf2 may backfire and promote further damage if the products of upregulation contribute to ROS generation.

Results from both chapter 2 and chapter 3 have shown that disruption in the redox state, as measured by the amount of reduced and oxidized glutathione, leads to neurite degeneration. In chapter 4, the effects of glutathione-mediated oxidative damage were investigated. Cells treated with AGEs experienced a significant loss of reduced glutathione and an increase in oxidized glutathione. This condition can result in a disruption of the thiol redox state, as oxidized glutathione reacts with free thiols on proteins and forms mixed disulfides (protein glutathionylation) [12]. Protein glutathionylation is reversible, but reversal is dependent on reduced glutathione dependent enzyme glutaredoxin-1 [13]. When exogenous membrane permeable oxidized glutathione (GSSGme) was added to the media of differentiated SH-SY5Y cells, significant neurite retraction was observed. Further disruption of the thiol redox state via inhibition of glutathione reductase and glutaredoxin-1 exacerbated neurite damage, resulting in a dramatic increase of thinning neurites and a loss of long neurites. The significant impact observed of glutathione reductase and glutaredoxin-1 inhibition suggested protein glutathionylation (potentially structural proteins such as tubulin) as a mechanism for neurite degeneration. Treating SH-SY5Y cells with AGEs to mimic diabetic conditions resulted in

significant protein glutathionylation. NAC treatment conferred complete protection against AGE-induced protein glutathionylation. Taken together the results show that maintenance of the thiol redox state is critical for maintaining neurite morphology, and antioxidants such as NAC that protect the thiol redox state will confer neurite protection in pro-oxidative conditions.

5.2 Future Directions

1. Establishing GRX-1 stable knockdown SH-SY5Y cells

Currently there is no known specific chemical inhibitor for GRX-1. 2-acetylamino-3-[4-(2-acetylamino-2-carboxyethylsulfanylthiocarbonylamino)phenylthiocarbamoylsulfanyl] propionic acid (AAPA) was used in our studies to inhibit both glutathione reductase and GRX-1 [14,15]. In our cell culture model of diabetic peripheral neuropathy, diabetic conditions and induction of oxidative stress in cells was mimicked with AGEs. The observed increase in oxidative stress results in a loss of reduced glutathione (GSH) and an increase in oxidized glutathione (GSSG). When the GSH:GSSG ratio decreases, it can disrupt the thiol redox state of the cell [16]. One potential outcome of this disruption is the increase in protein glutathionylation. In chapter 4, it is shown that there is a significant increase in protein glutathionylation when cells are stressed with AGEs. We show evidence that NAC, which confers complete protection against AGE-induced neurite degeneration, protects against the observed increase in glutathionylation. It was hypothesized that NAC would confer protection by maintaining cellular GSH, which would allow GRX-1 to reduce glutathionylated proteins and prevent neurite degeneration. However, this question cannot be answered using AAPA as an inhibitor of GRX-1. By inhibiting glutathione reductase, we are also disrupting other components of the endogenous antioxidant defense system that are dependent on GSH. Generation of a stable GRX-1 knockdown model, as was attempted in chapter 4, would allow us to establish the role of GRX-1 in neurite

maintenance. It was hypothesized that when GRX-1 is knocked down, NAC would no longer confer protection against neurite degeneration because the cell would not be able to reduce glutathionylated proteins.

2. Identifying glutathionylated proteins

In the present studies, we were able to quantify the total amount of glutathionylated proteins by running a Western blot under non-reducing conditions and then using an anti-GSH antibody. A major glutathionylated protein band appears at a molecular weight of approximately 55 kDa. It was hypothesized that this band could be the microtubule associated structural proteins α/β-tubulin. Studies done using differentiated NSC34 cells suggest tubulin glutathionylation could be driving neurite degeneration [17]. To identify the glutathionylated proteins conclusively, redox proteomics would need to be conducted as done by the Fratelli *et al* group [18]. Another protein of interest with a molecular weight matching our GSH band would be glutathione reductase. In chapter 3 it was shown that the combination of AGE and D3T treatment led to a significant decrease in glutathione reductase activity. There is a possibility that the loss of activity was due to glutathionylation of glutathione reductase.

3. Explanation of the glutathione reductase paradox

From our studies in chapter 3, a mechanism for how the potent Nrf2 inducer D3T exacerbated AGE-induced damage was developed. However, Nrf2 upregulation is an expected protective response to increased oxidative stress, and D3T is generally regarded as a protective antioxidant compound [19–22]. In our model system, D3T treatment induced an increase in G6PD protein expression. The increase of reducing equivalents (NADPH) would be expected to

confer protection, as glutathione reductase reduces GSSG to GSH in a NADPH-dependent manner. However, NADPH oxidases are also dependent on NADPH to generate superoxide. With the observed decrease in glutathione reductase activity, it is possible that increased NADPH generation via G6PD resulted in increased NADPH oxidase activity in AGE treated cells resulting in a pro-oxidative condition. Therefore, it is critical to understand the mechanism behind D3T inhibition of glutathione reductase activity. Preliminary data from our lab suggest protein carbonyl formation (irreversible protein oxidation) may play a role in glutathione reductase inhibition (data not shown).

4. Translation of results from SH-SY5Y cells to other models

As a transition step to future application of these results to humans, an intermediate step would involve animal studies. Prior to designing an animal study, testing other cellular models is warranted. Translation of the results presented here to a model in primary culture is important to show the results are not confined to differentiated SH-SY5Y cells. Isolated rat dorsal root ganglia sensory neurons (DRG) would be a good primary culture model. Rat DRG have been shown to express the receptor for advanced glycation end products (RAGE) and respond to RAGE ligand S100 [23]. Use of S100 in DRG resulted in a significant increase of ROS and neuronal injury [23]. Importantly, DRG isolated from STZ-diabetic rats showed significant accumulation of ROS in axons and abnormal changes in neuronal outgrowth compared to non-diabetic controls. Furthermore, NAC treatment of STZ-diabetic DRG enhanced neuronal outgrowth [24]. Important initial experiments to confirm in the rat DRG model would be evaluation of neurite degeneration and redox balance (GSH and GSSG quantification) in response to AGE treatment. Follow up experiments would include evaluation of the antioxidants

NAC and D3T in protection against AGE-induced damage. If D3T treatment exacerbates the condition as is observed in SH-SY5Y cells, it would be important to test whether other Nrf2 inducers such as diallyl sulfide and sulforaphane have a similar effect [25]. These follow up studies will need to be conducted (both primary culture and animal studies) before we can recommend or advise against the use phytochemicals such as D3T in patients suffering with diabetic peripheral neuropathy. NAC treatment has already been shown to be protective in STZ-diabetic DRG [24], but confirmation that protection is conferred via a GSH-mediated mechanism is necessary. If GSH maintenance is found to be critical for neurite protection, as is the case for SH-SY5Y cells, future studies should focus on evaluating the neuroprotective properties of both Nrf2 and non-Nrf2-mediated GSH-inducing substances.

5.3 References

[1] Effect of intensive therapy on the microvascular complications of type 1 diabetes mellitus., JAMA. 287 (2002) 2563–9. http://www.pubmedcentral.nih.gov/articlerender.fcgi?artid=2622728&tool=pmcentrez&rendertype=abstract (accessed October 28, 2014).

[2] A.M. Stino, A.G. Smith, Peripheral neuropathy in prediabetes and the metabolic syndrome., J. Diabetes Investig. 8 (2017) 646–655. doi:10.1111/jdi.12650.

[3] T.J. Lindsay, B.C. Rodgers, V. Savath, K. Hettinger, Treating diabetic peripheral neuropathic pain., Am. Fam. Physician. 82 (2010) 151–8. http://www.ncbi.nlm.nih.gov/pubmed/20642268 (accessed September 16, 2014).

[4] T. Saarto, P.J. Wiffen, Antidepressants for neuropathic pain: a Cochrane review., J. Neurol. Neurosurg. Psychiatry. 81 (2010) 1372–3. doi:10.1136/jnnp.2008.144964.

[5] Centers for Disease Control Prevention, Diabetes 2014 Report Card, 2014. www.cdc.gov/diabetes/library/reports/congress.html (accessed April 29, 2018).

[6] E.L. Feldman, Oxidative stress and diabetic neuropathy: a new understanding of an old problem., J. Clin. Invest. 111 (2003) 431–3. doi:10.1172/JCI17862.

[7] J.W. Baynes, S.R. Thorpe, Role of oxidative stress in diabetic complications: a new perspective on an old paradigm., Diabetes. 48 (1999) 1–9. http://www.ncbi.nlm.nih.gov/pubmed/9892215 (accessed September 2, 2014).

[8] E.L. Feldman, K.-A. Nave, T.S. Jensen, D.L.H. Bennett, New Horizons in Diabetic Neuropathy: Mechanisms, Bioenergetics, and Pain, Neuron. 93 (2017) 1296–1313. doi:https://doi.org/10.1016/j.neuron.2017.02.005.

[9] K.R. Atkuri, J.J. Mantovani, L.A. Herzenberg, L.A. Herzenberg, N-Acetylcysteine--a safe antidote for cysteine/glutathione deficiency., Curr. Opin. Pharmacol. 7 (2007) 355–9. doi:10.1016/j.coph.2007.04.005.

[10] I.A. Cotgreave, N-acetylcysteine: pharmacological considerations and experimental and clinical applications., Adv. Pharmacol. 38 (1997) 205–27. http://www.ncbi.nlm.nih.gov/pubmed/8895810 (accessed April 27, 2018).

[11] R. Pazdro, J.R. Burgess, The antioxidant 3H-1,2-dithiole-3-thione potentiates advanced glycation end-product-induced oxidative stress in SH-SY5Y cells., Exp. Diabetes Res. 2012 (2012) 137607. doi:10.1155/2012/137607.

[12] D. Giustarini, R. Rossi, A. Milzani, R. Colombo, I. Dalle-Donne, S-glutathionylation: from redox regulation of protein functions to human diseases., J. Cell. Mol. Med. 8 (n.d.) 201–12. http://www.ncbi.nlm.nih.gov/pubmed/15256068 (accessed June 13, 2018).

[13] A.P. Fernandes, A. Holmgren, Glutaredoxins: Glutathione-Dependent Redox Enzymes with Functions Far Beyond a Simple Thioredoxin Backup System, Antioxid. Redox Signal. 6 (2004) 63–74. doi:10.1089/152308604771978354.

[14] S.S. Sadhu, E. Callegari, Y. Zhao, X. Guan, T. Seefeldt, Evaluation of a dithiocarbamate derivative as an inhibitor of human glutaredoxin-1, J. Enzyme Inhib. Med. Chem. 28 (2013) 456–462. doi:10.3109/14756366.2011.649267.

[15] Y. Zhao, T. Seefeldt, W. Chen, X. Wang, D. Matthees, Y. Hu, X. Guan, Effects of glutathione reductase inhibition on cellular thiol redox state and related systems., Arch. Biochem. Biophys. 485 (2009) 56–62. doi:10.1016/j.abb.2009.03.001.

[16] T. Seefeldt, Y. Zhao, W. Chen, A.S. Raza, L. Carlson, J. Herman, A. Stoebner, S. Hanson, R. Foll, X. Guan, Characterization of a novel dithiocarbamate glutathione reductase inhibitor and its use as a tool to modulate intracellular glutathione., J. Biol. Chem. 284 (2009) 2729–37. doi:10.1074/jbc.M802683200.

[17] B. Carletti, C. Passarelli, M. Sparaco, G. Tozzi, A. Pastore, E. Bertini, F. Piemonte, Effect of protein glutathionylation on neuronal cytoskeleton: a potential link to neurodegeneration, Neuroscience. 192 (2011) 285–294. doi:10.1016/j.neuroscience.2011.05.060.

[18] M. Fratelli, H. Demol, M. Puype, S. Casagrande, I. Eberini, M. Salmona, V. Bonetto, M. Mengozzi, F. Duffieux, E. Miclet, A. Bachi, J. Vandekerckhove, E. Gianazza, P. Ghezzi, Identification by redox proteomics of glutathionylated proteins in oxidatively stressed human T lymphocytes, Proc. Natl. Acad. Sci. 99 (2002) 3505–3510. doi:10.1073/pnas.052592699.

[19] K.-R. Li, S.-Q. Yang, Y.-Q. Gong, H. Yang, X.-M. Li, Y.-X. Zhao, J. Yao, Q. Jiang, C. Cao, 3H-1,2-dithiole-3-thione protects retinal pigment epithelium cells against Ultra-violet radiation via activation of Akt-mTORC1-dependent Nrf2-HO-1 signaling., Sci. Rep. 6 (2016) 25525. doi:10.1038/srep25525.

[20] J. Dong, D. Yan, S. Chen, Stabilization of Nrf2 Protein by D3T Provides Protection against Ethanol-Induced Apoptosis in PC12 Cells, PLoS One. 6 (2011) e16845. doi:10.1371/journal.pone.0016845.

[21] Z. Jia, H. Zhu, M.A. Trush, H.P. Misra, Y. Li, Generation of superoxide from reaction of 3H-1,2-dithiole-3-thione with thiols: implications for dithiolethione chemoprotection., Mol. Cell. Biochem. 307 (2008) 185–91. doi:10.1007/s11010-007-9598-z.

[22] M. Kobayashi, L. Li, N. Iwamoto, Y. Nakajima-Takagi, H. Kaneko, Y. Nakayama, M. Eguchi, Y. Wada, Y. Kumagai, M. Yamamoto, The antioxidant defense system Keap1-Nrf2 comprises a multiple sensing mechanism for responding to a wide range of chemical compounds., Mol. Cell. Biol. 29 (2009) 493–502. doi:10.1128/MCB.01080-08.

[23] A.M. Vincent, L. Perrone, K. a Sullivan, C. Backus, A.M. Sastry, C. Lastoskie, E.L. Feldman, Receptor for advanced glycation end products activation injures primary sensory neurons via oxidative stress., Endocrinology. 148 (2007) 548–58. doi:10.1210/en.2006-0073.

[24] E. Zherebitskaya, E. Akude, D.R. Smith, P. Fernyhough, Development of selective axonopathy in adult sensory neurons isolated from diabetic rats: role of glucose-induced oxidative stress., Diabetes. 58 (2009) 1356–64. doi:10.2337/db09-0034.

[25] H. Kumar, I.-S. Kim, S.V. More, B.-W. Kim, D.-K. Choi, Natural product-derived pharmacological modulators of Nrf2/ARE pathway for chronic diseases, Nat. Prod. Rep. 31 (2014) 109–139. doi:10.1039/C3NP70065H.

APPENDIX

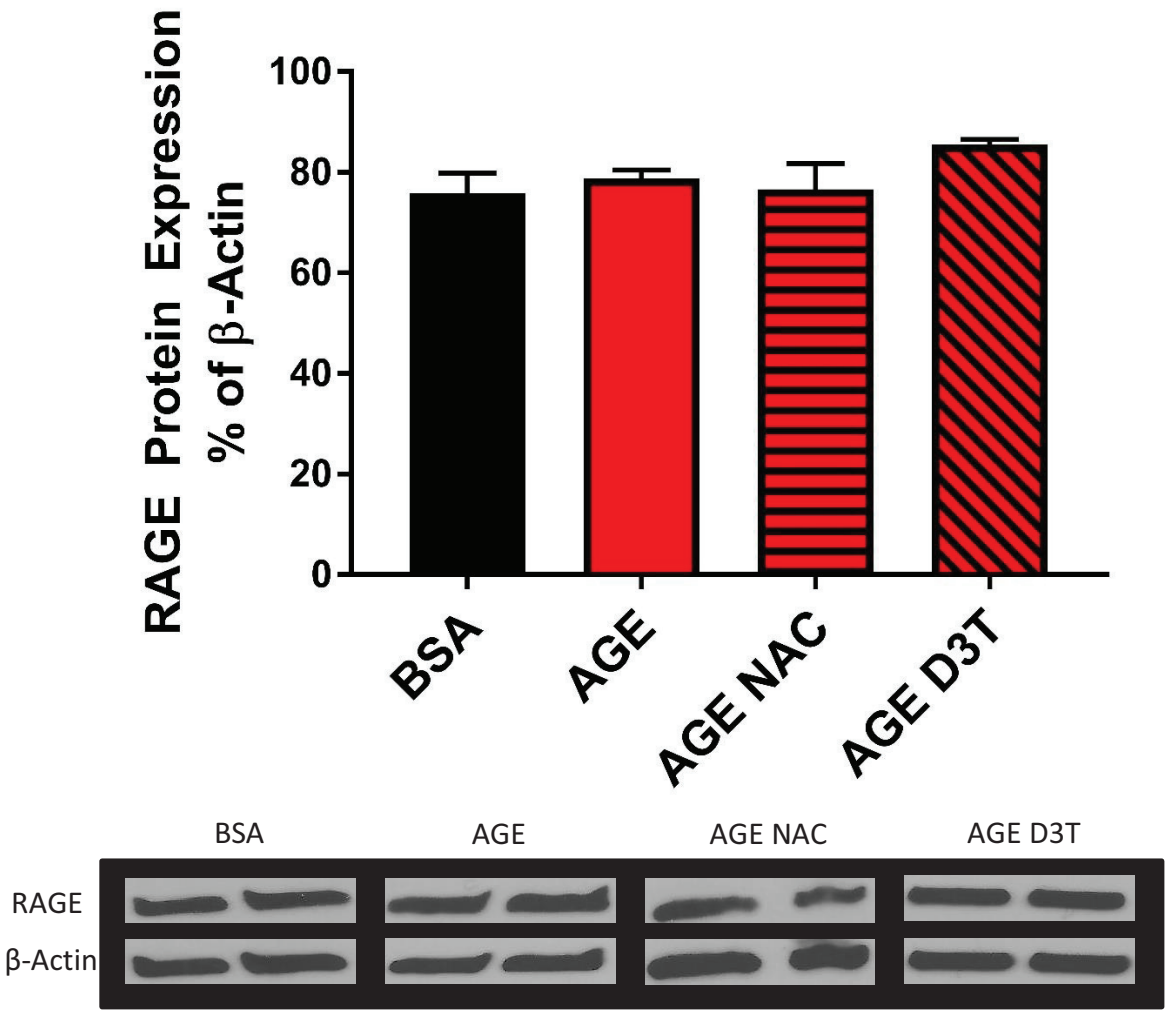

Figure A. 1 Treatment does not affect RAGE expression.
Differentiated cells were treated with 1 mM NAC or 100 μM D3T for 24 hours prior to 5 mg/mL BSA or AGE treatment. NAC and D3T were replenished during the 24-hour AGE treatment. Blots shown are representative samples of each group. Data were analyzed by one-way ANOVA with Dunnett's post-hoc analysis from 3 independent experiments. Bars with an * are significantly different from the BSA group ($p < 0.05$).

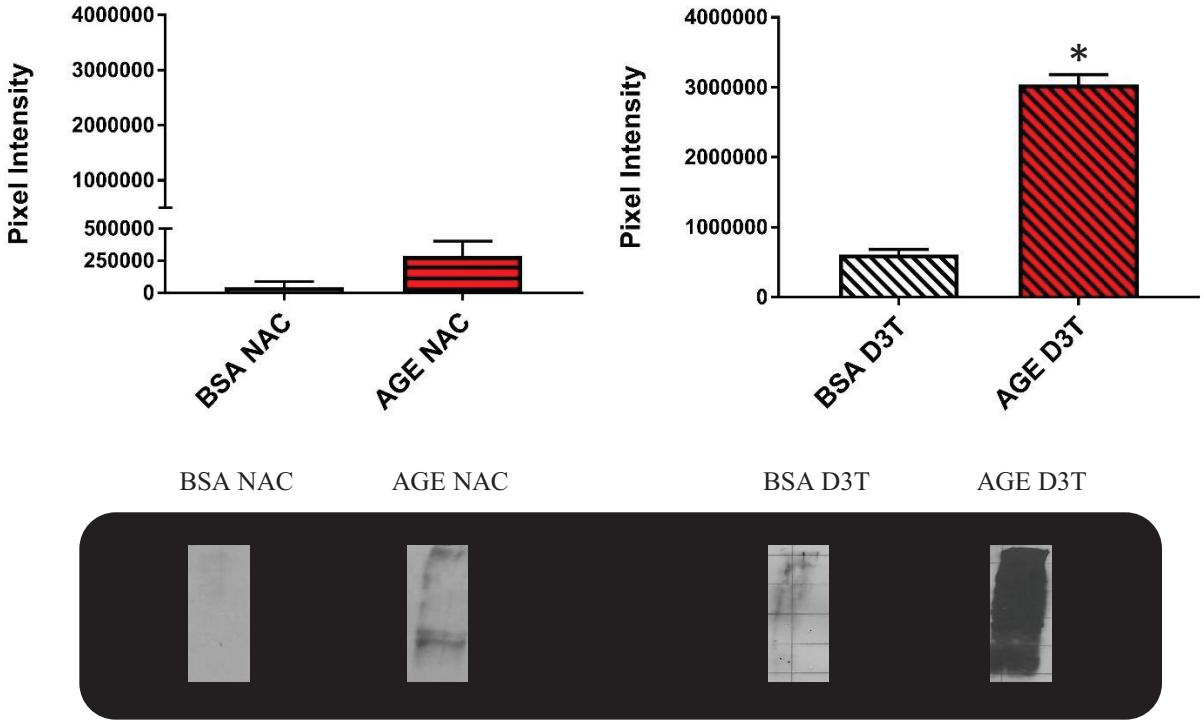

Figure A. 2 NAC protects against AGE-induced protein carbonyl formation whereas D3T does not.

Differentiated cells were treated with 1 mM NAC or 100 μM D3T for 24 hours prior to 5 mg/mL BSA or AGE treatment. NAC and D3T were replenished during the 24-hour BSA and AGE treatments. Western blots of DNPH-modified protein carbonyls shown are representative lane samples of each group. Data were analyzed via 2-tailed Student's t-test from 3 independent experiments. Bars with an * are significantly different ($p < 0.05$) from the respective BSA control group.

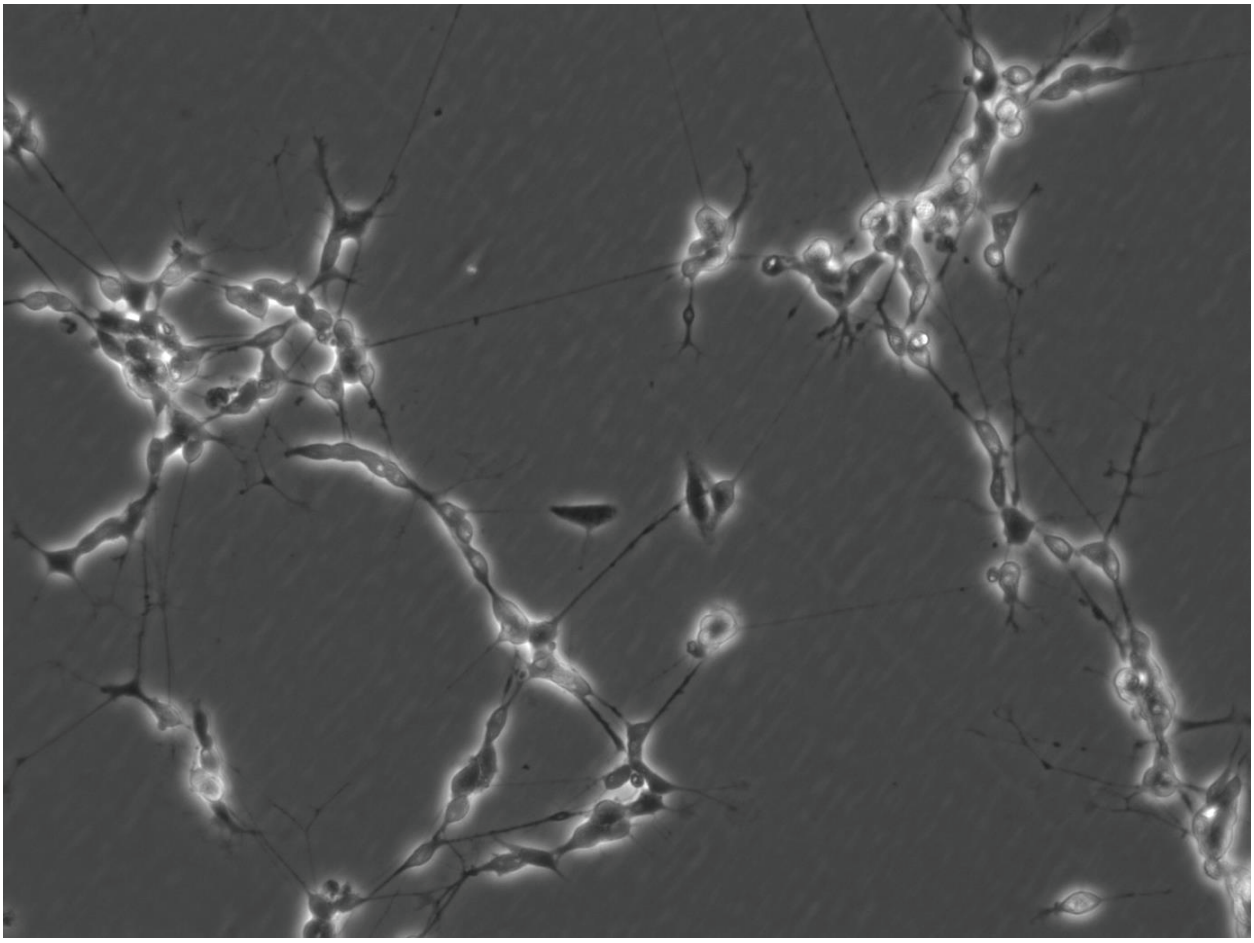

Figure A. 3 Differentiated SH-SY5Y cells before treatment.
Neurite length in 10x images was quantified using ImageJ with NeuronJ plugin. Representative image is shown.

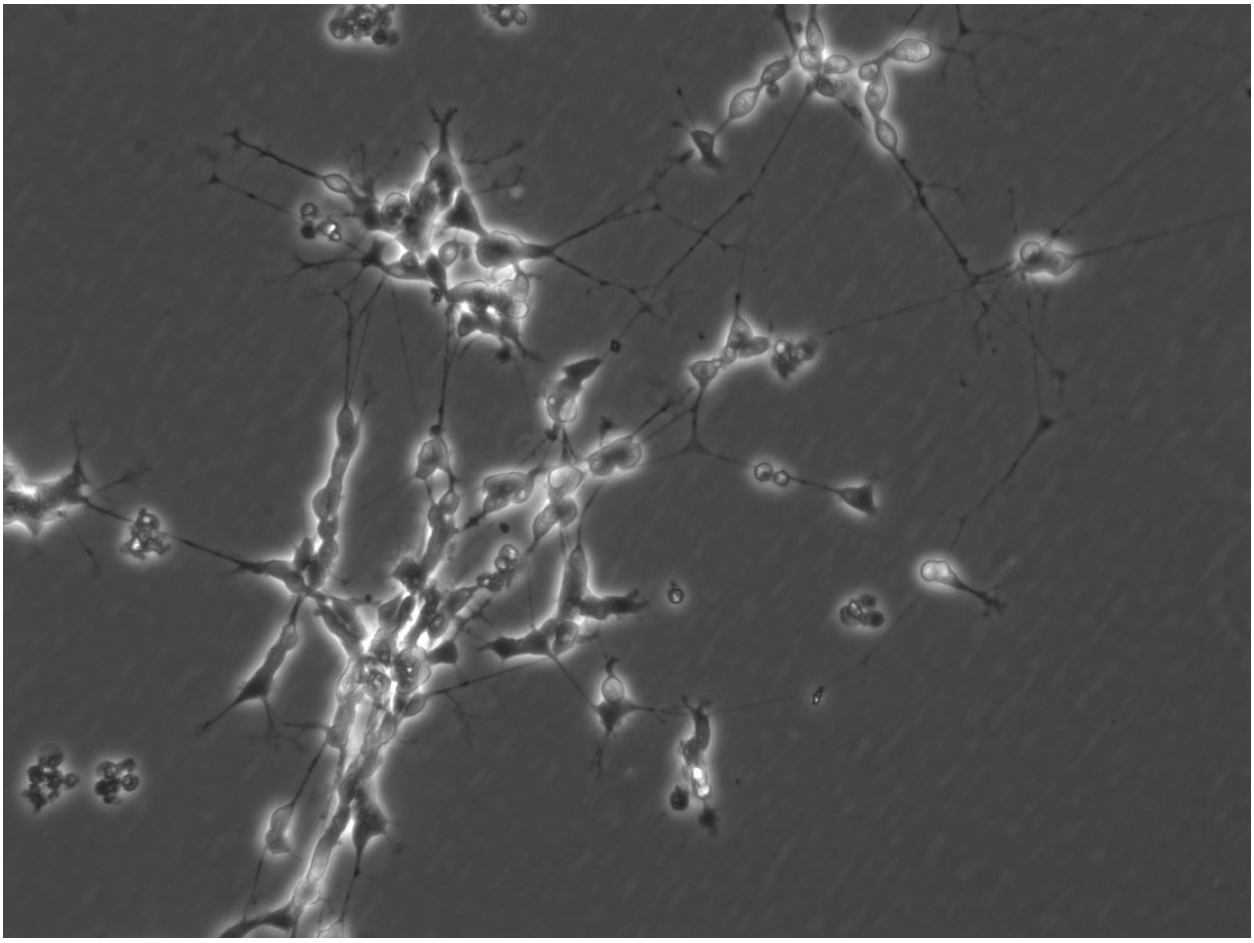

Figure A. 4 Differentiated SH-SY5Y cells after 40-minute treatment with GSSGme. Following differentiation, SH-SY5Y cells were treated with 200 μM GSSGme for 40 minutes. Neurite length in 10x images was quantified using ImageJ with NeuronJ plugin. Representative image is shown.

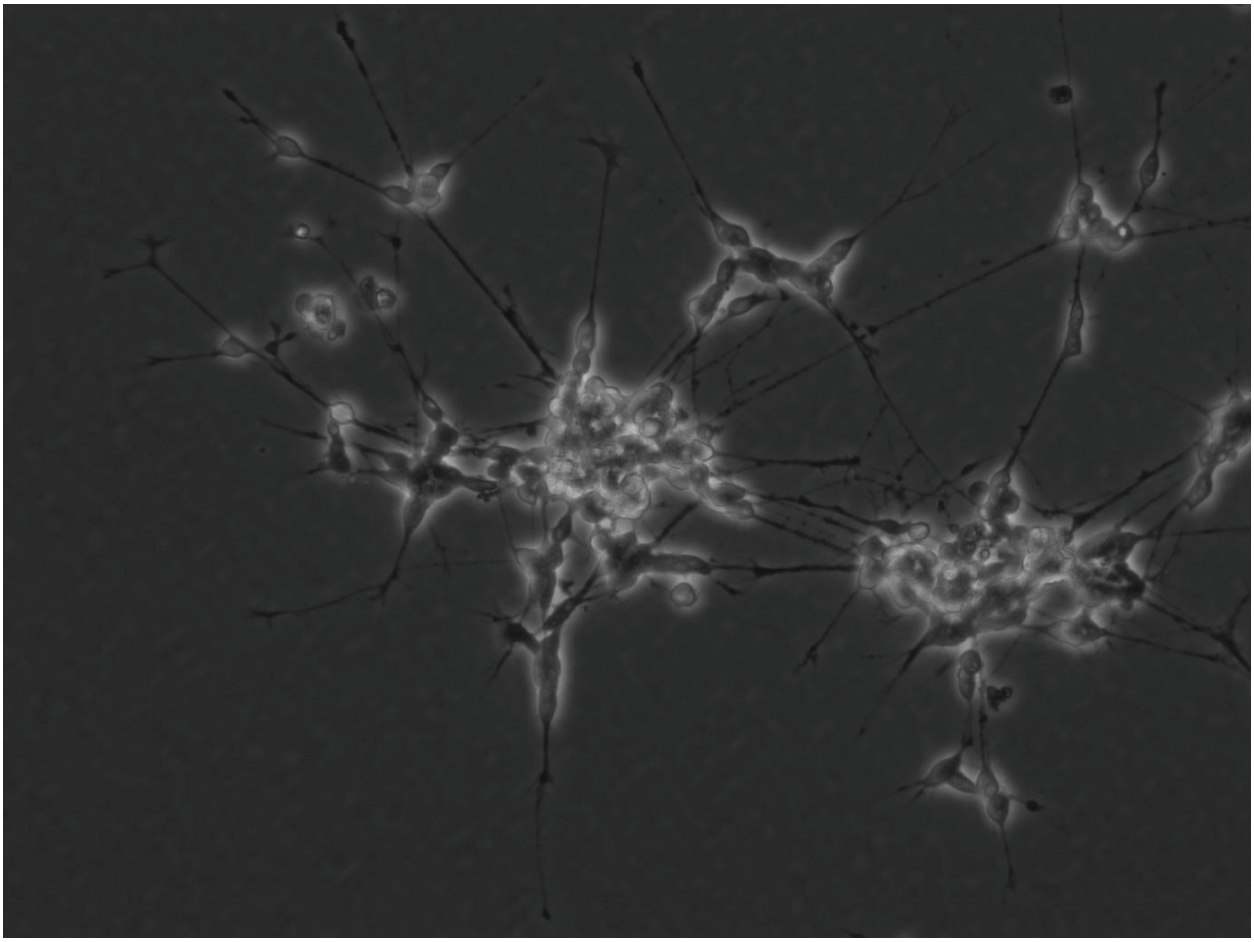

Figure A.5 Differentiated SH-SY5Y cells after 40-minute treatment with AAPA.
Following differentiation, SH-SY5Y cells were treated with 15 μM AAPA for 40 minutes. Neurite length in 10x images was quantified using ImageJ with NeuronJ plugin. Representative image is shown.

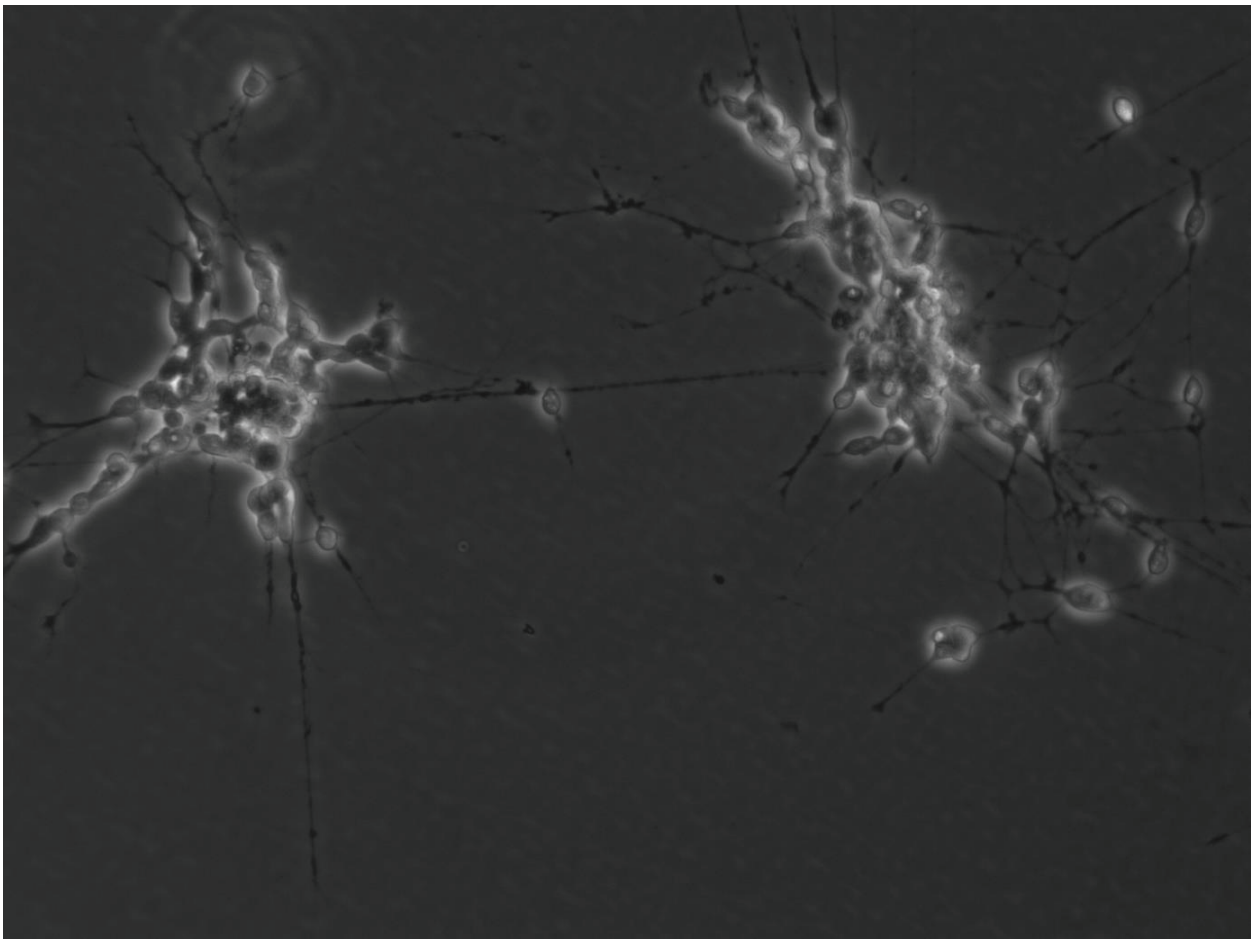

Figure A. 6 Differentiated SH-SY5Y cells after 40-minute treatment with GSSGme and AAPA. Following differentiation, SH-SY5Y cells were treated with 200 μM GSSGme and 15 μM AAPA for 40 minutes. Neurite length in 10x images was quantified using ImageJ with NeuronJ plugin. Representative image is shown.